AD-A211 651

②

REPORT DOCUMENTATION PAGE

Form Approved
OMB No. 0704-0188

1a. REPORT SECURITY CLASSIFICATION	1b. RESTRICTIVE MARKINGS
2a. SECURITY CLASSIFICATION AUTHORITY	3. DISTRIBUTION / AVAILABILITY OF REPORT
2b. DECLASSIFICATION / DOWNGRADING SCHEDULE	Approved for public release, distribution unlimited

DTIC ELECTE AUG 21 1989 B

4. PERFORMING ORGANIZATION REPORT NUMBER(S)

Ceramatec Report No. 8961701

5. MONITORING ORGANIZATION REPORT NUMBER(S)

AFOSR-TR- 89-1097

6a. NAME OF PERFORMING ORGANIZATION	6b. OFFICE SYMBOL (If applicable)	7a. NAME OF MONITORING ORGANIZATION
Ceramatec, Inc.		Air Force Office of Scientific Research/NE

6c. ADDRESS (City, State, and ZIP Code)	7b. ADDRESS (City, State, and ZIP Code)
2425 South 900 West Salt Lake City, UT 84119	Bolling Air Force Base Washington, DC 20332-6448

8a. NAME OF FUNDING / SPONSORING ORGANIZATION	8b. OFFICE SYMBOL (If applicable)	9. PROCUREMENT INSTRUMENT IDENTIFICATION NUMBER
AFOSR	NE	Contract No. F49620-87-C-0077

8c. ADDRESS (City, State, and ZIP Code)

c/o AFOSR, Directorate of Materials Sci.
Bldg. 410, Bolling AFB 20332-6448

10. SOURCE OF FUNDING NUMBERS

PROGRAM ELEMENT NO.	PROJECT NO.	TASK NO.	WORK UNIT ACCESSION NO.
61102F	DARPA	999999	

11. TITLE (Include Security Classification)

New Mechanism for Toughening Ceramic Materials

12. PERSONAL AUTHOR(S)
Raymond A. Cutler and Anil V. Virkar

13a. TYPE OF REPORT	13b. TIME COVERED	14. DATE OF REPORT (Year, Month, Day)	15. PAGE COUNT
Final	FROM 7-15-87 TO 12-14-88	1989, May, 19	93

16. SUPPLEMENTARY NOTATION
Zirconium oxides, Ceramic materials,

17. COSATI CODES			18. SUBJECT TERMS (Continue on reverse if necessary and identify by block number)
FIELD	GROUP	SUB-GROUP	Tetragonal Zirconate Polycrystals (TZP)

19. ABSTRACT (Continue on reverse if necessary and identify by block number)

A 14 month study by Ceramatec, with a subcontract to the University of Utah, was initiated in order to determine if ferroelastic switching contributes to toughening in ceramic materials. Domain switching in ZrO_2 single crystals (heat treated to minimize transformation) at 1400°C was used to show that ferroelastic switching is a process which occurs at temperatures in excess of the monoclinic to tetragonal transformation temperature. These data, coupled with fracture toughness measurements of 8 MPa·m$^{1/2}$ at 1000°C, show that ferroelastic toughening has the potential for toughening at temperatures in excess of that possible by transformation toughening. Experiments on PZT, $SrZrO_3$ and $Gd_2(MoO_4)_3$ were used to show that ferroelastic switching can contribute to toughening. The time dependence of switching was demonstrated using PZT ceramics. Dopants were added to polycrystalline TZP materials in order to substantially increase their fracture toughness. In the case of SrO additions, strontium aluminate platelets, formed in-situ during sintering, contributed to toughness

UNCLASSIFIED

20. DISTRIBUTION / AVAILABILITY OF ABSTRACT	21. ABSTRACT SECURITY CLASSIFICATION
☒ UNCLASSIFIED/UNLIMITED ☐ SAME AS RPT. ☐ DTIC USERS	

22a. NAME OF RESPONSIBLE INDIVIDUAL	22b. TELEPHONE (Include Area Code)	22c. OFFICE SYMBOL
Dr. Liselotte J. Schioler	(202) 767-4933	NE

DD Form 1473, JUN 86   Previous editions are obsolete.   SECURITY CLASSIFICATION OF THIS PAGE

89 8 1

NEW MECHANISM FOR TOUGHENING CERAMIC MATERIALS

AFOSR.TR. 89-1097

Final Report
DARPA Contract No. F49620-87-C-0077

Submitted by

Raymond A. Cutler
Ceramatec, Inc.
2425 South 900 West
Salt Lake City, Utah 84119

and

Anil V. Virkar
Department of Materials Science
University of Utah
Salt Lake City, Utah 84112

Submitted to

Dr. Liselotte J. Schioler
Electronic and Material Sciences
Air Force Office of Scientific Research
Bolling Air Force Base, DC 20332-6448

Ceramatec Report No. 8961701
May 1989

FINAL REPORT

May 1989

NEW MECHANISM FOR TOUGHENING CERAMIC MATERIALS

Submitted by
Ceramatec, Inc.
2425 South 900 West
Salt Lake City, Utah 84119

SUMMARY

Background

Ceramatec, Inc. proposed to DARPA that the toughening of zirconia-based ceramics be investigated to see if ferroelastic switching contributes to toughening. Virkar and Matsumoto[1,2]. suggested that ferroelastic switching, which was observed on the ground surfaces of tetragonal zirconia polycrystalline (TZP) ceramics, could contribute to the high toughness measured for zirconia ceramics. While it was recognized that transformation toughening[3-5] is the primary mechanism for toughening at low temperatures, another mechanism is responsible for the high toughness observed by Ingel et al.[6,7] for single crystals at temperatures in excess of the transformation temperature.

The x-ray diffraction data of Virkar and Matsumoto clearly showed ferroelastic switching upon grinding ceria and yttria TZP ceramics, showing that the grinding stress exceeded the ferroelastic switching stress (i.e., coercive stress) in zirconia. They also examined a wide variety of dopants in order to change the switching strain. Dopants composed of trivalent (group III (Sc, Y, La), lanthanide (Ce, Pr, Nd, Sm, Eu, Gd, Tb, Dy, Ho, Er, Tm, Yb, and Lu)) and pentavalent (V, Nb, or Ta) ions in the form of mixed oxides were very effective in increasing the fracture toughness of zirconia. $LaNbO_4$, which is expected to increase the c/a ratio of TZP materials, was among the most promising dopants identified in the in-house funded work. Additionally, SrO additions were shown to increase the fracture toughness of Ce-TZP materials. SrO had previously been added to Mg-PSZ as a sintering aid. A 14 month effort (July 15, 1987-Sept. 14, 1988) was initially funded by DARPA through AFOSR in order to determine the feasibility of ferroelastic toughening and other novel toughening approaches which have the possibility of allowing high toughness at temperatures in excess of 1000°C.

Program Objectives

The objectives of the research were to: 1) Determine the effect of additives ($SrZrO_3$ and $LaNbO_4$) on the mechanical behavior of TZP. Particular focus was on optimizing high temperature strength and toughness by determining compositions which promoted ferroelastic behavior; 2) Increase understanding of ferroelastic toughening (or alternate mechanism if ferroelastic toughening was determined not to be valid) by identifying key parameters (effects of temperature, composition, coercive stress, and other factors) which affect toughening in a system (such as VO_2) which is not transformation toughened; 3) Conduct a literature search to identify new materials which undergo ferroelastic toughening; 4) Develop mathematical models which are consistent with experimental data; and 5) Study toughening by combined mechanisms (i.e., ferroelastic toughening and whisker reinforcement).

The research effort awarded to Ceramatec with David W. Richerson as Program Manager and Raymond A. Cutler as Principal

1

Investigator had a subcontract to the University of Utah under the direction of Professor Anil V. Virkar. The work at Ceramatec was directed mainly at examining the role of dopants in toughening polycrystalline zirconia ceramics while the University of Utah subcontract focused on understanding ferroelasticity. The University of Utah research used ZrO_2 single crystals for deformation studies and high temperature processing to obtain fine domain structure in polycrystalline structures.

Accomplishments

X-ray diffraction of Y_2O_3-doped ZrO_2 single crystals (heat treated to 2100°C to eliminate any monoclinic ZrO_2) showed that ferroelastic domains underwent reorientation (switching) in compression. Prior to loading in compression to 2.25 GPa and 300 MPa at 25°C and 1400°C, respectively, the ZrO_2 cubes (<100> axes orthogonal to the surfaces of the cube) were x-rayed on the surface to which compression was applied and to a side surface. After compression testing, the same two surfaces were x-rayed again. In each case, the intensity of the (002) peak decreased and the (200) peak intensity increased on the surface that was subjected to stress. On the side surface, however, the (002) peak increased and the (200) peak decreased in accord with ferroelastic domain switching.

Fracture toughness measurements made on tetragonal ZrO_2 single crystals using the SENB technique resulted in fracture toughness at room temperature of approximately 12 $MPa \cdot m^{1/2}$ and approximately 8 $MPa \cdot m^{1/2}$ at 1000°C. X-ray diffraction of the fractured surfaces showed an increase in intensity of the (002) peak and a decrease in intensity of the (200) relative to the pristine surface.

Polycrystalline ZrO_2 samples were sintered at temperatures in excess of 2100°C. The fracture toughness was measured as 7.7 $MPa \cdot m^{1/2}$ at room temperature. No monoclinic phase was detected on the fracture surface despite grain size in excess of 100 μm. Polycrystalline Y_2O_3 TZP (Y-TZP) samples sintered at 1500°C and annealed above the t-->c transformation temperature and rapidly cooled showed no dependence of hardness on grain size over a range of grain sizes between approximately 0.5 and 100 μm. This suggests that the fine domain structure formed upon cooling from the cubic to tetragonal stability regime controlled hardness.

Experiments on commercially available lead zirconate titanate (PZT) ceramics were conducted since no transformation toughening occurs in these materials. It was observed that either the application of compressive mechanical stress or an electric field resulted in domain switching in these ferroelastic-ferroelectric materials. Relaxation time studies show that switching is dependent on rate and composition[9]. These fundamental studies help explain why switching was not initially observed on fractured polycrystalline samples. Fracture toughness measurements showed that fracture toughness decreases with increasing temperature up to the Curie temperature (350°C) and is independent of temperature above that temperature

2

(up to at least 500°C). Domain switching was observed on some samples fractured at room temperature. Indentations were introduced into samples which were both mechanically and electrically poled. The difference in crack lengths could be explained on the basis of ferroelastic domain switching. These data suggest that ferroelastic domain switching does contribute to the overall toughness in the PZT ceramics tested.

Further understanding in the role of dopants in toughening ZrO_2 was gained. In all cases investigated, several toughening mechanisms appeared to be operating simultaneously. The contribution of ferroelastic toughening was therefore difficult to ascertain. For all materials sintered in the stability range of the t-phase, significant transformation toughening occurred. Additions of $LaNbO_4$ (up to 2 wt. %) to polycrystalline Ce-TZP/Al_2O_3 increased toughness from 10 to 16 MPa·m$^{1/2}$ at room temperature.

Additions of $SrZrO_3$ to Ce-TZP lowers the fracture toughness and increases the strength and hardness. The addition of $SrZrO_3$ to Ce-TZP decreases grain growth, resulting in smaller grain size for Ce-TZP doped with as little as 0.5 wt. % $SrZrO_3$. The addition of $SrZrO_3$ to Ce-TZP/Al_2O_3 markedly improved the fracture toughness as measured by the double cantilever beam technique. Values as high as 20 MPa·m$^{1/2}$ were measured at room temperature. The addition of SrO to Ce-TZP/Al_2O_3 allows the formation of $SrO·6Al_2O_3$, which form as platelets in the zirconia matrix. The formation of platelets occurs simultaneously with increased fracture toughness, although further work is needed to show that crack bridging is aiding toughening. The addition of alumina to zirconia in the absence of SrO decreases ZrO_2 grain growth, thereby increasing the hardness and strength, while decreasing the fracture toughness. The formation of strontium aluminate platelets allows an excellent combination of room temperature mechanical properties (K_C=15.2 MPa·m$^{1/2}$, σ_f=530 MPa, H=13.7 GPa) with SrO-doped ZrO_2(12 mol. % CeO_2)-30 vol. % Al_2O_3.

An advantage of in-situ aluminate formation is that materials which react to give high platelet contents can be densified, whereas it is difficult to obtain high volume loadings of platelets when sintering (i.e., hot pressing) mixtures of powders and platelets. Initial alumina concentrations of 15, 30 and 60 vol. %, at constant SrO/Al_2O_3 molar ratios, could be densified to greater than 97% of theoretical density. Creep testing at 1200°C under 45-85 MPa stress resulted in strain rates of $2x10^{-8}$ to $9x10^{-8}$/s for Ce-TZP with strontium aluminate platelets (Ce-TZP with 30 vol. % Al_2O_3 with 2 wt. % $SrZrO_3$). These creep rates were two orders of magnitude lower than conventional Y-TZP. Further creep testing is needed before it can be concluded that interlocking strontium aluminate platelets limit creep. It is expected that the materials developed will have promise as creep-resistant structural members. Further work is needed to optimize compositions and to determine if high platelet loading allows retention of strength and toughness to high temperatures. Additional work is also needed to see if

3

these materials can be further aided by ferroelastic toughness through heat treatment (i.e., heat treatment in the cubic regime).

Carlsson[10] has shown that $SrZrO_3$, in which the paraelastic/ferroelastic transition can be lowered below room temperature by the addition of $CaZrO_3$ or $BaZrO_3$, reorients (switches ferroelastically) under the application of compressive loading. Polycrystalline $SrZrO_3$, $Sr_{0.8}Ca_{0.2}ZrO_3$, $Sr_{0.8}Ba_{0.2}ZrO_3$, $Sr_{0.6}Ba_{0.4}ZrO_3$, and $Sr_{0.4}Ba_{0.6}ZrO_3$ ceramics were sintered and characterized. SENB fracture toughness was 25% higher for ferroelastic compositions than for the paraelastic composition, indicating that the ferroelastic toughening contribution is significant in this class of ceramics.

Degree to Which Objectives Were Met

Further understanding on the role of dopants was gained. Transformation toughening was observed with both $LaNbO_4$ and SrO doped ZrO_2-based ceramics, but transformation toughening alone does not explain the large difference in toughness with small dopant additions. High temperature strength testing performed by J. Swab at the Army Materials Laboratory on $SrZrO_3$-doped Ce-TZP made by Matsumoto and Mayhew showed that high temperature strength retention (73% of the strength retained to 1100°C (strength of 550±40 MPa at 25°C and 400±10 MPa at 1100°C)) is possible in this system[11]. The in-situ formation of strontium aluminate platelets was used to meet the objective of combined toughening mechanisms.

A survey of the literature showed that $SrZrO_3$ is ferroelastic. Additional work is necessary to optimize toughness in $SrZrO_3$-based ceramics. Work with nontransformable materials including PZT and $t'-ZrO_2$ were used to gain a further understanding of ferroelastic toughening and show that it can contribute to toughening. Relaxation times for switching under an electric field were modelled. Calculations on the contribution of ferroelastic switching to toughening are dependent on the depth and degree of switching, as well as the stress required for switching. The stress required for switching was measured but further work is needed to determine the zone depth and degree of switching. In both $t'-ZrO_2$ and PZT, two materials where transformation toughening does not contribute to toughening, x-ray diffraction data clearly showed that ferroelastic switching occurs. Fracture toughness data obtained in both systems suggest that switching contributes to toughness, which in the case of $t'-ZrO_2$, can be retained to temperatures above 1000°C.

In the following report is divided into two sections. The first covers important aspects of the Ceramatec research. The second contains a summary and two papers, which highlight the work performed by Professor Anil Virkar at the University of Utah under subcontract from Ceramatec. In addition, a patent application, based partly on this DARPA/AFOSR supported research, has been submitted by Ceramatec.

4

I. CERAMATEC

EXPERIMENTAL PROCEDURES

Compositions were prepared using a wide variety of ZrO_2 including undoped TZ-0 (TOSOH), SC-15 (Magnesium Electron), E-20 (Magnesium Electron) to which CeO_2 (Molycorp) was added and coprecipitated ZrO_2(12 mol. % CeO_2) (TZ-12CE, TOSOH) and ZrO_2(3 mol. % Y_2O_3) (TZ-3YA, TOSOH). Al_2O_3 (CR-30, Baikowski; HP-DBM, Reynolds; or A-16SG, Alcoa) and $SrZrO_3$ (TAM) were added to some compositions. $LaNbO_4$ was formed by reacting lanthanum and niobium oxides prior to adding it to the ZrO_2-based ceramics. Alternatively, $LaAl_{11}O_{18}$ and $AlNbO_4$ were formed and added to the other components. $SrZrO_3$, $Sr_{0.8}Ca_{0.2}ZrO_3$, $Sr_{0.8}Ba_{0.2}ZrO_3$, $Sr_{0.6}Ba_{0.4}ZrO_3$, and $Sr_{0.4}Ba_{0.6}ZrO_3$ compositions were made using $SrZrO_3$, $BaZrO_3$ and $CaZrO_3$ powders (TAM) or high purity $SrCO_3$, $BaZrO_3$ and $CaZrO_3$ powders (Alfa) with TZ-0 ZrO_2.

All compositions were vibratory milled using ZrO_2 media in methanol or n-hexane using appropriate dispersants. The powders were wet screened -325 mesh and dry screened -170 mesh. Bars were formed uniaxially at 35 MPa and subsequently isostatically pressed at 200 MPa. Compositions were sintered in air at either 1500 or 1550°C for two hours. Some Y-TZP compositions were subsequently annealed in argon at temperatures ranging between 1900 and 2200°C in a graphite resistance heated furnace. The heating rate was approximately 35°C/minute and the cooling rate to 1500°C was approximately 50°C/minute.

Density was determined by water displacement. Sintered bars were x-rayed and subsequently ground using a 220 diamond wheel. Four-point bend strength was measured using a universal testing machine with a crosshead speed of 0.5 cm/min, a support span of 40 mm and a loading span of 20 mm. The ground and fracture surfaces were x-rayed for selected compositions and % monoclinic, based on total ZrO_2 content, was made using the analysis of Toraya[12]. Fracture toughness was measured using the double cantilever beam (DCB) technique except for $SrZrO_3$-based compositions, which were measured using the single edge notched beam (SENB) technique (notch width of approximately 250 μm) in 3-point bending. For DCB tests, 3 bars were generally broken with 3-7 measurements on each bar. Hardness was determined using a 75 N indent made with a 136° Vickers diamond indenter. Ten measurements were made for each composition. Creep was measured in air at 1200°C with applied stress ranging between approximately 10 and 85 MPa using a technique previously described by Jou, et al.[13].

RESULTS AND DISCUSSION

Effect of Dopants

Lanthanum Niobate: When small additions of $LaNbO_4$ (up to 2 wt. %) were added to Ce-TZP (i.e., ZrO_2(12 mol. % CeO_2)) containing 15 vol. % Al_2O_3, there was no change in microstructure but a substantial increase in fracture toughness occurred. Table 1 lists the density, hardness, fracture toughness (DCB) and strength of compositions made using $LaNbO_4$ additions. Table 2 shows data from a set of compositions made using $LaAl_{11}O_{18}$ and $AlNbO_4$, showing the equivalent amount of $LaNbO_4$ added. In both sets of data, the fracture toughness shows a significant increase with small additions of $LaNbO_4$. Fracture surfaces showed large amounts of monoclinic ZrO_2, although the amount of monoclinic did not correlate with the fracture toughness. For the compositions in Table 1, the % monoclinic ZrO_2 on the fracture surface was measured as 73, 86, 66, 79 and 62% for 0.0, 0.15, 0.30, 0.60, and 1.20 wt. % $LaNbO_4$ additions, respectively. In Table 2, the % monoclinic ranged between 72 and 76, again showing no correlation with composition. The Table 2 data indicate that strength is not necessarily a strong function of composition. The Table 2 data also show that density and hardness are independent of composition.

Detailed grain size measurements were not made in order to determine if slight difference in grain size contributed to the increase in fracture toughness. X-ray diffraction data support the qualitative conclusion that grain size is similar for all compositions as there is no trend in monoclinic content. The x-ray data show that transformation toughening does not explain the increase in fracture toughness with increasing amounts of fracture toughness. The large degree of transformation and in x-ray diffraction scans, however, made it difficult to conclude whether ferroelastic toughening contributes to toughness in this system.

Table 1
Ce-TZP/15 vol. % Al_2O_3 Containing Small Additions of $LaNbO_4$

$LaNbO_4$ (wt. %)	Density (g/cc)	%T.D.	#[d]	σ_f[a] (MPa) x[e]	s[f]	K_{Ic}[b] (MPa·m$^{1/2}$) x	s	H[c] (GPa) x	s
0.00	5.86	99.0	5	536	27	10.6	0.1	11.1	0.7
0.15	5.86	99.0	5	511	16	11.1	0.2	11.6	0.2
0.30	5.83	98.5	5	449	10	12.1	0.4	11.1	0.3
0.60	5.85	98.5	5	407	32	14.0	0.3	10.4	0.3
1.20	5.81	98.1	5	379	14	13.8	0.5	10.4	0.3

a. Four-point bend strength.
b. DCB fracture toughness.
c. Vicker's hardness.
d. Number of strength specimens tested.
e. Mean value.
f. Standard deviation.

Table 2
LaNbO$_4$-Doped Ce-TZP/15 vol. % Al$_2$O$_3$ Made Using
Additions of LaAl$_{11}$O$_{18}$ and AlNbO$_4$

LaNbO$_4$ (wt. %)	Density (g/cc)	%T.D.	σ_f (MPa) #	σ_f (MPa) x	σ_f (MPa) s	K$_{Ic}$ (MPa·m$^{1/2}$) x	K$_{Ic}$ (MPa·m$^{1/2}$) s	H (GPa) x	H (GPa) s
0.25	5.86	99.0	5	522	4	12.4	0.4	12.0	0.3
0.50	5.85	98.8	10	449	80	13.2	0.6	12.2	0.1
0.75	5.89	99.5	10	436	94	13.8	0.5	11.2	0.4
1.00	5.87	99.2	10	431	70	15.8	0.5	11.3	0.2
1.50	5.86	99.0	10	457	63	15.7	0.6	11.4	0.2

The increase in fracture toughness with increasing LaNbO$_4$ addition is consistent with the prior unpublished work of Matsumoto and Virkar, although they measured values as high as 20 MPa·m$^{1/2}$. Further work was not performed with these compositions due to: 1) the inability of x-ray diffraction data to clearly show how LaNbO$_4$ was affecting the c/a ratio[14], 2) the large degree of transformation occurring within this system, and 3) the fact that SrO additions allowed one to see microstructural trends (see section on SrO additions).

A cursory investigation of the saturation level of LaNbO$_4$ in the ZrO$_2$ lattice suggested that with increased LaNbO$_4$ additions (i.e., greater than 5 wt. %), CeO$_2$ comes out of solution with ZrO$_2$, making the transformation from t-->m occur more readily[14]. Matsumoto showed that LaNbO$_4$ additions to Y-TZP did not affect toughness. Further work needed in this system includes 1) evaluation of elevated temperature properties, 2) characterization of LaNbO$_4$ doped ZrO$_2$ (no Al$_2$O$_3$ additions) in order to see the effect of Al$_2$O$_3$ and to observe peak switching, 3) high temperature heat treatment in air in order to form t'-ZrO$_2$ with LaNbO$_4$ additions (the tendency of CeO$_2$ to reduce to Ce$_2$O$_3$ at elevated temperatures will make this difficult), and 4) an understanding of why LaNbO$_4$ affects the toughness of Ce-TZP and not Y-TZP. For the purpose of determining the contribution of ferroelastic switching to toughening, further work will only involve materials which do not show a significant amount of transformation.

Strontium Oxide: Strontium oxide additions, like LaNbO$_4$ additions, have a strong effect on fracture toughness. Table 3 shows data for Ce-TZP compositions made with 15 vol. % Al$_2$O$_3$. The SrO was added as SrZrO$_3$. No extra CeO$_2$ was added to compensate for the small amount of ZrO$_2$ added from the SrZrO$_3$. This did not strongly influence the results, however, since CeO$_2$ content in ZrO$_2$ ranged from 12.0 mol. % for no SrZrO$_3$ addition to 11.4 mol. % for 4 wt. % SrZrO$_3$. Figure 1 shows that the density decreased with increasing amounts of SrZrO$_3$ added above 1 wt. %. Polished cross-sections viewed under the SEM showed an increasing tendency to form plate-shaped grains with increasing SrZrO$_3$ additions, as shown in Figure 2. Energy dispersive spectroscopy (EDS) revealed a high concentration of Al and Sr in these grains,

Table 3
Ce-TZP/15 vol. % Al_2O_3 Containing Small Additions of SrO

$SrZrO_3$ (wt. %)	Density (g/cc)	%T.D.	#	σ_f (MPa) x	s	K_{Ic} (MPa·m$^{1/2}$) x	s	H (GPa) x	s
0.0	5.88	99.3	5	634	19	8.3	0.2	11.5	0.9
0.5	5.91	99.9	5	589	17	11.0	0.2	11.5	0.1
1.0	5.85	99.0	5	574	46	12.5	0.4	11.5	0.2
2.0	5.68	96.3	5	520	53	14.0	0.7	10.3	0.3
4.0	5.72	96.9	5	570	38	12.2	0.3	10.2	0.4

with no Sr detected in the matrix. This suggested that strontium aluminate ($SrO·6Al_2O_3$) was forming in-situ during sintering, as would be expected based on phase equilibria (see Figure 3) between SrO and Al_2O_3[15]. Fracture surfaces showed that the strontium aluminate grains were platelets (see Figure 4). The formation of platelets, therefore, competes with sintering and leads to the lower density observed when sintering at 1500°C. When the sintering temperature was raised 50°C, the density was greater than 99% of theoretical for all compositions.
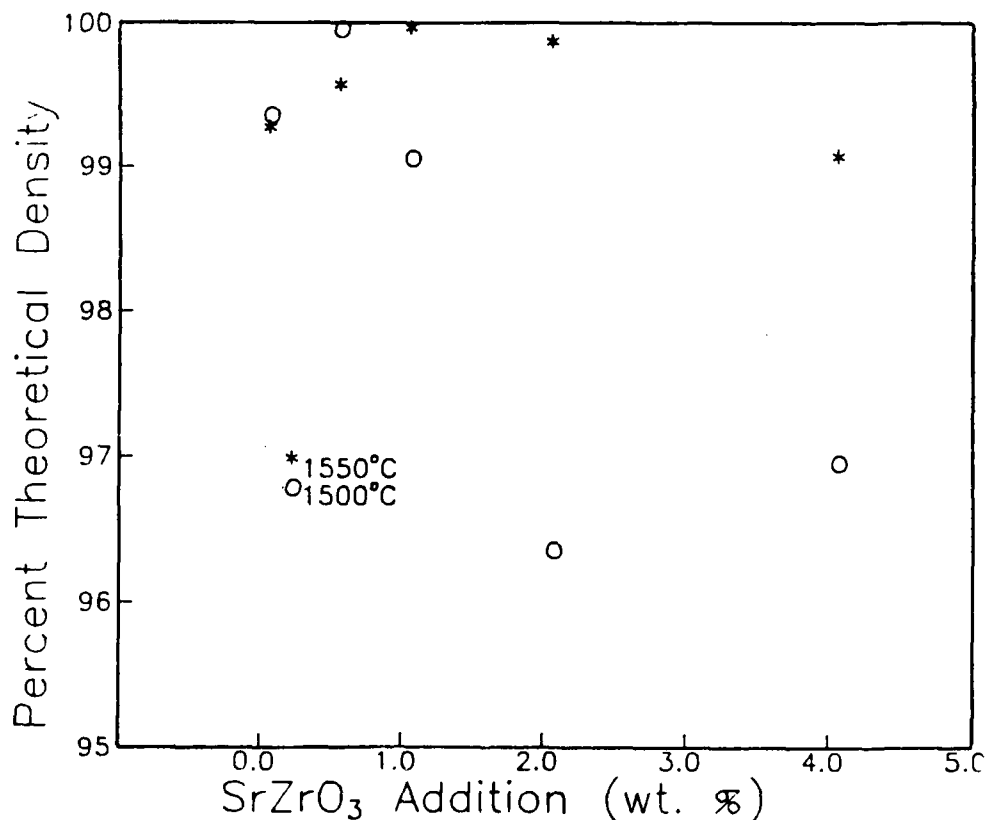
Figure 1. Effect of $SrZrO_3$ content and sintering temperature on the density of Ce-TZP/15 vol. % Al_2O_3 compositions.

8

Ce-TZP   2 μm

(a)

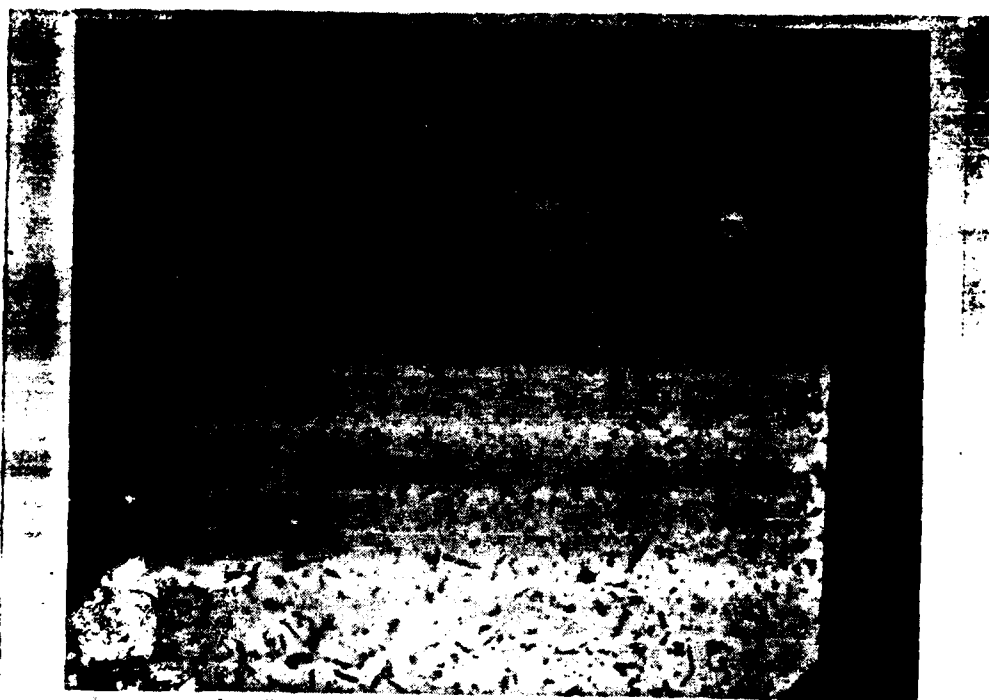Ce-TZP+15^V/o Al$_2$O$_3$ 2 μm

(b)

Figure 2. SEM micrographs of polished cross-sections of Ce-TZP and Ce-TZP/15 vol. % Al$_2$O$_3$ compositions showing strontium aluminate platelet formation with increasing SrO content. (a) Ce-TZP, (b) Ce-TZP/15 vol. % Al$_2$O$_3$.

9

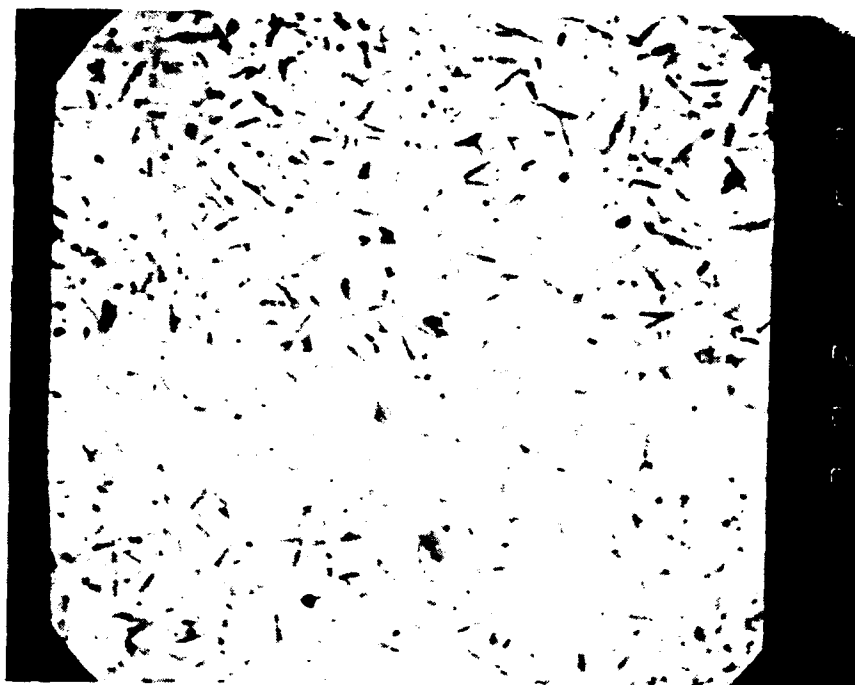Ce–TZP+15^V/o Al$_2$O$_3$ +0.5^W/o SrZrO$_3$ 10μm

(c)

Ce–TZP+15^V/o Al$_2$O$_3$ +1 ^{W}/o SrZrO$_3$ 10μm

(d)

Figure 2 (continued).   Ce-TZP/15 vol. % Al$_2$O$_3$ with (c) 0.5 and (d) 1.0 wt. % SrZrO$_3$.

10

Ce−TZP+15^V/o Al$_2$O$_3$+2^W/o SrZrO$_3$ 10μm

(e)
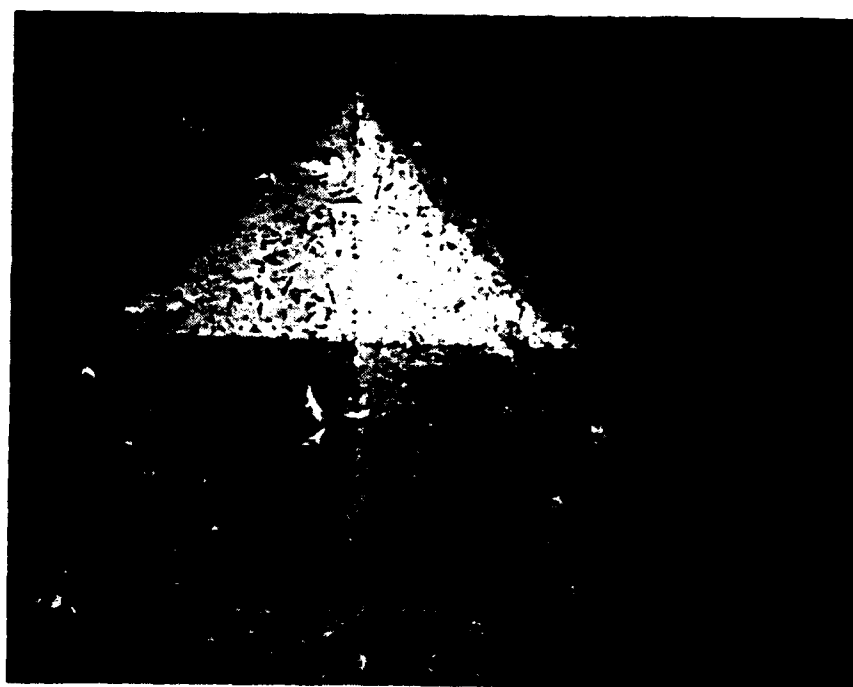
10μm

(f)

Figure 2 (continued).   Ce-TZP/15 vol. % Al$_2$O$_3$ with (e) 2.0 and (f) 4.0 wt. % SrZrO$_3$.   Note hardness indentation and change in magnification in (f) as compared to (a)-(e).

11

Ce—TZP+15^V/o Al$_2$O$_3$+4^W/o SrZrO$_3$ ___5μm___

(g)

Figure 2 (continued). (g) Ce-TZP/15 vol. % Al$_2$O$_3$-4 wt. % SrZrO$_3$ showing crack from indentation. Note crack branching and bridging.
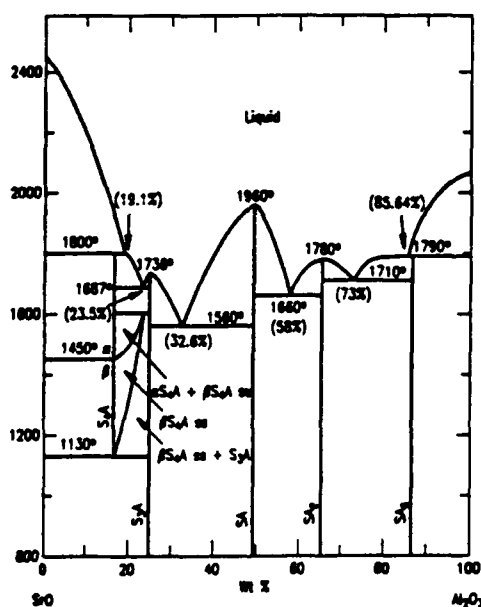
Figure 3. Al$_2$O$_3$-SrO phase diagram[15]. The addition of small amounts of SrO to Al$_2$O$_3$ results in the formation of hexagonal SrO·6Al$_2$O$_3$.

12
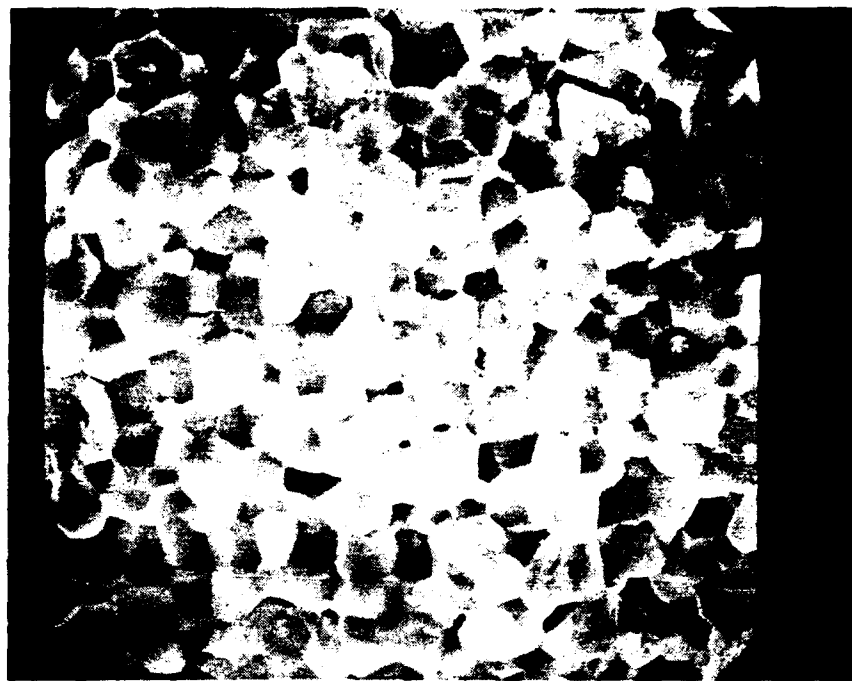
Ce–TZP   5μm

(a)

Ce–TZP+15 ᵛ/o Al₂O₃   5μm

(b)

Figure 4. SEM micrographs of fracture surfaces of Ce-TZP and Ce-TZP/15 vol. % Al₂O₃ compositions. (a) Ce-TZP, (b) Ce-TZP/15 vol. % Al₂O₃. Note decrease in grain size with alumina addition.
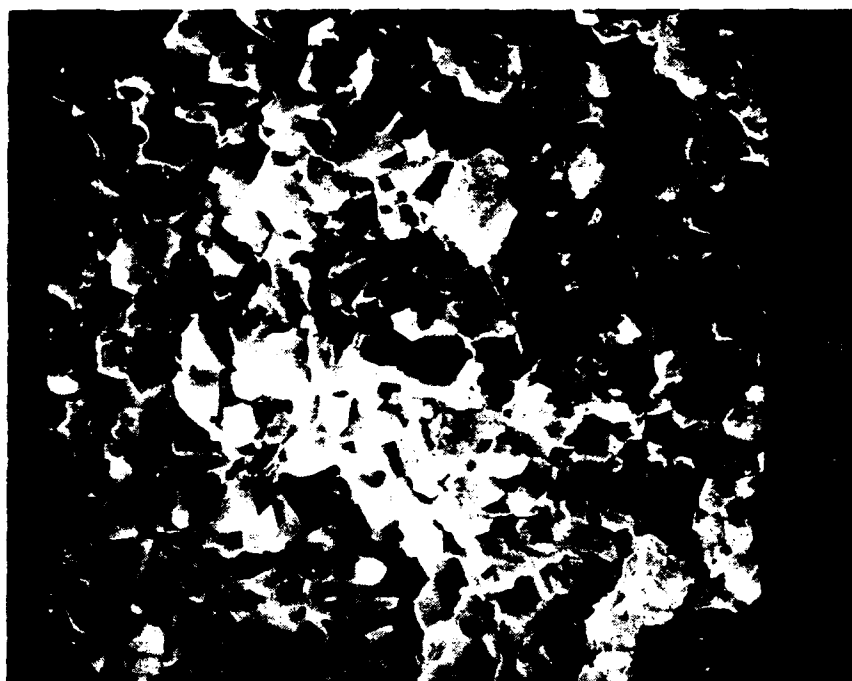
13

Ce–TZP

$2\mu m$

(c)
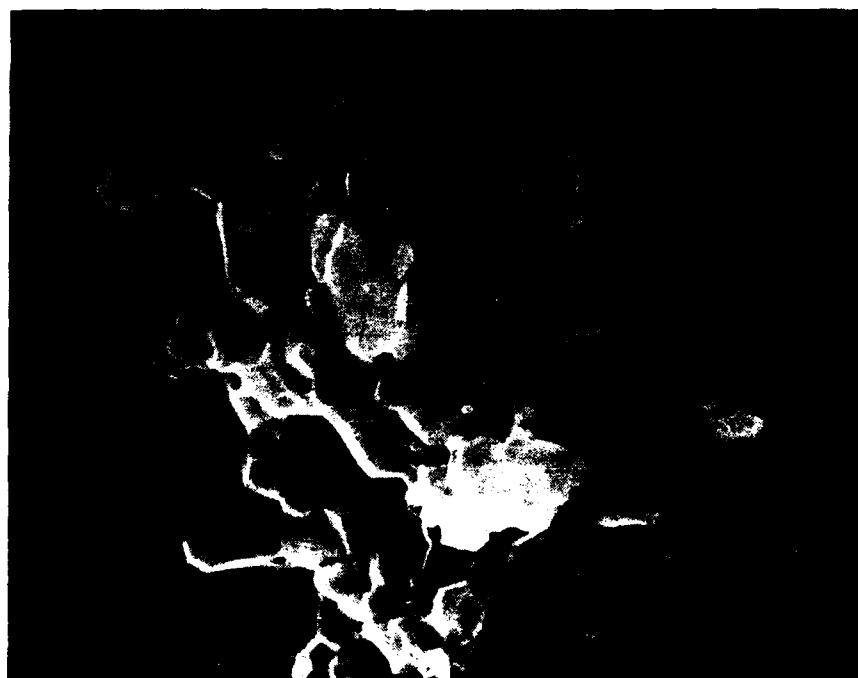
Ce–TZP+15^V/o Al$_2$O$_3$

$10\mu m$

(d)

Figure 4 (continued). (c) Ce-TZP and (d) Ce-TZP/15 vol. % Al$_2$O$_3$ at higher magnification.

14

Ce−TZP+15^V/o Al$_2$O$_3$+2^W/o SrZrO$_3$ $\overline{\quad 5\mu m \quad}$

(e)

Ce−TZP+15^V/o Al$_2$O$_3$+4^W/o SrZrO$_3$ $\overline{\quad 5\mu m \quad}$

(f)

Figure 4 (continued). Ce-TZP/15 vol. % Al$_2$O$_3$ with (e) 2.0 and (f) 4.0 wt. % SrZrO$_3$. Note strontium aluminate platelet formation.

15

Ce—TZP+15^V/o Al$_2$O$_3$ +2^W/o SrZrO$_3$ 1μm

(g)

Figure 4 (continued).   (g) Ce-TZP/15·vol. % Al$_2$O$_3$ with 4.0 wt. % SrZrO$_3$. Platelet shape of strontium aluminate is clearly evident.

The addition of Al$_2$O$_3$ to Ce-TZP increased the hardness and strength, but decreased the fracture toughness (ZrO$_2$(12 mol. % CeO$_2$ had a density of 6.21 g/cc, strength of 388+17 MPa, fracture toughness of 12.6+1.1 MPa·m$^{1/2}$, and hardness of 9.5+0.2 GPa) in agreement with the work of Tsukuma and Takahata[16]. The value of SrZrO$_3$ additions were that fracture toughness was increased without decreasing strength significantly (see Figures 5 and 6). By adding SrO to Ce-TZP/Al$_2$O$_3$ it is therefore possible to have the toughness of Ce-TZP and the strength and hardness of Ce-TZP/Al$_2$O$_3$ compositions.

The amount of monoclinic ZrO$_2$ on fracture surfaces increased from 67% for no SrZrO$_3$ to 73-75% for 0.5-4.0 wt. % SrZrO$_3$ additions, showing only a slight correlation of fracture toughness with the degree of transformation (see Figure 7). The amount of monoclinic ZrO$_2$ on ground surfaces was 5.4, 11.7, 12.3, 18.2, and 16.2% for 0.0, 0.5, 1.0, 2.0 and 4.0 wt. % SrZrO$_3$ additions, respectively, showing a much stronger correlation with fracture toughness than the % monoclinic on fracture surfaces.

Since the amount of monoclinic on Ce-TZP fracture surfaces was measured as 83% and its toughness is comparable or less than that of Ce-TZP/Al$_2$O$_3$ composites with strontium aluminate platelets, one can look for toughening mechanisms in addition to t--->m ZrO$_2$ transformation. Figure 2(g) suggests that both crack branching and crack bridging are contributing, although more
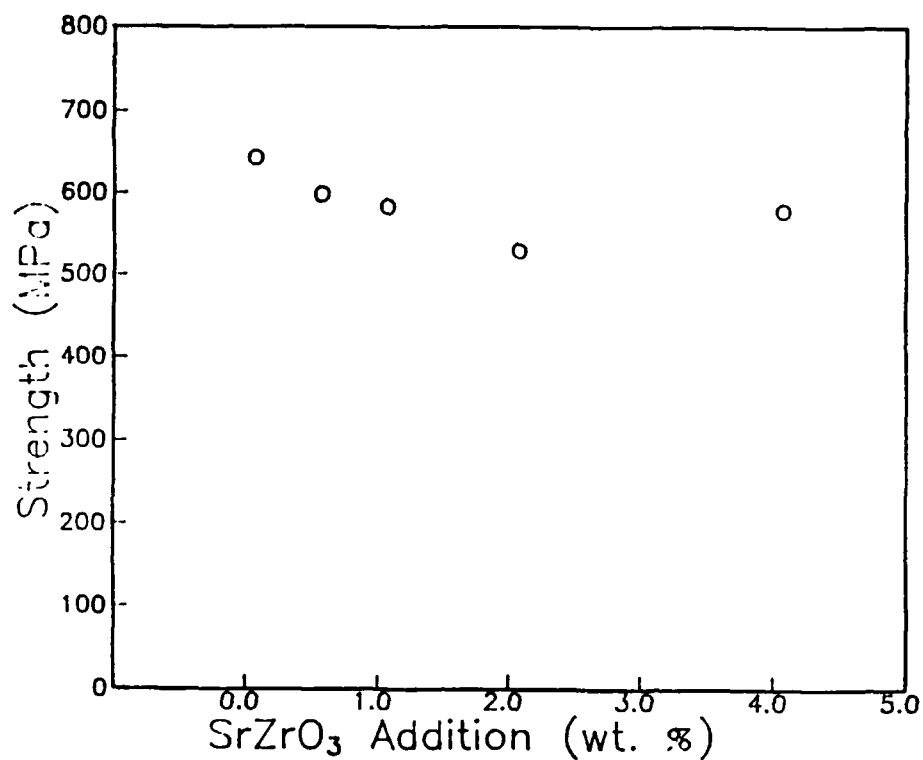
16

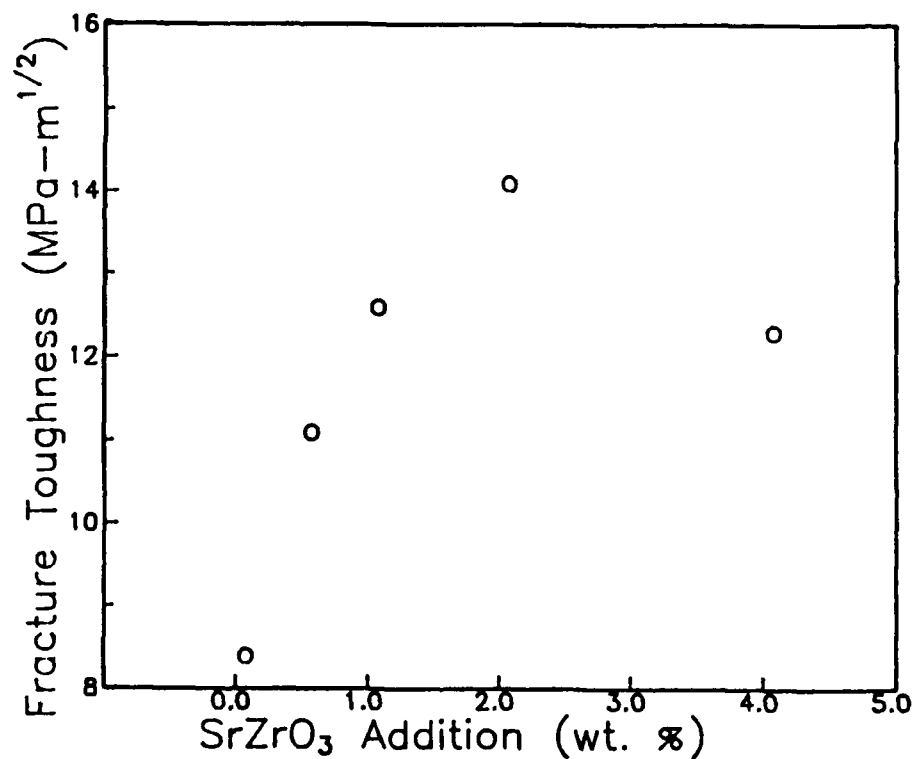Figure 5. Strength of Ce-TZP/15 vol. % Al_2O_3 compositions as a function of $SrZrO_3$ content added to the starting powder.

Figure 6. DCB fracture toughness of Ce-TZP/15 vol. % Al_2O_3 compositions as a function of $SrZrO_3$ content added to the starting powder.
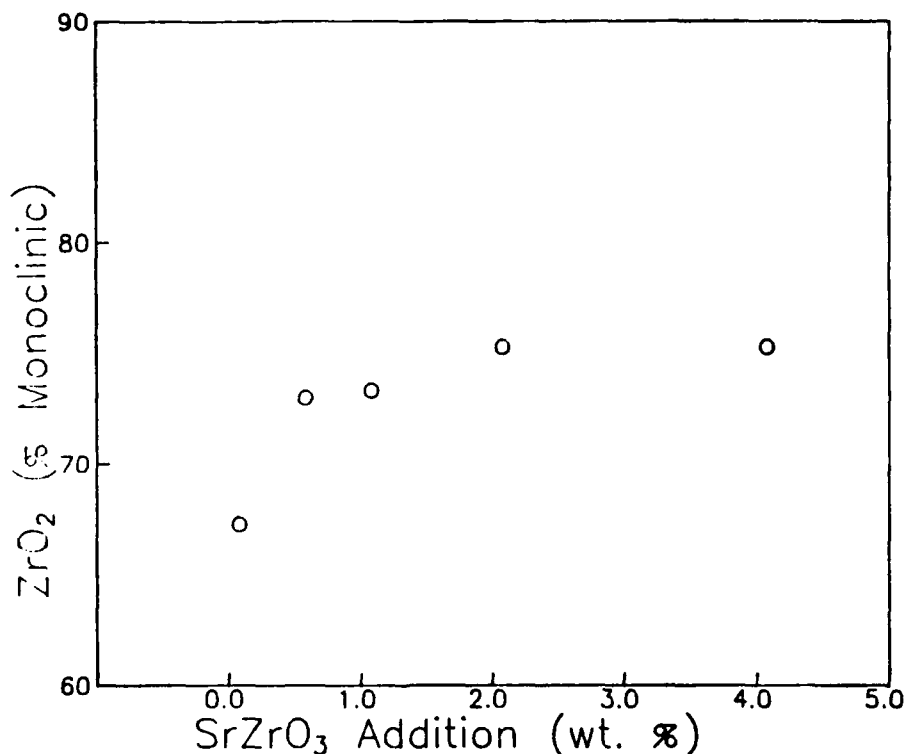
17

90

80

ZrO_2 (% Monoclinic)

70

60

0.0   1.0   2.0   3.0   4.0   5.0

$SrZrO_3$ Addition (wt. %)

Figure 7. Percent monoclinic ZrO_2 (based on total ZrO_2 content) on fracture surfaces of Ce-TZP/15 vol. % Al_2O_3 compositions as a function of $SrZrO_3$ content added to the starting powder.

detailed work is needed in order to explore crack-platelet interactions. As previously stated, it is also possible that ferroelastic toughening is operative, although such characterizations are more easily performed on materials which do not show a large degree of transformation.

Ce-TZP/15 vol. % Al_2O_3 with 2 wt. % $SrZrO_3$ sintered at 1550°C instead of 1500°C had similar strength (519$\pm$20 MPa) but much higher toughness (19.2$\pm$2.8 MPa·m$^{1/2}$). Acoustic noise and permanent deformation characteristic of transformation was noted during room temperature strength testing. The sintering temperature will affect the ZrO_2 size and therefore the degree of transformation. In order to optimize the toughening due to crack bridging, one should promote weak bonding between platelets and the matrix and control the distribution and size of the platelets. The platelets are approximately 0.5 μm in width and 5-10 μm in breadth. Further work is needed to determine the chemistry and interfacial characteristics of the platelets.

In order to determine how $SrZrO_3$ additions affect the fracture toughness of Ce-TZP, compositions were made as before, except without Al_2O_3. ZrO_2 and CeO_2 powders were milled together due to a limited supply of coprecipitated Ce-TZP. It will be shown below that this same approach results in similar properties to those discussed above for Ce-TZP/Al_2O_3 ceramics. Mechanical property data, as presented in Table 3 for Ce-TZP/15

18

vol. % Al_2O_3 compositions, are give in Table 4 for Ce-TZP compositions. Polished cross-sections showed no evidence of second phase formation. This is consistent with aluminate platelet formation in the case of Ce-TZP/Al_2O_3 compositions. Since no platelets were formed in Ce-TZP with SrO added, one would expect no problem sintering high $SrZrO_3$ additions, consistent with the experimental data (see Figure 8). The strength (see Figure 9)increases significantly with 0.5 and 1.0 wt. % $SrZrO_3$ additions, as does the hardness. Conversely, the DCB fracture toughness decreases dramatically with increasing $SrZrO_3$ content, as shown in Figure 10. The amount of monoclinic ZrO_2 on fracture surfaces was measured as 90.1, 88.5, 74.3 and 76% for 0.0, 0.5, 1.0 and 4.0 wt. % $SrZrO_3$ additions, respectively. The amount of monoclinic ZrO_2 does not correlate with fracture toughness when comparing Ce-TZP ($SrZrO_3$ doped) with Ce-TZP/15 vol. % Al_2O_3 ($SrZrO_3$ doped) since both types of materials have similar % monoclinic ($\approx$75%) but fracture toughness is lower in Ce-TZP by a factor of at least 2 (compare Tables 3 and 4). These data also suggest that the lower CeO_2 contents with increasing $SrZrO_3$ additions do not promote higher toughness.

The major factor which could be found to influence the properties of Ce-TZP doped with $SrZrO_3$ was grain size. The addition of $SrZrO_3$ affects grain size, as grain refinement is obvious with as little as 0.5 wt. % $SrZrO_3$ (see Figure 11). The grain size did not change appreciably with $SrZrO_3$ additions between 1 and 4 wt. %. The decreasing grain size with small additions of $SrZrO_3$ suggests that all of the SrO is not going into solution with the Ce-TZP matrix, although this was not detected by SEM microscopy. If the SrO additions limit grain growth, then hardness would be expected to increase. Strength would also increase if the critical flaw size, such as agglomerate size, is controlled by the grain size. The grain size also has a strong effect on the degree of transformation, with smaller grain sizes transforming less readily than larger grains.

Figure 12 shows a comparison of the degree of transformation in Ce-TZP and Ce-TZP with $SrZrO_3$. Without a second phase, transformation in Ce-TZP is unrestrained and large transformation bands are formed under stress (i.e., in region of indent (Fig.

Table 4
Ce-TZP Containing Small Additions of SrO

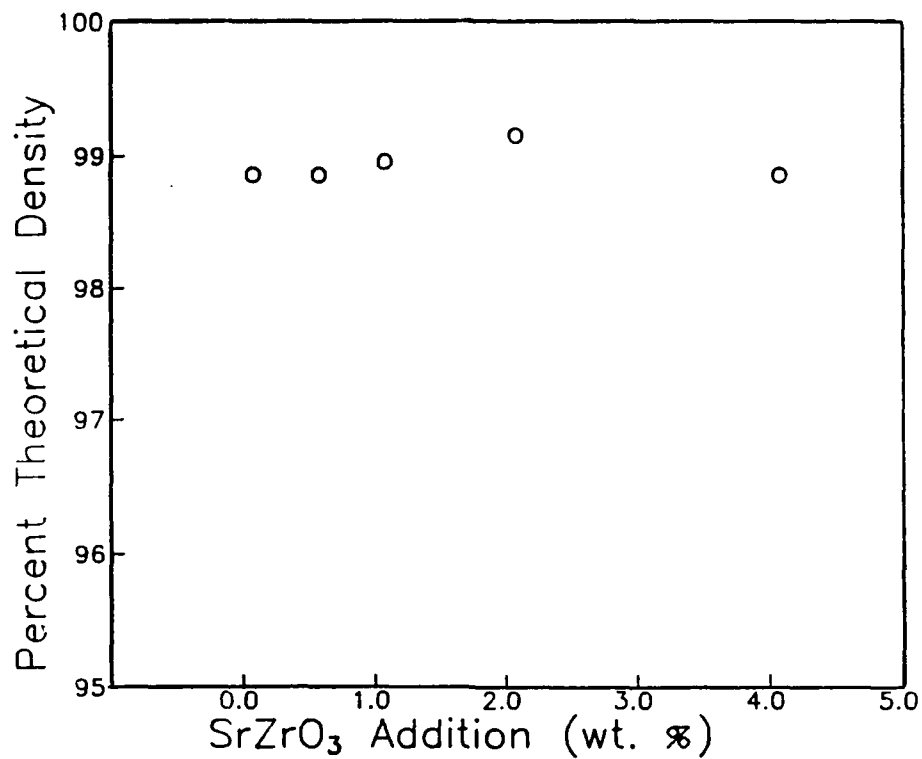| $SrZrO_3$ (wt. %)	Density (g/cc)	%T.D.	σ_f (MPa)			K_{IC} (MPa·m$^{1/2}$)		H (GPa)	
			#	x	s	x	s	x	s
0.0	6.21	98.8	10	172	7	13.3	0.6	7.7	0.1
0.5	6.21	98.8	9	264	8	10.1	0.6	not measured	
1.0	6.21	98.8	13	388	31	5.8	0.2	9.5	0.2
2.0	6.22	99.1	9	389	13	5.8	0.2	not measured	
4.0	6.20	98.8	11	392	23	5.8	0.2	9.9	0.2

Figure 8. Density of Ce-TZP as a function of $SrZrO_3$ content added to the starting powder.
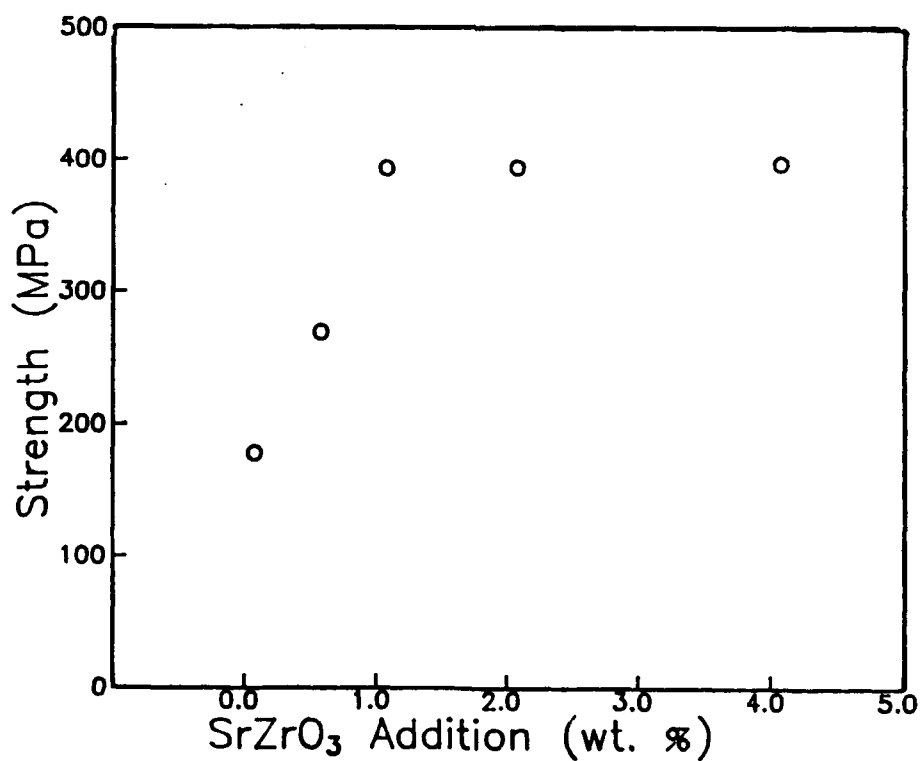

Figure 9. Strength of Ce-TZP as a function of $SrZrO_3$ content added to the starting powder.
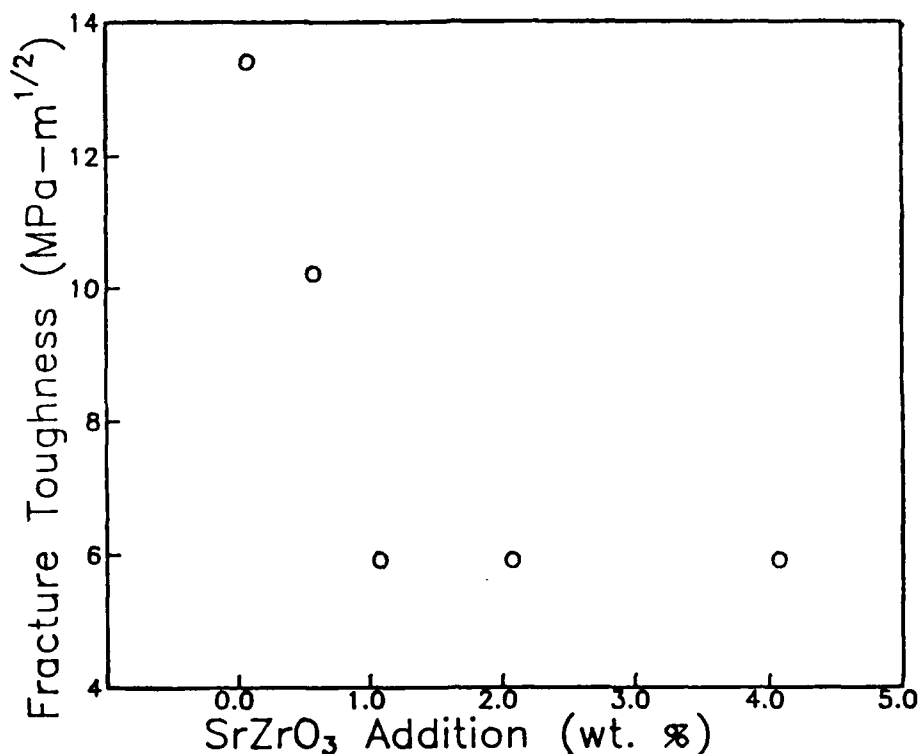
20

Figure 10.   DCB fracture toughness of Ce-TZP as a function of
             SrZrO₃ content added to the starting powder.

12(a,b))) and extend beyond the indentation cracks (Fig. 12(c)).
Increasing SrZrO₃ additions limit the degree of transformation
(Fig. 12(d-f)), but transformation is still much more prevalent
than in Ce-TZP containing strontium aluminate platelets, as will
be shown below.

These data give strong evidence that strontium aluminate
platelets allow increased toughness since SrO additions to Ce-TZP
lead to a decrease in toughness.   The strength and hardness of
Ce-TZP/Al₂O₃ compositions containing strontium aluminate
precipitates are also superior to those of Ce-TZP ceramics, with
or without SrZrO₃ additions.

The fact that strontium aluminate platelets form in-situ
suggests that SrO, not SrZrO₃, is the important constituent and
that strontium can be added as an oxide, carbonate, nitrate, etc.
and achieve a similar effect.   Since the aluminates form in-situ,
higher platelet loadings should be possible than if SrO·6Al₂O₃
platelets were first synthesized and then the composite was
sintered.   Depending on sintering parameters (i.e., rate of
heating, sintering temperature, etc.) it should also be possible
to form higher contents of strontium aluminate platelets in the
matrix.   Consequently, both Ce-TZP/30 vol. % Al₂O₃ and Al₂O₃/40
vol. % Ce-TZP where made with SrZrO₃, keeping the SrO/Al₂O₃ molar
ratio similar to those used in the Ce-TZP/15 vol. % Al₂O₃
composites discussed above.

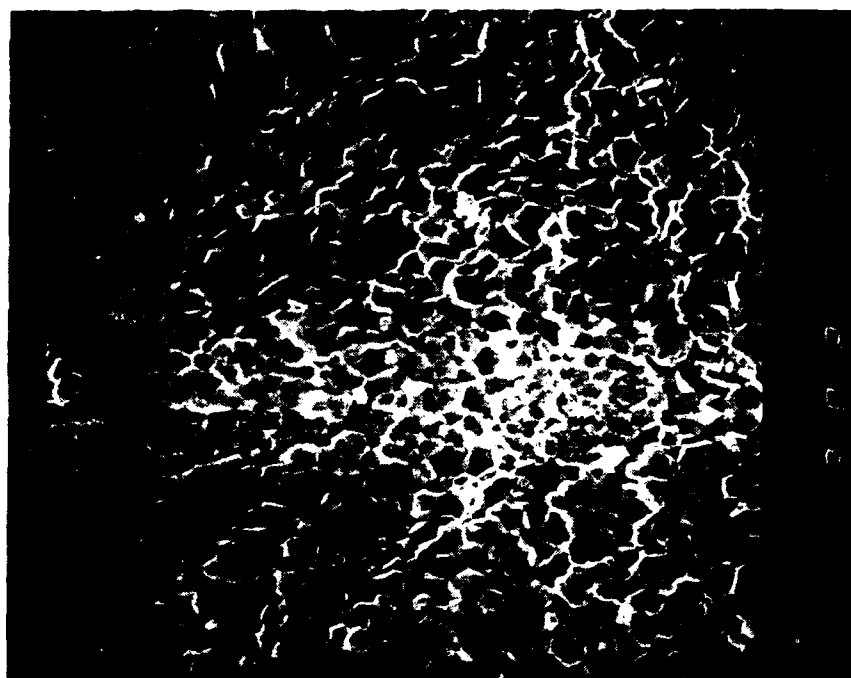21
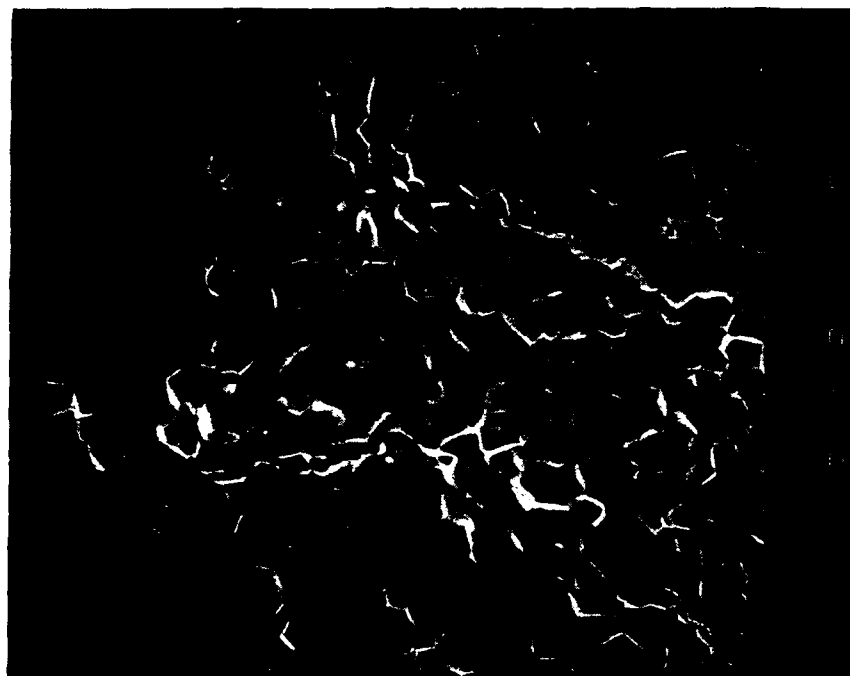
Ce–TZP   10μm

(a)

Ce–TZP+0.5 ^{W}/o SrZrO$_3$ 10μm

(b)

Figure 11.   SEM micrographs of fracture surfaces of Ce-TZP
             with and without SrZrO$_3$ additions. (a) Ce-TZP, (b)
             Ce-TZP with 0.5 wt. % SrZrO$_3$. Note decrease in grain
             size with SrZrO$_3$ addition.
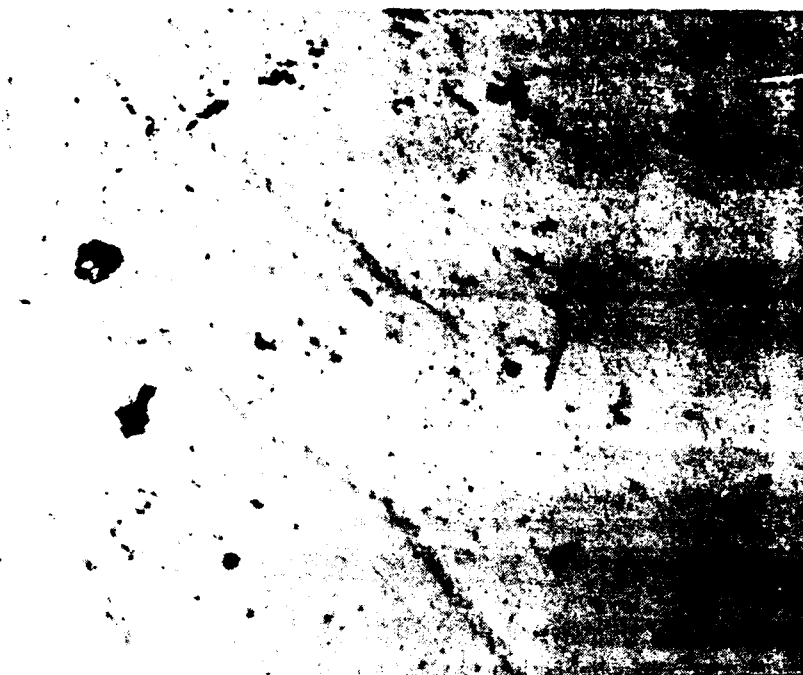
22

Ce-TZP+1.0 ^{W}/o SrZrO$_3$ $\overline{10\mu m}$

(c)

Ce-TZP+4.0 ^{W}/o SrZrO$_3$ $\overline{10\mu m}$

(d)

Figure 11 (continued).   Ce-TZP with (c) 1.0 and (d) 4.0 wt. % SrZrO$_3$. Compare with Fig. 11(a,b).

23

Ce–TZP $\overline{100\mu m}$

(a)

Ce–TZP $\overline{100\mu m}$

(b)

Figure 12.   Nomarski optical micrographs of polished surfaces of Ce-TZP, with and without $SrZrO_3$ additions, near Vickers hardness indentations. (a,b) Ce-TZP showing transformation bands extending from indentation.

24

Ce–TZP $\overline{100\mu m}$

(c)

Ce–TZP+0.5 ^{W}/o SrZrO$_3$ $\overline{100\mu m}$

(d)
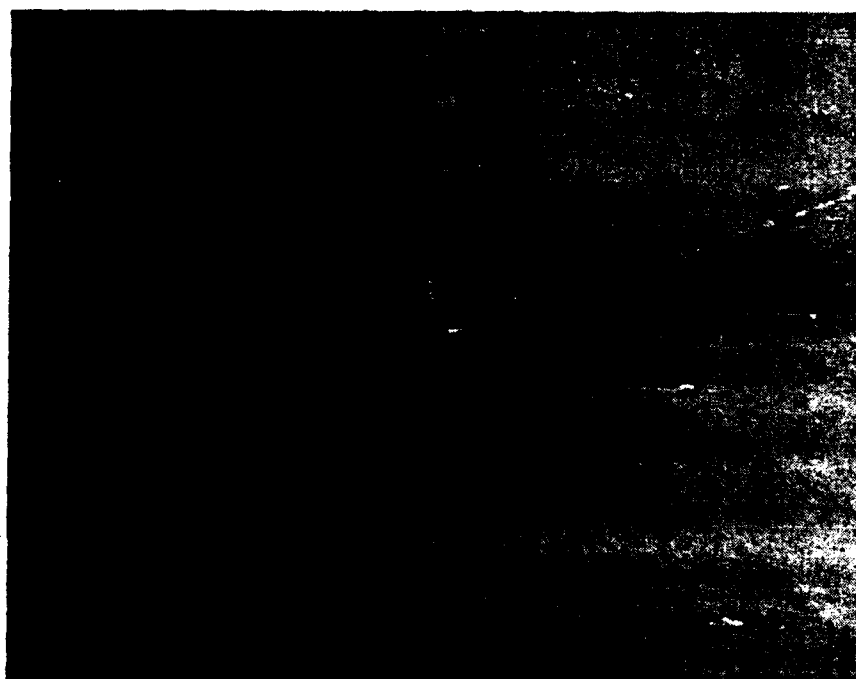
Figure 12 (continued).   (c) Ce-TZP showing bands extending
                          beyond indentation crack, (d) Ce-TZP
                          with 0.5 wt. % SrZrO$_3$.

25

Ce–TZP+1.0 W/o SrZrO$_3$ $\overline{100\mu m}$

(e)

Ce–TZP+4.0 W/o SrZrO$_3$ $\overline{100\mu m}$

(f)

Figure 12 (continued).   Ce-TZP with (e) 1.0 and (f) 4.0 wt. %
   SrZrO$_3$. Compare with Fig. 12(a-d).

Table 5 shows density, strength, DCB fracture toughness and hardness values measured on sintered (1500°C for 2 hours) samples made from reactants containing Ce-TZP/30 vol. % Al_2O_3 with various amounts of $SrZrO_3$. ZrO_2 and CeO_2 powders were used instead of coprecipitated Ce-TZP in an identical manner to Ce-TZP compositions discussed above. The molar ratio of CeO_2 ranged between 12.0 mol. % for no $SrZrO_3$ addition to 11.3 mol. % for 8 wt. % $SrZrO_3$ addition. The trends were similar to those observed for sintered samples made from coprecipitated Ce-TZP powders with 15 vol. % Al_2O_3 and $SrZrO_3$ additions between 0 and 4 wt. %.

The density decreases with increasing $SrZrO_3$ content due to the formation of strontium aluminate platelets which impede densification. Sintering at 1550°C resulted in densities greater than 97% of theoretical for all compositions. The strength decreases at higher loadings of strontium aluminate due to the platelets acting as stress risers and the lower density of these compositions. Strengths were comparable or superior to those measured for corresponding compositions of Ce-TZP/15 vol. % Al_2O_3 (compare Tables 3 and 5) with the exception of the highest $SrZrO_3$ content. The main advantage of increased alumina in the starting composition is increased hardness, which was 2-3 GPa higher than the corresponding compositions in Table 3. Higher alumina content should also result in improved high temperature properties[15], although these measurements have not been made on compositions containing strontium aluminates.

High fracture toughness increased with increasing $SrZrO_3$ content up to 4 wt. % and then decreased (see Table 5). The fracture toughness of 15 MPa·m$^{1/2}$ measured for a 30 vol. % Al_2O_3 Ce-TZP composition is exceptional. A large degree of transformation toughening was evident on fracture surfaces, as the % monoclinic ZrO_2 increased from 42.1% with no $SrZrO_3$ to 85.7% with 4 wt. % $SrZrO_3$. These data suggest that the formation of strontium aluminate platelets allow easier transformation than is possible with an equiaxed microstructure. Nomarski interference contrast optical photographs (Figure 13) showed that the transformation zone was larger with $SrZrO_3$ additions to Ce-TZP/30 vol. % Al_2O_3 than for the alumina dispersed Ce-TZP. However, no transformation bands were observed and zone sizes

Table 5
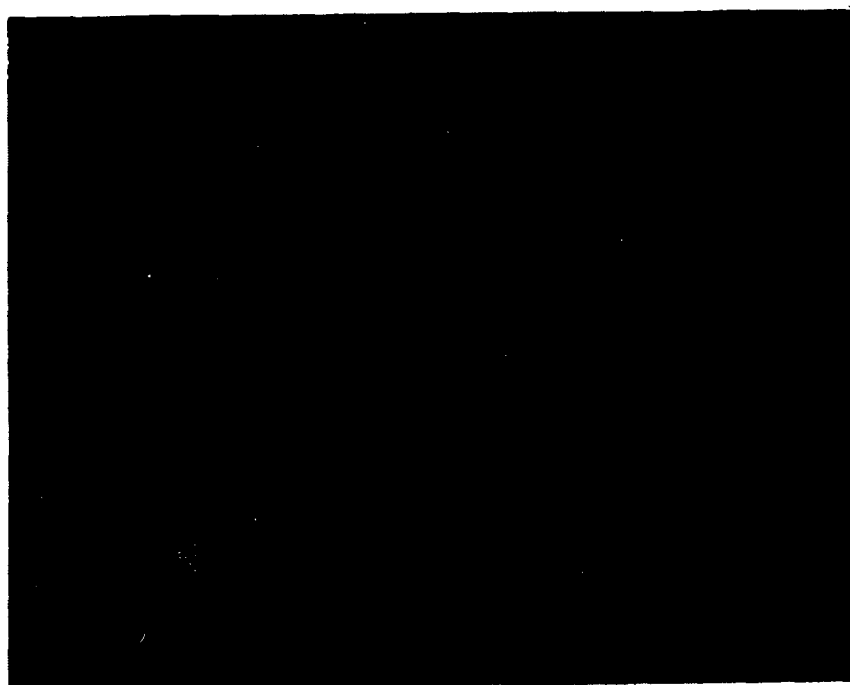Ce-TZP/30 vol. % Al_2O_3 Containing Additions of SrO

$SrZrO_3$ (wt. %)	Density (g/cc)	%T.D.	σ_f (MPa) #	x	s	K_{IC} (MPa·m$^{1/2}$) x	s	H (GPa) x	s
0.0	5.53	99.1	8	632	37	7.8	0.3	14.5	0.2
1.0	5.53	99.1	10	648	45	9.9	0.1	14.6	0.1
2.0	5.52	99.1	7	726	29	11.2	0.5	13.7	0.5
4.0	5.47	98.2	8	530	28	15.1	0.3	12.7	0.2
8.0	5.15	92.5	12	407	43	11.8	0.3	12.1	1.6

27
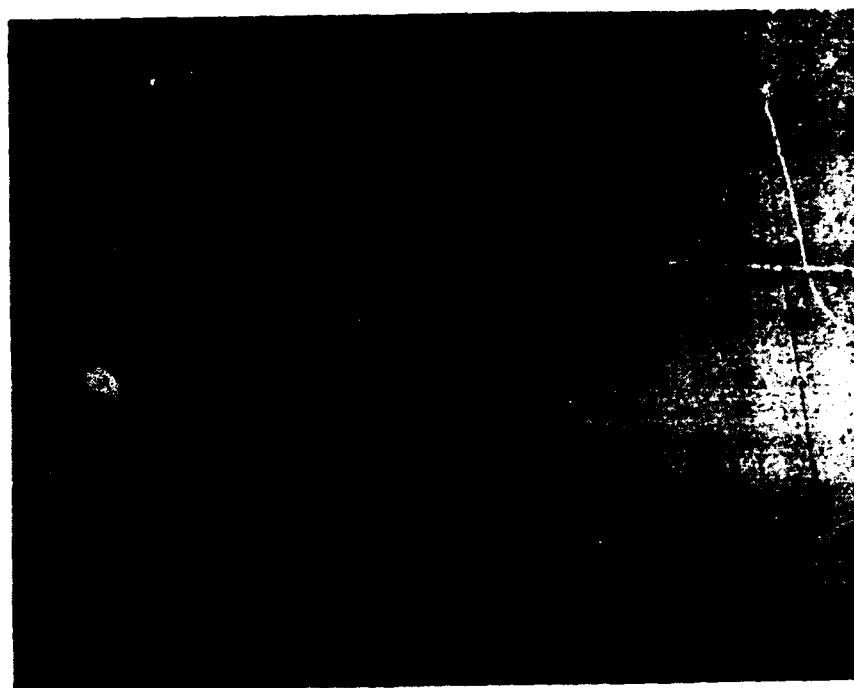
Ce–TZP+30^v/o Al$_2$O$_3$ $\overline{100\mu m}$

(a)

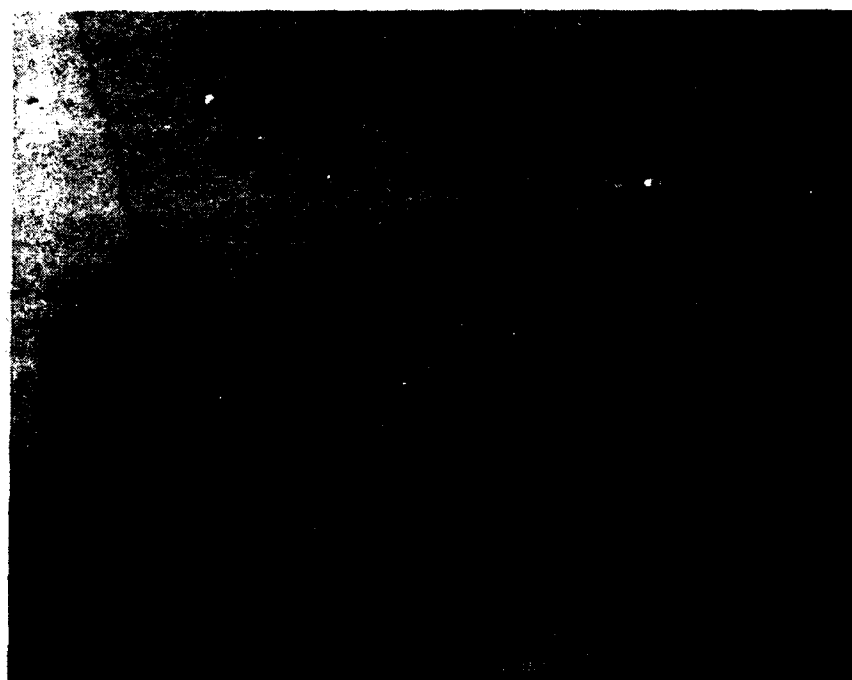Ce–TZP+30^v/o Al$_2$O$_3$ +1 ^{w}/o SrZrO$_3$ $\overline{100\mu m}$

(b)

Figure 13. Nomarski optical micrographs of polished surfaces of Ce-TZP/30 vol. % Al$_2$O$_3$, with and without SrZrO$_3$ additions, near Vickers hardness indentations. Ce-TZP with (a) no and (b) 1 wt. % SrZrO$_3$.

28

Ce-TZP+30^v/o Al$_2$O$_3$ +2^w/o SrZrO$_3$ $\overline{100\mu m}$

(c)

Ce-TZP+30^v/o Al$_2$O$_3$ +8^w/o SrZrO$_3$ $\overline{100\mu m}$

(d)

Figure 13 (continued).   Ce-TZP/30 vol. % Al$_2$O$_3$ showing bands
with (c) 2.0 and (d) 8.0 wt. % SrZrO$_3$.
Compare with Fig. 12 and Fig. 13 (a,b).

were smaller than in Ce-TZP compositions (compare Figures 12 and 13). Modulus measurements should be made for Ce-TZP with strontium aluminate platelets in comparison to the same matrix with dispersed alumina.

SEM micrographs of polished cross-sections and fracture surfaces clearly reveal strontium aluminate platelet formation (see Figure 14). X-ray diffraction showed peaks corresponding to hexagonal $SrO \cdot 6Al_2O_3$.

Table 6 lists properties of sintered bars made from starting compositions consisting of Al_2O_3/ZrO_2(12 mol. % CeO_2) with $SrZrO_3$ ranging between 0 and 16 wt. %. The CeO_2 content was kept constant at 12 mol. % by adding extra CeO_2 to starting compositions which were made without coprecipitated Ce-TZP. A sintering temperature of 1600°C was required to densify these materials, with compositions containing less than 8 wt. % $SrZrO_3$ obtaining densities greater than 98% of theoretical. Strength, hardness and toughness did not improve as compared to Ce-TZP/30 vol. % compositions. The important point, however, is that high toughness (14 MPa·m$^{1/2}$) was achieved in one composition containing a high alumina content. Figure 15 shows that high platelet loadings were achieved in-situ during sintering.

Figure 16 compares the fracture toughness of all three alumina concentrations based on their SrO/Al_2O_3 molar ratio. It appears that keeping the CeO_2 content constant at 12 mol. % (60 vol. % Al_2O_3 starting compositions) shifts the peak toughness to a lower SrO/Al_2O_3 ratio. The fact that peak toughness occurs over the same SrO/Al_2O_3 range for all three alumina contents gives strong support for toughening due to strontium aluminate platelet formation. The data in Figure 16 also indicate that the SrO/Al_2O_3 range over which high toughness occurs narrows with increasing alumina content. It is noteworthy that the peak toughness does not change significantly, despite the fact that the amount of ZrO_2 deceases by a factor of four, further evidence that mechanisms in addition to transformation toughening are operative in these compositions.

Creep testing was performed in air on Ce-TZP/30 vol. % Al_2O_3 containing 2 wt. % $SrZrO_3$ in comparison to Y-TZP (ZrO_2(3 mol. % Y_2O_3)) at 1200°C and stress levels ranging between 11 and 84 MPa (see Figure 17). The creep resistance of the platelet containing

Table 6
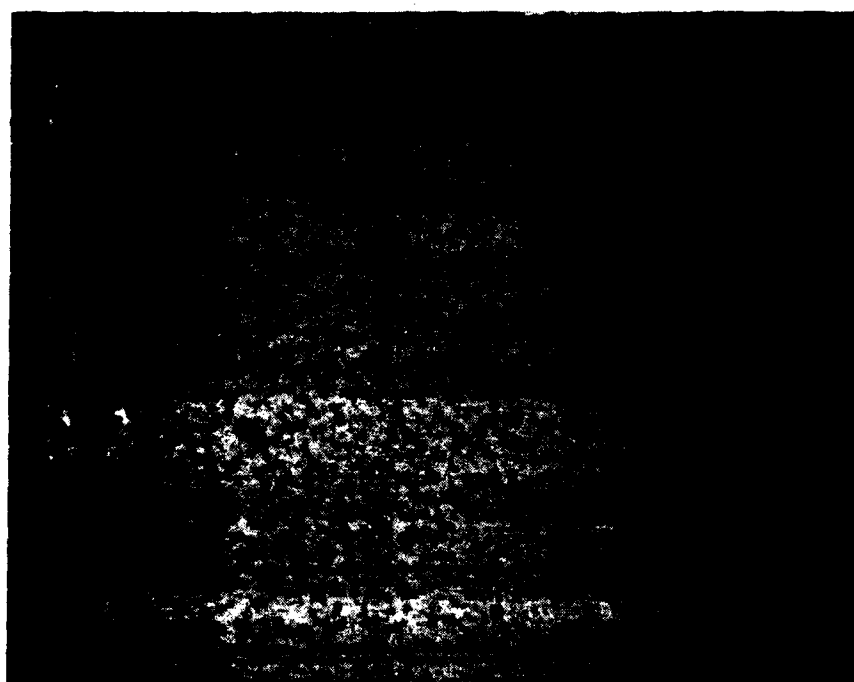Al_2O_3/40 vol. % ZrO_2(12 mol. % CeO_2) Containing Additions of SrO

SrZrO3 (wt. %)	Density (g/cc)	%T.D.	σ_f (MPa)	K_{IC} (MPa·m$^{1/2}$) X	s	H (GPa) X	s
0.0	4.78	97.8	612	7.5	0.2	13.1	0.2
2.0	4.83	98.6	650	7.8	0.2	14.6	0.2
4.0	4.81	98.0	524	14.0	0.8	13.6	0.2
8.0	4.71	95.6	464	8.4	0.9	11.7	0.2
16.0	4.40	88.4	309	6.1	0.1	8.1	0.2

30
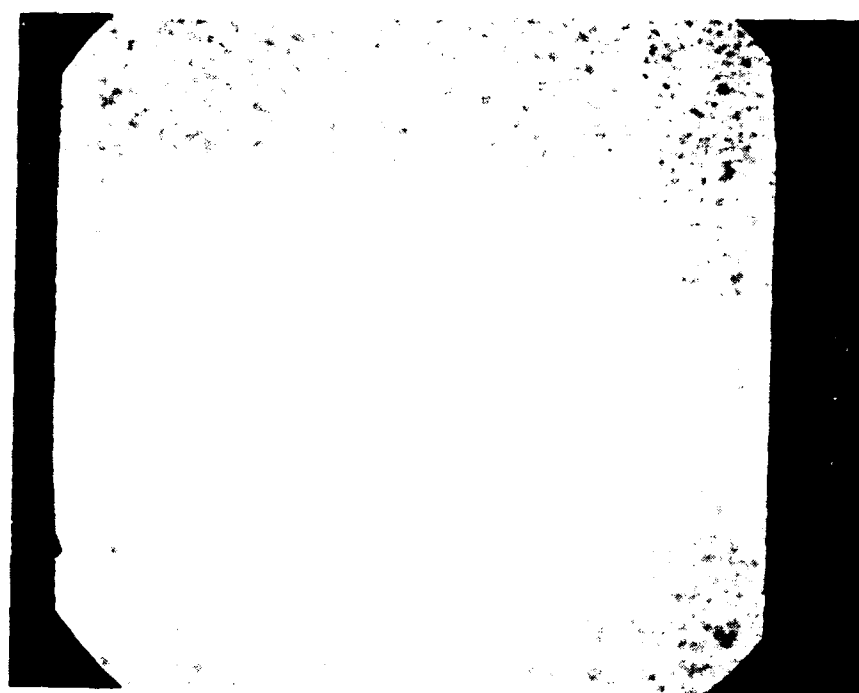
Ce—TZP+30^v/o Al$_2$O$_3$ $\overline{10\mu m}$

(a)

Ce—TZP+30^v/o Al$_2$O$_3$ +1 ^{w}/o SrZrO$_3$ $\overline{10\mu m}$
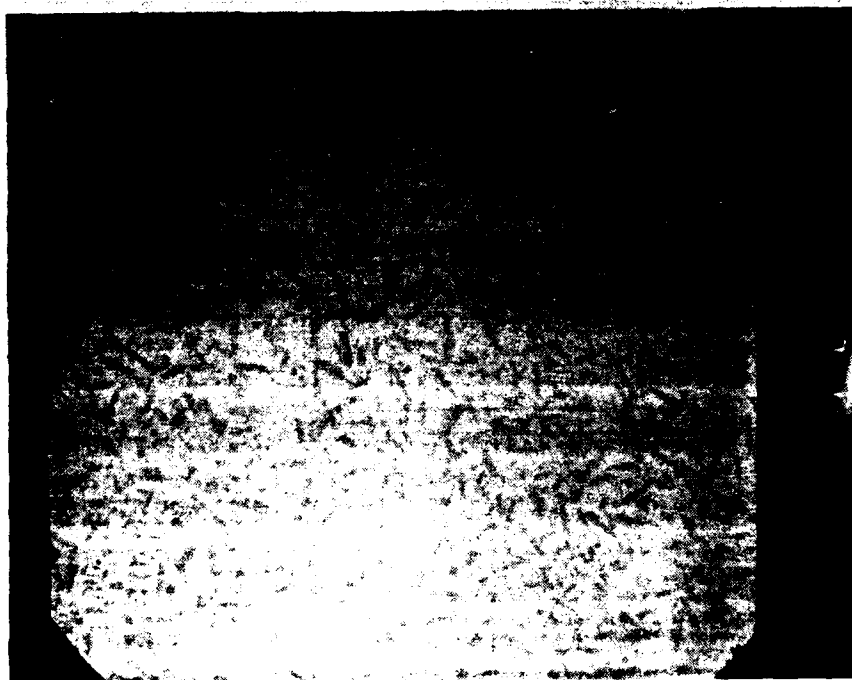
(b)

Figure 14.   SEM micrographs of Ce-TZP/30 vol. % Al$_2$O$_3$, with
increasing SrZrO$_3$ additions.   Ce-TZP with (a) no and
(b) 1 wt. % SrZrO$_3$.
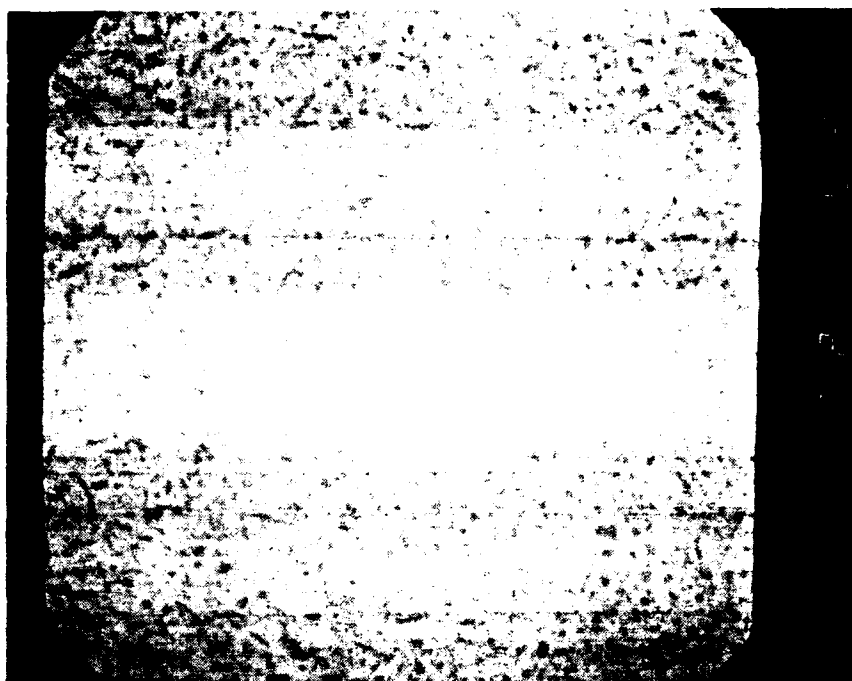
Ce–TZP+30^V/o Al$_2$O$_3$+2^W/o SrZrO$_3$ 10μm

(c)

Ce–TZP+30^V/o Al$_2$O$_3$+4^W/o SrZrO$_3$ 10μm

(d)

Figure 14 (continued).   Ce-TZP/30 vol. % Al$_2$O$_3$ with (c) 2.0 and (d) 4.0 wt. % SrZrO$_3$.

Ce–TZP+30^{V}/o Al$_2$O$_3$ +8^{W}/o SrZrO$_3$ 10μm

(e)

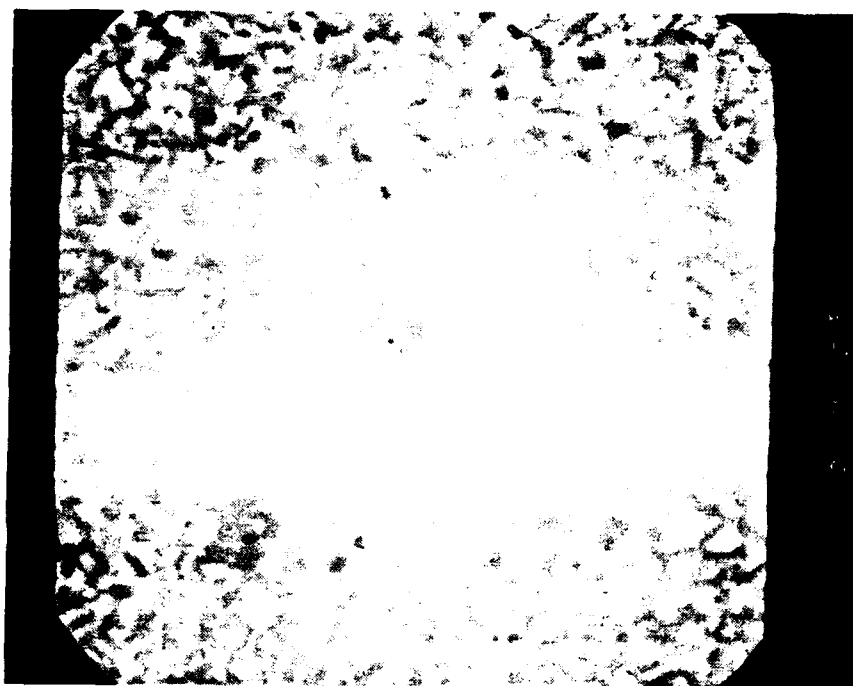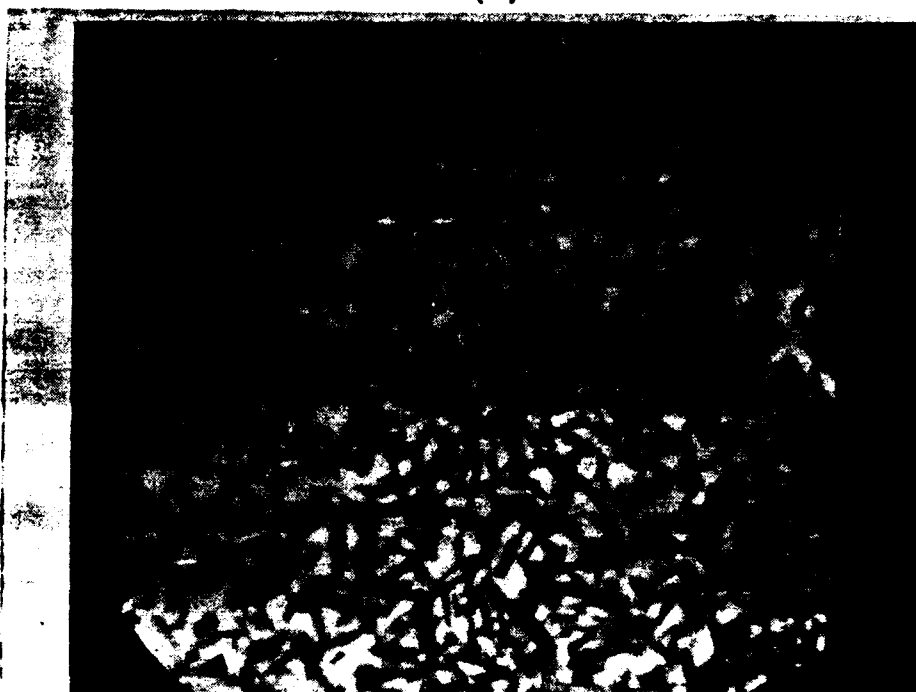Ce–TZP+30^{V}/o Al$_2$O$_3$+8^{W}/o SrZrO$_3$ 5μm
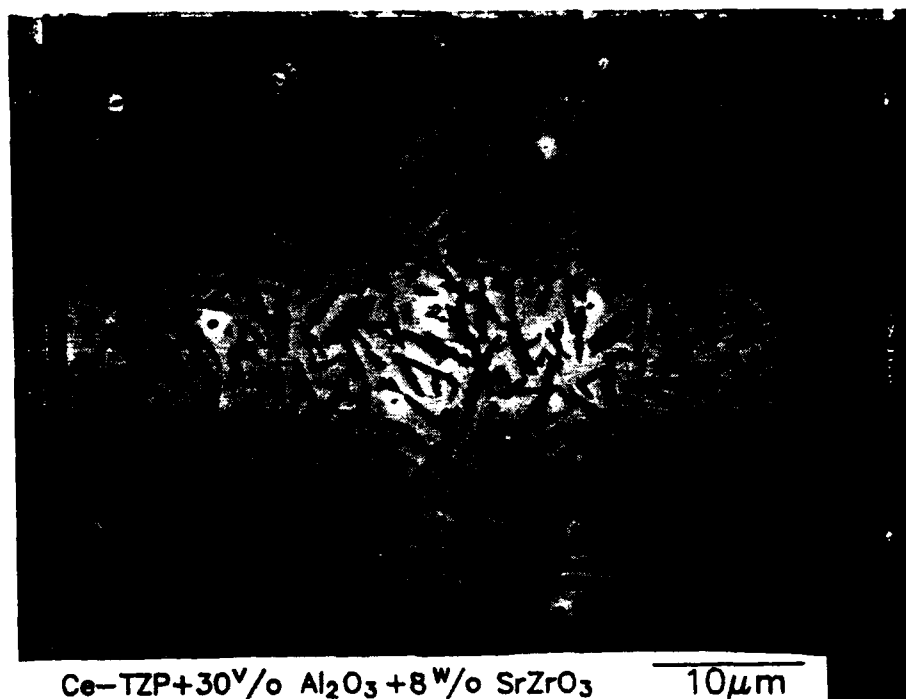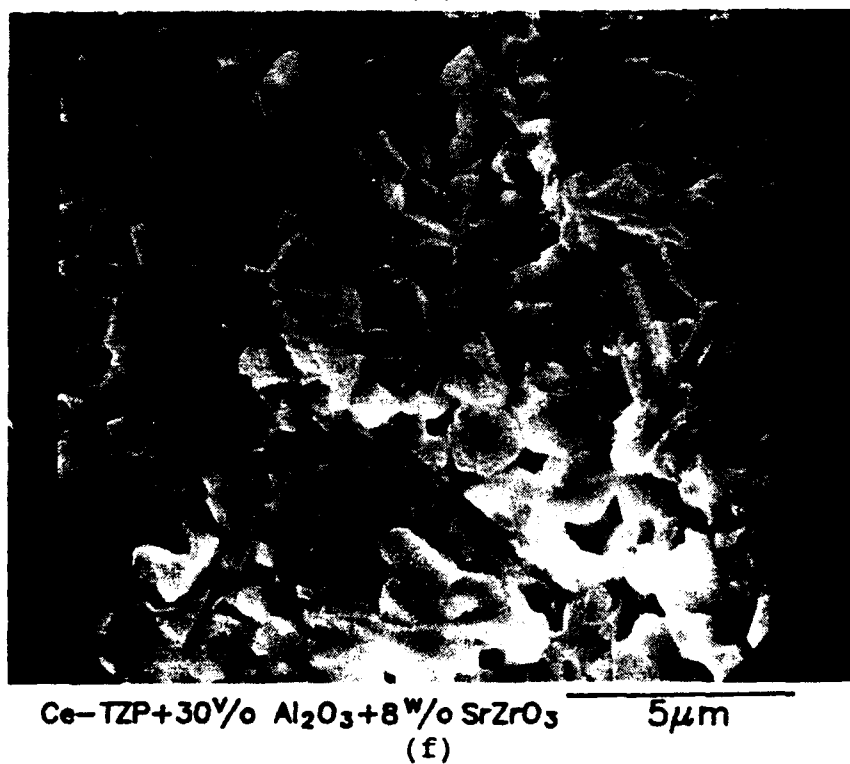
(f)

Figure 14 (continued).   Ce-TZP/30 vol. % Al$_2$O$_3$ with 8.0 wt. % SrZrO$_3$. (a) Polished cross-section, (b) fracture surface.

33

Al$_2$O$_3$+40 ^{V}/o Ce–TZP+8 ^{W}/o SrZrO$_3$ ⎯⎯ 10μm

(a)

Al$_2$O$_3$+40 ^{V}/o Ce–TZP+16 ^{W}/o SrZrO$_3$ ⎯⎯ 10μm

(b)

Figure 15.   SEM micrographs of polished surfaces of Al$_2$O$_3$/40 vol. % ZrO$_2$(12 mol. % CeO$_2$ with (a) 8 and (b) 16 wt. % SrZrO$_3$ added to starting powders. Note strontium aluminate platelet formation.

34

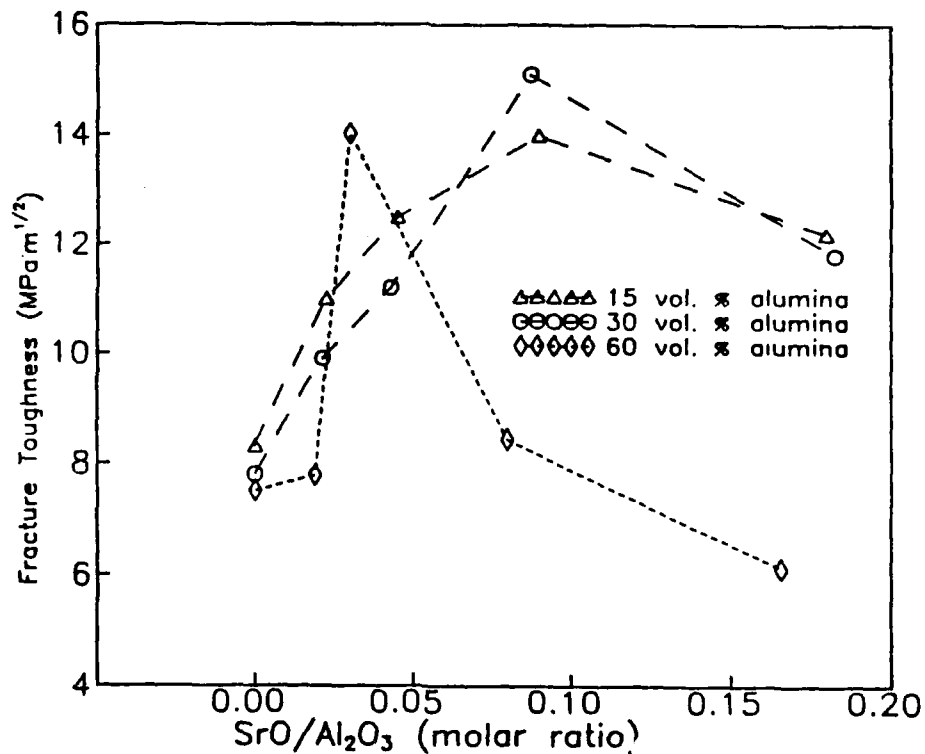Figure 16.   Fracture toughness of Ce-TZP with 15 (triangles), 30
              (circles) and 60 (diamonds) volume percent alumina in
              the starting Ce-TZP composition, as a function of
              SrO/Al_2O_3 molar ratio.
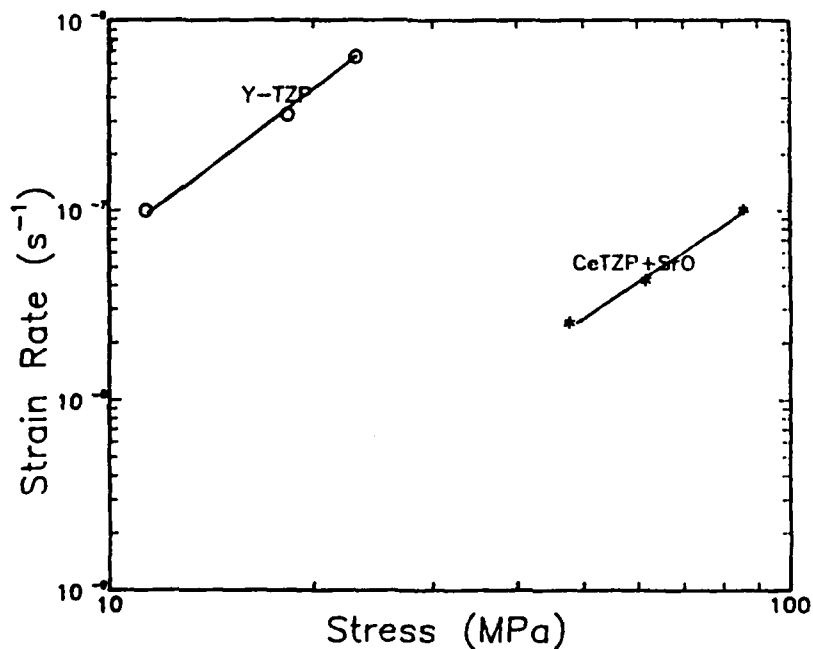

Figure 17.   Creep of ZrO_2(3 mol. % Y_2O_3) (circles) and Ce-TZP/30
              vol. % Al_2O_3 containing 2 wt. % $SrZrO_3$ (stars) in air
   at 1200°C.

Ce-TZP composition is two orders of magnitude higher than the Y-TZP. While this is encouraging, the comparisons which should be made are between Ce-TZP, Ce-TZP/Al_2O_3, and Ce-TZP/Al_2O_3 compositions with high strontium aluminate platelet loadings. The finer grain size of the Y-TZP may be the reason for the high creep rate in this material. Stress exponents in both materials were approximately 2.4.

While this investigation into the role of dopants did not shed further light on ferroelastic toughening, it does show that alternate mechanisms are operative with small amounts of dopants. Work is needed to determine the degree of toughening in Al_2O_3 due to in-situ strontium aluminate formation. Transmission electron microscopy should be used to look at the degree of bonding between platelets and matrix. High temperature properties need to be investigated.

Non-transformable ZrO_2

Based on the work at the University of Utah in retaining high toughness in yttria-doped single crystals at high temperatures (see Part II) ZrO_2(3 mol. % Y_2O_3) coprecipitated powders were sintered at 1500°C for two hours. These polycrystalline Y-TZP materials had a density of 6.02 g/cc after sintering, bend strength of 727 MPa, hardness of 13.0$\pm$0.3 GPa and fracture toughness of approximately 5 MPa·m$^{1/2}$. The grain size was approximately 0.5 μm and 26% monoclinic ZrO_2 was detected on the fracture surface. Upon heating rapidly in a reducing environment to 1900°C, holding 5 minutes and cooling rapidly (50°C/minute), the density increased to 6.11 g/cc. The strength at room temperature was 648, the fracture toughness was 5.5 MPa·m$^{1/2}$ and the hardness remained nearly constant (12.8$\pm$0.2 GPa), despite an increase in grain size by approximately one order in magnitude. Heat treating at 1950°C for 5 minutes resulted in material with similar strength (650 MPa), hardness (12.9$\pm$0.2 GPa), grain size less than 10 μm and 3.4% monoclinic ZrO_2 on fracture surfaces. The x-ray diffraction pattern showed a mixture of t and t' ZrO_2. At temperatures above 2000°C, only t' ZrO_2 was observed and no monoclinic ZrO_2 was noted on fracture surfaces. While the strength at 2000°C dropped to 548 MPa, due to increasing grain size, the hardness remained constant at 12.7$\pm$0.3 GPa, indicating that the size of domains, not grain size, controls hardness in this material. Upon heating treating at 2050°C, the density remained high (6.09 g/cc), and the strength and hardness remained constant at 552 MPa and 12.8 GPa, respectively. The grain size was generally less than 100 μm and mixed mode fracture was observed, as shown in Figure 18(b).

Bars heat treated at 1950°C were sent to Professor A. G. Evans of University of California for strength testing at 1000°C in an inert atmosphere furnace. Work is planned to look at domain size using TEM and to control oxidation of heat treated samples so that high temperature testing can occur in oxidizing atmospheres. ZrO_2 (2.5 mol. % Y_2O_3) will be used to avoid elevated temperature phase separation.

36

Y-TZP $\overline{2\,\mu m}$

(a)
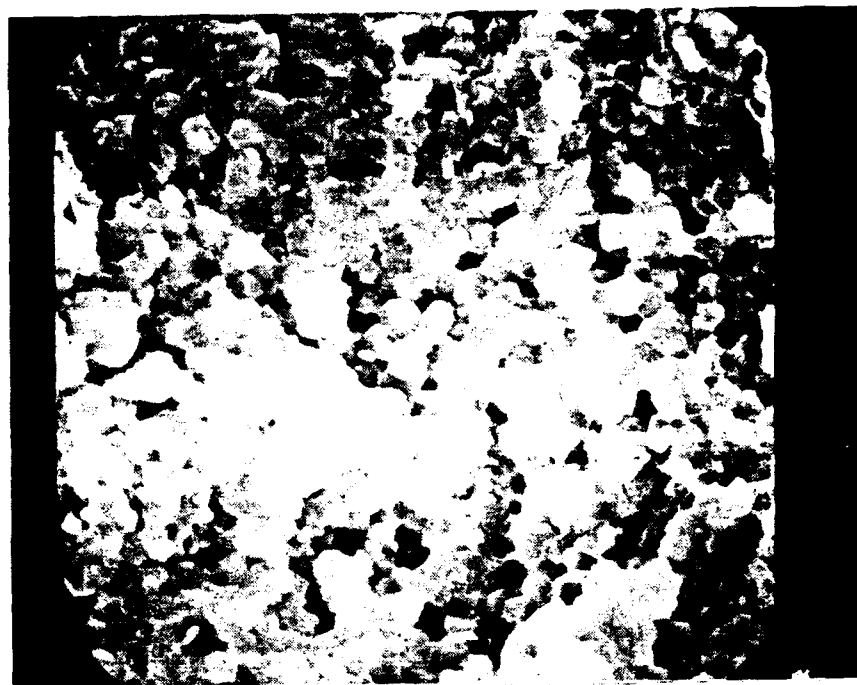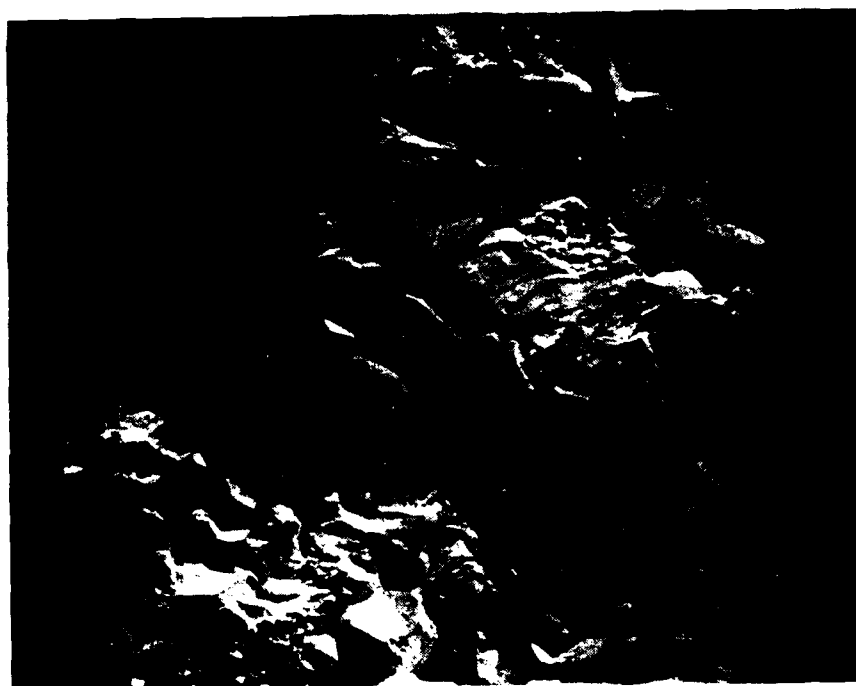
Y-TZP $\overline{100\mu m}$

(b)

Figure 18.   SEM micrographs of fracture surfaces of ZrO_2(3 mol. % Y_2O_3 sintered at 1500°C for two hours.   (a) No heat treatment, (b) Heat treated at 2050°C for 5 minutes.

37

Strontium Zirconate

$SrZrO_3$ has a density of 5.48 g/cc and is orthorhombic at room temperature. Upon heating, strontium zirconate becomes tetragonal at 700°C (c/a < 1), changes to another form of tetragonal (c/a > 1) above 830°C, and is cubic above ≈1200°C[10]. The melting point of $SrZrO_3$ is ≈2650°C. Carlsson[10] investigated the plastic behavior of $SrZrO_3$ by measuring compressive strength of $SrZrO_3$ and zirconates based on the substitution of Ca and Ba for Sr, which change lattice parameters and phase stability. He showed plastic deformation and associated nonlinearity in strength testing for orthorhombic and the first tetragonal structure (c/a < 1) but no plasticity for the second tetragonal structure (c/a > 1) and cubic $Sr_{0.1}Ba_{0.9}ZrO_3$. Although Carlsson did not explain his work based on ferroelasticity, he did discuss the effect of domain reorientation on plasticity.

Table 7 lists the strength and SENB fracture toughness of compositions based on the work of Carlsson[10]. Polycrystalline $SrZrO_3$, $Sr_{0.8}Ca_{0.2}ZrO_3$, $Sr_{0.8}Ba_{0.2}ZrO_3$, $Sr_{0.6}Ba_{0.4}ZrO_3$, and $Sr_{0.4}Ba_{0.6}ZrO_3$ ceramics were sintered at 1550°C for 2 hours with densities above 98.5% of theoretical. All of the compositions except for $Sr_{0.4}Ba_{0.6}ZrO_3$ are orthorhombic or tetragonal 1 (i.e., capable of ferroelastic switching). SENB fracture toughness was 25% higher for ferroelastic compositions than for the paraelastic composition, indicating that the ferroelastic toughening contribution is significant in this class of ceramics. Further work is needed to optimize strength and toughness in order for these materials to be attractive for structural applications. The use of high purity starting materials, rather than the commercially available zirconates used in the present study, is recommended for such optimization work.

Table 7
Zirconates Based on Work of Carlsson[10]

Composition	Density (g/cc)	Strength (MPa)	SENB K_{IC} (MPa·m$^{1/2}$)
$Sr_{0.8}Ca_{0.2}ZrO_3$	5.18	203±27	3.07±0.1
$SrZrO_3$	5.38	157±7	2.96±0.7
$Sr_{0.8}Ba_{0.2}ZrO_3$	5.51	131±7	3.14±0.1
$Sr_{0.6}Ba_{0.4}ZrO_3$	5.65	131±4	2.71±0.1
$Sr_{0.4}Ba_{0.6}ZrO_3$	5.80	135±9	2.36±0.1

REFERENCES

1. A. V. Virkar and R. L. K. Matsumoto, "Ferroelastic Domain Switching as a Toughening Mechanism in Tetragonal Zirconia," J. Am. Ceram. Soc., 69[10] C-224-C-226 (1986).

2. A. V. Virkar and R. L. K. Matsumoto, "Toughening Mechanism in Tetragonal Zirconia," to appear in Advances in Ceramics, Science and Technology of Zirconia III. Ed. by N. Claussen, M. Rühle and A. H. Heuer. Am. Ceram. Soc., Columbus, OH. 1988.

3. R. C. Garvie, R. H. Hannink and R. T. Pascoe, "Ceramic Steel?," Nature (London), 258[5537] 703-704(1975).

4. Advances in Ceramics, Vol. 3, Science and Technology of Zirconia I. Ed. by A. H. Heuer and L. W. Hobbs. Am. Ceram. Soc., Columbus, OH, 1981.

5. Advances in Ceramics, Vol. 12, Science and Technology of Zirconia II. Ed. by N. Claussen, M. Rühle, and A. H. Heuer. Am. Ceram. Soc., Columbus, OH, 1984.

6. R. P. Ingel, D. Lewis, B. A. Bender and R. W. Rice, "Temperature Dependence of Strength and Fracture Toughness of ZrO_2 Single Crystals," J. Am. Ceram. Soc., 65[9] C-150-C-151 (1982).

7. R. P. Ingel, D. Lewis, B. A. Bender and R. W. Rice, "Physical, Microstructural and Thermomechanical Properties of ZrO_2 Single Crystals," pp. 408-414 in Advances in Ceramics, Vol. 12, Science and Technology of Zirconia II. Ed. by N. Claussen, M. Rühle, and A. H. Heuer. Am. Ceram. Soc., Columbus, OH, 1984.

8. G. V. Srinivasan, J. F. Jue, S. Y. Kuo and A. V. Virkar, "Ferroelastic Domain Switching in Polydomain Tetragonal Zirconia Single Crystals," accepted for publication in J. Am. Ceram. Soc.

9. K. Mehta and A. V. Virkar, "Fracture Mechanisms in Ferroelectric-Ferroelastic Lead Zirconate Titanate Ceramics," submitted to J. Am. Ceram. Soc.

10. L. Carlsson, "Non-elastic Mechanical Behavior in $SrZrO_3$ by Reorientation," J. Mater. Sci., 5 325-339 (1970).

11. R. L. K. Matsumoto and R. J. Mayhew, "High Temperature Evaluation of New Ferroelastic Toughened Ceramic Materials," Army SBIR Final Report on Contract #DAAL04-87-C-0058 (February 1988).

12. H. Toraya, M. Yoshimura and S. Somiya, "Calibration Curve for Quantitative Analysis of the Monoclinic-Tetragonal ZrO_2 System by X-Ray Diffraction," J. Am. Ceram. Soc., 68[6] C-119-C-121 (1984).

13. Z. C. Jou, S. Y. Kuo and A. V. Virkar, "Elevated Temperature Creep of Silicon Carbide-Aluminum Nitride Ceramics: Role of Grain Size," J. Am. Ceram. Soc., 69[11] C-279-C-281 (1986).

14. J. J. Hansen, "Investigation into the Solubility of $LaNbO_4$ Doped in Unstabilized and 12 Mole % Ceria Partially Stabilized Zirconia and the Resulting Ferroelastic Response," Senior Thesis, Department of Materials Science and Engineering, University of Utah (1988).

15. R. S. Roth, J. R. Dennis, and H. F. McMurdie, Phase Diagrams for Ceramists, Vol. VI (Am. Ceram. Soc., Columbus, OH, 136-137 (1987)).

16. K. Tsukuma and T. Takahata, "Mechanical Property and Microstructure of TZP and TZP/Al_2O_3 Composites," Advanced Structural Ceramics, Vol. 78, ed. by P. F. Becher, M. V. Swain and S. Somiya (Materials Research Society, Pittsburgh, PA, 123-135, 1987)).

II. UNIVERSITY OF UTAH

FINAL REPORT

NEW MECHANISM FOR TOUGHENING CERAMIC MATERIALS

Submitted by

Prof. Anil V. Virkar

Department of Materials Science and Engineeing, 304 EMRO

University of Utah

Salte Lake City, Utah 84112.

to

Ceramatec, Inc.

2425 South 900 West

Salt Lake City, Utah 84119.

Attn: Dr. Raymond A. Cutler

May, 1989.

SUMMARY

During the period July 15, 1987 to December, 14 1988, efforts were directed on determining the potential contribution of ferroelasticity.to toughness. The specific objective was determine if tetragonal zirconia is indeed ferroelastic. And if so what contribution, if any, results from ferroelastic domain switching. Since many tetragonal zirconia materials undergo transformation to the monoclinic phase, unequivocal determination of the ferroelastic effects is expected to be difficult. To circumvent this problem, efforts were also directed on other ferroelastic materials which are known to be ferroelastic but do not undergo a martensitic transition unlike zirconia. During the course of this work, experimental work was conducted on three materials: Zirconia, commercial lead zirconate-titanate, and rare earth molybdates.

A: Experiments on Zirconia:

A:(I): Polydomain, 2.4 mol% Y_2O_3-Stabilized Single Crystals:

The work on zirconia was conducted on three types of materials: yttria-stabilized single crystals, yttria-stabilized polycrystalline zirconia, and ceria-stabilized polycrystalline zirconia. The objective of the work was to determine the role of ferroelasticity on toughness. Single crystals cotainign 2.4 mol.% Y_2O_3 were purchased from Ceres corporation. The as-received crystals also contained some amount of the monoclinic phase. The crystals were thus annealed in air at $\geq 2100^\circ C$ This treatment led to the formation of essentially single phase tetragonal material. Both X-ray diffraction and electron microscopy indicated that the crystals were polydomain with the <001> axes of the domains in three mutually orthogonal directions. compression testing at room temperature as well as at $1000^\circ C$ and $1400^\circ C$ showed that ferroelastic domain switching can be effected. Fracture toughness was measured using the single edge notched beam in bending. The toughness was ~12 MPa√m at room temperature and ~8 MPa√m at $1000^\circ C$. X-ray diffraction from fracture surfaces of samples broken at $1000^\circ C$ showed that domain switching had occurred. In none of the tests, monoclinic phase was detected. The results of this work indicated that ferroelastic domain switching can occur in polydomain tetragonal (the socalled t'-phase) zirconia single crystals. A manuscript based on this work has been approved for publication in the Journal of the American ceramic Society. A copy of the same is attached along with this report.

A:(II): Polycrystalline Y_2O_3-Stabilized t'-Zirconia: It is well known that the yttria-stabilized (partially) materials must be very fine-grained to ensure that they do not spontaneously

transform into the monoclinic phase. For samples containing ~3 mol.% Y_2O_3, the critical grain size is on the order of a micron or so. Thus, the grain size of the polycrystalline material must be less than about 1 μm. Indeed, experimental work on materials sintered at ~1500°C are in accord with this. Yet, single crystals several milllimeters are stable and do not transform spontaneously. This suggested that it must be the domain size and not the grain size that is important in the t'-materials; i.e. tetragonal zirconia that has been formed by the cubic → tetragonal displacive transition. It was thus thought that if polycrystalline zirconia ceramics can be made by first heatign to the cubic phase field, nontransformable tetragonal zirconai of very large grain siez can be made. In order to test this hypothesis, samples containign various amounts of Y_2O_3 (3 to 6 mol.%) were first sintered at 1500°C followed by heating to ~2100°C in air. Optical microscopy showed that the grain size of the samples was about 200 μm. Yet the samples were fully tetragonal and did not transform to the monoclinic phase upon grinding. No monoclinic phase was detected on the fracture surfaces either. The toughness of the samples at room temperature was as high as about 8 MPa√m depending upon the yttria content. The process of grinding led to the development of texture consistent with the occurrence of ferroelastic switching. One sample was X-rayed while under a tensile stress. It was observed that the intensity ratio of the (002) and the (200) peaks changed consistent with the occurrence of ferroelastic domain switching. No monoclinic peaks were observed. Additional experiments are underway.

A:(III): Ceria-Stabilized Polycrystalline Zirconia: Preliminary experiments have shown that ceria-stabilized materials under certain conditions exhibit high toughness values. High toughness of these materials is known to be due to reverse tetragonal → monoclinic phase transition. The plasticity associated with t → m → t transition is probably the cause of high toughness. Yet, some materials, particulary those containing $SrZrO_3$ and Al_2O_3 often have high toughness without exhibiting a great deal of plasticity. It was thus deemed necessary to examine the deformation behavior of polycrystalline zirconia. The most convenient method of examining defromation behavior is in compression. This was accomplished by mounting two starin gahes on each of the two opposite surfaces; one for the measurement of longitudinal and one for the lateral strains, respectively. The two strain gages from the opposite faces were connected in series to eliminate any buckling effects. In many of these materials reverse transformation was observed. Yet, the toughness did not scale with the amount of deformation. Currently, experiments are underway to examine deformation behavior at elevated temperatures. This work is beign done at Oak Ridge National Laboratory (ORNL) by one of our graduate students. In the next report, discussion of these experiments will be included.

B: Experiments on Lead Zirconate Titanate:

Lead zirconate titanate (PZT) ceramics are known to be simultaneously ferroelectric-ferroelastic. As there is no possibility of martensitic transformation in this material, this is an ideal material to identify contribution of ferroelastic domain switching in toughening. Toughness of a commercial PZT was measured between room temperature to 500°C, which is well above the Curie temperature (~350°C). The toughness decreased with increasing temperature upto ~350°C and remained constant thereafter. X-ray diffraction from fracture surfaces indicated the occurrence of ferroelastic domain switching. The observed toughening effect (~40%), is in accord with theoretical calculation. The principal calculation of this work is that ferroelastic domain switching does occur in PZT and does contribute to the overall toughness. A manuscript based on this work has been submitted to the Journal of the American ceramic Society. A copy of the same is included here as an appendix.

C: Experiments on Gadolinium Molybdate:

Gadolinium molybdate, $Gd_2(MoO_4)_3$, GMO, is a simultaneously ferroelastic-ferroelectric material. In the ferroic state, GMO is orthorhombic with a ≈ b. (with b slightly greater than a) The direction of polarization is along the c-axis. Application of a suitable stress can switch a into b and b into a. Concurrently, the c-axis inverts (through 180°). It was hypothesized that the crack sizes will be of different lengths in single crystals depending upon the orientation. In GMO, the twinning plane is of {110} type. Indents were introduced in single crystals in such a way that the edges of the indents were parallel (and perpendicular) to the twin boundaries. Thus, the ensuing cracks from the indent corners are at ~45° with respect to the twin boundaries. That is, the cracks are along [100] and [010] directions. The cracks along [010] are expected to be shorter in comparison to those along [100] if ferroelastic domain switching can occur under the influence of a stress field of a crack tip. The reason is that when the crack is along [010], the normal to the crack surface is along [100], i.e. along the a direction. In the tensile stress field of the crack tip, a can switch into b. This process will absorb some energy. As a result, less energy is available for driving the crack. For cracks along [100], the crack surfaces are normal to [010], i.e., along b. In a tansile stress field of the crack tip, no reoientation is to be expected since the domais.are already oriented in the prospective direction. That is, no energy is absorbed in the reorientation process and all of the enrgy is available to drive the crak. The crack lengths are thus expected to be longer. This is precisely what was observed. Indents were also introduced with the indent edges at 45° with respect to the twin boundaries. In this case, the cracks are parallel and normal to the twin boundaries. That is, the

cracks are along <110>. In this orientation, no domnain reorientation is expected for either of the cracks. The expectation is that the cracks will be of the same length. This is precisely what was observed. A manuscript based on this work is currentlly being prepared and will be submitted for publication shortly. Experiments on polycryatslline rare earth molybdates are currently underway.

FERROELASTIC DOMAIN SWITCHING IN POLYDOMAIN TETRAGONAL ZIRCONIA SINGLE CRYSTALS

by

G. V. Srinivasan, J. F. Jue, S. Y. Kuo and A. V. Virkar

Department of Materials Science & Engineering
University of Utah
Salt Lake City, Utah 84112.

ABSTRACT

As-received, yttria-doped (4.2 wt.% Y_2O_3) single crystals of zirconia were heated to $\geq 2100°C$ in air. Cube-shaped samples with faces perpendicular to <100> axes on the basis of the pseudocubic symmetry were cut from the crystals. X-ray and electron diffraction indicated that the crystals are polydomain with [001] axes, on the basis of the tetragonal symmetry, in three mutually orthogonal directions (perpendicular to the cube faces). The cube-shaped crystals were tested in compression at temperatures as high as 1400°C. X-ray diffraction indicated that ferroelastic domains underwent reorientation (switching) in compression. Subsequently, notched samples with the long direction of the beams along <100> on the basis of the pseudocubic symmetry, were fractured in three point bending at temperatures as high as 1000°C. X-ray diffraction from fracture surfaces showed that domain reorientation had occurred and that no monoclinic phase was observed on fracture or ground surfaces. The fracture toughness at room temperature and at 1000°C was measured to be ~12 and ~8 MPa√m, respectively. Preliminary experiments on polycrystalline tetragonal zirconia samples containing 5.4 wt. % Y_2O_3 and sintered at $\geq 2100°C$ also showed no evidence of the monoclinic phase on fracture or ground surfaces. The toughness of the polycrystalline samples was typically 7.7 MPa√m. These results indicate that ferroelastic domain switching can occur during fracture and may contribute to toughness.

I. INTRODUCTION

High toughness and/or strength of many zirconia-based ceramics are known to be due to transformation toughening. In these materials, the toughness and the strength decrease with

1

increasing temperature since the thermodynamic driving force for transformation of the metastably retained tetragonal phase into the stable monoclinic polymorph decreases with increasing temperature. As a result, above about 800°C to 900°C, no contribution of transformation to the overall toughness is expected. Indeed, numerous zirconia-based materials do exhibit loss of strength and toughness with increasing temperature. There are, however, some tetragonal zirconia materials in which high strength and toughness can be retained to temperatures above the monoclinic → tetragonal transition temperature. Also, there are materials in which the toughness and the strength do not decrease with increasing temperature. The data of Ingel et. al. [1,2] on yttria-stabilized tetragonal zirconia single crystals showed strength ~700 MPa up to 1600°C. By contrast, the strength of the corresponding cubic crystals was only 350 MPa. In a study by Michel et. al. [3], the toughnesses of tetragonal and cubic crystals were determined to be ~6 and ~1.8 MP√m, respectively. Similarly, the work of Yuan et. al. [4] on polycrystalline ceramics containing 40 vol.% ZrO_2 and 60 vol.% MgO shows that the strength is independent of temperature up to the maximum testing temperature of 1000°C. X-ray diffraction from fracture surfaces of either the single crystals or the MgO-ZrO_2 ceramics failed to reveal the existence of the monoclinic phase. Failure to observe the monoclinic phase could possibly be explained on the premise that reverse transformation to the tetragonal phase may have occurred during the fracture process as observed in some other polycrystalline zirconia materials. However, the high strength of tetragonal zirconia single crystals above 1000°C in the study by Ingel et. al. [1,2] can not be explained on the basis of reverse transformation as the m → t transition in zirconia containing 4.2 wt.% Y_2O_3 is ≤ 700°C. Also, the constancy of strength and toughness upto 1000°C, the maximum test temperature, in a study by Yuan et. al. [4] cannot be explained on the basis of transformation toughening.

During an investigation of a polycrystalline, ceria-stabilized, tetragonal zirconia (CeTZP) ceramic, no monoclinic phase was observed on ground surfaces [5]. However, surface grinding led to the development of crystallographic texture [5]. After surface grinding, the X-ray peak intensity of the (002) peak increased significantly while that of the (200) peak decreased. Similar effects were observed for the (113) and (131) peaks also. The enhancement of the intensity of the (002) peak indicates that many of the crystallites in the near surface region reoriented themselves upon grinding in such a way that their c-axes became orthogonal to the surface. According to Michel et. al. [3], the cubic → tetragonal displacive transformation in zirconia is a ferroelastic transition. Using Aizu's [6,7] notations, the representative species is given by m3mF4/mmm. Based on group theory considerations, the tertagonal phase is expected to be a ferroelastic phase. For a material to be ferroelastic, the crystal must exist in at least two energetically equivalent orientational states and that it must be possible, at least in principle, to shift the crystal from one state into the other by the application of an external stress. The development of texture upon grinding is consitent with the

existence of ferroelasticity in tetragonal zirconia. Later work showed that similar texture can be developed in $BaTiO_3$ and PZT which are known to be simultaneously ferroelectric-ferroelastic materials [8,9].

The objective of the present work was to examine the role of ferroelasticity in zirconia ceramics. Majority of the zirconia ceramics do exhibit transformation which makes unequivocal identification of ferroelastic effects difficult. Published information on tetragonal zirconia single crystals indicates that these crystals do not undergo transformation to the monoclinic phase [3]. This suggests that tetragonal single crystals are ideally suited to examine the ferroelastic behavior. For this reason, the experimental part of this investigation was primarily confined to single crystals of tetragonal zirconia stabilized by the addition of 4.2 wt.% Y_2O_3 although a few experiments were conducted on sintered, polycrystalline zirconia ceramics.

II. EXPERIMENTAL PROCEDURE

As-received crystals[*] (4.2 wt.% Y_2O_3) were mounted on a two axes goniometer and were oriented using Laue back reflection. Cube-shaped crystals, approximately 3 mm x 3 mm x 3 mm in dimensions, were cut out of the crystals in such a way that the <100> axes on the basis of the pseudocubic symmetry were orthogonal to the surfaces of the cubes. Bar-shaped samples of dimensions 3 mm x 3 mm x 25 mm were also cut in such a way that the long direction of the bar was along <100>. Some of the samples were then heated in a gas-fired furnace to a temperature $\geq$ 2100°C in air. The exact temperature could not be accurately determined for lack of a direct view of the hot zone. The temperature at the flame entry tube was as high as ~2400°C. It is believed that the actual sample temperature must be $\geq$ 2100°C. The hold time at temperature was about 10 minutes. However, about two hours were necessary to raise the temperature from ~1600°C to $\geq$ 2100°C. After 10 minutes at $\geq$ 2100°C, the platform containing the samples was immediately lowered to a region in the furnace where the temperature was ~1400°C. The reason for relatively rapid cooling to 1400°C was to prevent (or minimize) the precipitation of tetragonal phase by a diffusive process. Subsequently, the crystals were furnace cooled to room temperature. A few polycrystalline zirconia samples containing 5.4 wt.% Y_2O_3 (Tosoh powder), presintered at 1500°C/2 hours, were heat treated in the gas-fired furnace at $\geq$ 2100°C. The objective of this work was to determine if nontransformable polycrystalline zirconia samples can be fabricated by heating them in the stability range of the cubic phase field.

---

* Ceres Corp., Waltham, Mass.

3

The cube-shaped samples were subjected to compressive loading at room temperature as well as at temperatures up to 1400°C. Compressive testing at elevated temperatures was conducted using a silicon carbide loading fixture heated by molybdenum disilicide heating elements. At room temperature, the applied stresses were as high as ~2.25 GPa. At elevated temperatures, the maximum applied stress was on the order of 300 MPa. The objective of the compression tests was to determine if domain reorientation (switching) can be effected by compressive loading. Thin notches were machined in the bar-shaped samples for the measurement of fracture toughness, K_c, using the single edge notched beam (SENB) technique in three point bending. The samples were broken at room temperature and at 1000°C.

X-ray diffraction traces using CuKα radiation were obtained from: (1) ground surfaces, (2) fracture surfaces, and (3) surfaces of the cube-shaped crystals subjected to compression testing. The obejective was to determine if domain reorientation occurred in any of these processes. It was also the objective to determine if any monoclinic phase was present in these crystals.

For examination in a scanning transmission electron microscope, samples were prepared by dimple grinding followed by ion-milling to perforation. Samples were oriented in such a way that the foil surfaces were orthogonal to <001> axis on the basis of the pseudocubic symmetry. Polycrystalline samples were polished and etched in HF to reveal the grain structure.

III. RESULTS

III(a): X-Ray Diffraction: In the range of 2θ from 33° to 37° and from 72° to 76°, generally either two, or three or even four peaks were observed from the surfaces of the cube-shaped samples cut from the as-received single crystals. A typical X-ray diffractometer trace in the 2θ range between 72° and 76° from the as-received crystal is shown in Figure #1(a). In the same ranges of 2θ, only two peaks were observed in samples that had been annealed at ≥ 2100°C as shown in Figure #1(b). X-ray traces shown in Figures #1(a) and #1(b) are typical of the traces obtained from any of the six cube surfaces. The peaks in the annealed sample are identified as (400)d and (004)d of the single phase tetragonal crystals. The corresponding c/a is about 1.015. Of the four peaks observed in the X-ray traces from the as-received crystal, the inner two and the outer two are labeled (400)d & (004)d and (400)p & (004)p, respectively. The c/a ratios corresponding to the inner and outer sets of peaks are 1.006 and 1.0215, respectively.

X-ray diffraction traces from cube-shaped samples that had been annealed at ≥ 2100°C (and polished) show (002) & (004) peaks of lower intensities than the (200) & (400) peaks,

4

respectively. This result is consistent with an X-ray diffraction trace from a powder of the tetragonal phase. After surface grinding and/or cutting, however, the intensities of the (002) and (004) peaks were invariably greater than those of the (200) and (400) peaks, respectively. The sample whose X-ray trace is shown in Figure #1(b) was ground. After polishing the ground sample, the intensity of the (002) peak decreased and that of the (200) peak increased. However, even after removing the surface layer to a depth of ~15 μm, the intensity ratio of (002) to (200) was greater than the one corresponding to the powder pattern. This suggests that the depth of the texture developed by grinding was at least 15 μm.

Polycrystalline zirconia samples fabricated by first sintering at 1500°C followed by heating to ≥ 2100°C were also examined by X-ray diffraction. Samples were found to be of the tetragonal symmetry. No monoclinic phase was observed in the X-ray diffraction traces from ground and fracture surfaces. However, increase in the intensities of (002) & (004) peaks readily occurred upon surface grinding.

Prior to compression testing of cube-shaped crystals, X-ray diffraction traces were obtained from two surfaces; the surface upon which compressive loads were to be applied and one of the side surfaces. After compression testing, X-ray diffraction traces were again obtained from the same two surfaces. Figure #2 shows X-ray diffraction traces from the surface of an annealed and ground sample subjected to compression (~2.25 GPa) at room temperature, before and after the test. As shown in the figure, the intensities of (002) and (004) peaks decrease and those of (200) and (400) peaks increase after compression testing. Figure #3 shows X-ray traces from the side subjected to compression (~300 MPa) at 1400°C and from one of the side faces, both before and after the test. After compression testing, the intensity of the (002) peak decreased and that of the (200) peak increased from the surface that was subjected to compressive stress. This observation is consistent with that at room temeparture (Figure #2). By contrast, the intensity of the (002) peak increased and that of (200) decreased from the side surfaces. Similar results were obtained from samples tested at 1000°C and 1200°C. Samples tested at 1000°C and 1200°C were subjected to compressive stresses of 450 MPa and 300 MPa, respectively.

III(b): Microscopy: Figures #4(a) and #4(b) show electron diffraction patterns of the as-received and annealed samples, respectively. As seen in Figure #4(b), higher order spots are split. Diffraction pattern from the as-received crystal is similar to that from the annealed sample except that there are several additional spots (Figure #4(a)). These additional spots are due to the tetragonal precipitates, some of which transformed to the monoclinic phase. These precipitates are formed by a diffusional process during the presumably slow cool down after the crystal growth.

An electron micrograph of the annealed sample for zone axis <001> is shown in Figure #5. This structure is similar to the one reported by Lanteri and coworkers [10] and Sakuma [11].

An optical micrograph of a polycrystalline sample annealed at $\geq 2100^\circ$C is shown in Figure #6. The sample was etched in HF. The grain size of the sample is ≥ 100 μm. The density of the sample was measured to be 6.05 gm./ml.

III(c): Fracture Toughness Measurements: The toughness values of the single crystals at room temperature and at 1000°C were ~12 and ~8 MPa$\sqrt{m}$, respectively. As mentioned previously, no monoclinic phase was observed on the fracture surfaces. As indicated by Michel et. al. [3], two peaks corresponding to the monoclinic phase, if present, are expected on the low angle side of the (004) peak. No such peaks were observed. On the other hand, an enhancement of the (002) peak intensity was observed. X-ray diffraction traces obtained from samples fractured at room temperature and at 1000°C are shown in Figures # 7(a) and #7(b), respectively. As seen in these figures, the intensity of the (002) peak increased and that of the (200) peak decreased for the sample fractured at 1000°C. For the sample fractured at room temperature also the intensity of the (002) peak is greater than that from the pristine surface. Toughness of the polycrystalline zirconia samples sintered at $\geq 2100^\circ$C, measured by the SENB technique, was typically 7.7 MPa$\sqrt{m}$.

IV. DISCUSSION

IV(a): Structure of Single Crystals: As shown in Figure #1(a), between $2\theta = 7\mathcal{5}^\circ$ to 77°, four peaks were observed in the X-ray diffraction traces from the as-received crystals. These peaks are labeled (400)d, (004)d, (400)p and (004)p. The letter d indicates that the peaks correspond to the tetragonal phase formed by c $\rightarrow$ t displacive transformation (the so-called t'-phase) [10]. The letter p indicates that the peaks correspond to the tetragonal phase which precipitated out of the cubic phase by a diffusive process. As the tetragonal phase formed by a diffusive process has a lower yttria content in accordance with the phase diagram, the corresoponding c/a ratio is larger.

X-ray diffraction from surfaces of cube-shaped crystals annealed at $\geq 2100^\circ$C gave identical patterns consisting of two peaks each in the 2θ ranges between 33° & 37° and between 72° & 76°. The two sets of peaks are (002) & (200) and (400) & (004) corresponding to the tetragonal phase formed displacively. The presence of doublets indicates that the crystal is not a true single crystal, but is a polydomain crystal. If it were a true single crystal, it should yield only one peak in each of the ranges. The corresponding peaks would be (002) & (004) or (200) & (400) depending upon the crystal orientation. Thus, X-ray diffraction alone shows that the crystal must be a polydomain

crystal.

IV(b): Ferroelasticity and Zirconia: According to the group theory, for a transition to be ferroelastic, it must satisfy the following criteria [12]:

1)   Reduction in the point group symmetry must occur for a transition to be ferroic.
2)   A change in the crystal system must occur for the ferroic transition to be ferroelastic.

The point groups of cubic and tetragonal zirconia are m3m and 4/mmm, respectively. The change from cubic (m3m) to tetragonal (4/mmm) is accompanied by a reduction in the order of symmetry from 48 to 16. Thus, in accordance with the above criteria, this transition is ferroelastic and may be represented by Aizu's notation, m3mF4/mmm [6]. The number of possible variants may be deduced by simply dividing the order of symmetry in the prototype by that in the ferroelastic phase [7]. Thus, in cubic $\rightarrow$ tetragonal transition in zirconia, 48/16 = 3 variants are expected. Negita [13] has shown that in zirconia the cubic $\rightarrow$ tetragonal is a first order transition and tetragonal zirconia is an improper ferroelastic.

As shown by Tendeloo et. al. [14], based on the space group considerations (cubic (Fm3m) $\rightarrow$ tetragonal ($P4_2$/nmc)), upon transition a doubling of primitive cell is expected with the occurrence of two types of anti-phase domains separated by APB's.

The formation of the three variants and the APB's has been experimentally confirmed by Heuer and coworkers [10,15] and Sakuma [16]. These authors have imaged the three variants by choosing {112} type of reflections with <111> zone axis. The electron diffraction pattern shown in Figure #4 is consistent with the presence of the three variants. The fact that only two peaks were observed in X-ray diffraction patterns in a given 2θ range suggests that the split spots seen in Figure #4 can not be due to tetragonal precipitates. If tetragonal precipitates are present, X-ray diffraction traces should contain four peaks since the c/a ratio of the precipitates is different from that of the displacively formed tetragonal (t') phase.

IV(c): Ferroelastic Domain Switching in Compression: An important characteristics of a ferroic material is that by the application of the pertinent field, it should in principle be possible to shift the crystal from one state into another energetically equivalent state [6]. In the present experiments, when a compressive stress was applied along <100> (on the basis of the pseudocubic symmetry), the intensity of the (002) peak decreased and that of the (200) peak increased on the face that was subjected to compression (Figures #2 & #3). By contrast, the change in the intensities of the two peaks on faces parallel to the compression direction was in the opposite direction (Figure #3). This is consistent with the expectation that the c-axes of the domains should switch to

directions orthogonal to the compressive loading direction. Lankford et. al.[17] observed a step in load-deflection traces of single crystals compressed along <100> direction but not when compressed along <110> direction. The step observed by Lankford et. al. is consistent with the occurrence of ferroelastic domain switching.

It could be argued that the changes in the intensities observed in the present studies can be explained on the basis of reversible t $\rightarrow$ m transition. In ceria-doped polycrystalline tetragonal zirconia, tested in compression, this has been documented [18]. Samples in the present work were compression tested at temperatures as high as 1400°C. For zirconia containing 2.4 mol.% (4.2 wt.%) Y_2O_3, the t $\rightarrow$ m transition temperature is $\leq 700°C$ [19]. As the volume change from m $\rightarrow$ t is negative, according to the Clausius-Clapeyron relation hydrostatic pressure (1/3 uniaxial compression) decreases the t $\rightarrow$ m transition temperature [20]. Clearly, the changes in the intensities of the (002) and the (200) peaks observed at temperatures $\geq$ 1000°C cannot be explained on the basis of t $\rightarrow$ m reversible transition. Michel et. al. [3] reported that even after the single crystal (3 mol.% Y_2O_3) used in their study was crushed to a powder of size less than 1 μm, the amount of the monoclinic phase was less than 1 %. These results also suggest that the changes in the intensities of the (002) and the (200) peaks observed in our studies at room temperature are probably not due to reversible t $\rightarrow$ m transition but are due to domain switching.

IV(d): Toughening Mechanisms: The higher toughness values of tetragonal single crystals in comparison to cubic crystals in the work by Ingel et. al. [1,2] was attributed to crack deflection. Similarly, Michel et. al. [3] also suggested crack deflection by domain boundaries as the probable toughening mechanism. In a recent paper, Heuer et. al. [21] have suggested that at elevated temperatures, precipitation strengthening in tetragonal single crystals containing 4.5 mol.% Y_2O_3 can occur. In the present work, toughness of tetragonal single crystals was measured to be 12 and 8 MPa√m at room temperature and at 1000°C, respectively. These mechanisms of toughening are probably operative in the single crystals studied in the present work. Wadhavan [22] has suggested ferroelastic domain switching as a possible toughening mechanism. Changes in the intensities of the (002) and (200) peaks observed in compression tests as well as on fracture surfaces suggest that the phenomenon of domain switching can contribute to the overall toughness. At 1000°C, no contribution of transformation toughening is expected for the reasons mentioned previously. At room temperature also no monoclinic phase was observed on ground or fracture surfaces of single crystals annealed at $\geq$ 2100°C. Yet, changes in the intensities of (002) and (200) peaks occurred consistent with the occurrence of domain switching. This suggests that toughening by ferroelastic domain switching is probably operative at room temperature also. However, the possible contribution of reversible t $\rightarrow$ m transition at room temparture in toughening can not be ruled out.

In materials such as lead-zirconate-titanate (PZT), on the other hand, the contributions of the domain switching can be clearly identified as no transformation toughening is possible [9].

V. SUMMARY AND CONCLUSIONS

Group theoretical considerations suggest that tetragonal zirconia is a ferroelastic material [6,7,12-14]. An important characteristic of a ferreoelastic material is that it should be possible, at least in principle, to change domain orientation by the application of an external stress. In the present work X-ray diffraction evidence was presented in support of the contention that domain switching occurred during compression testing and fracture. The observation that high toughness can be retained far above the t $\rightarrow$ m transition temperature suggests that there is little contribution from transformation toughening. By contrast, the occurence of domain switching indicates that ferroelastic domain switching can contribute to toughening. Finally, nontransformable tetragonal zirconia polycrystalline samples containing 5.4 wt.% (3 mol.%) Y_2O_3 with grain size $\geq$ 100 μm can be fabricated by annealing the samples in the stability range of cubic zirconia ($\geq$ 2100°C).
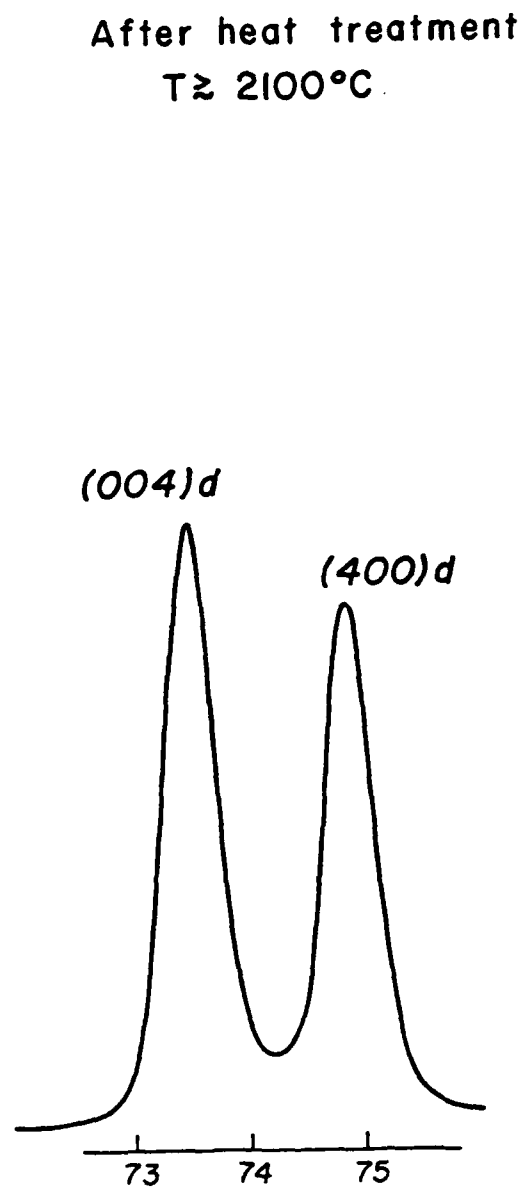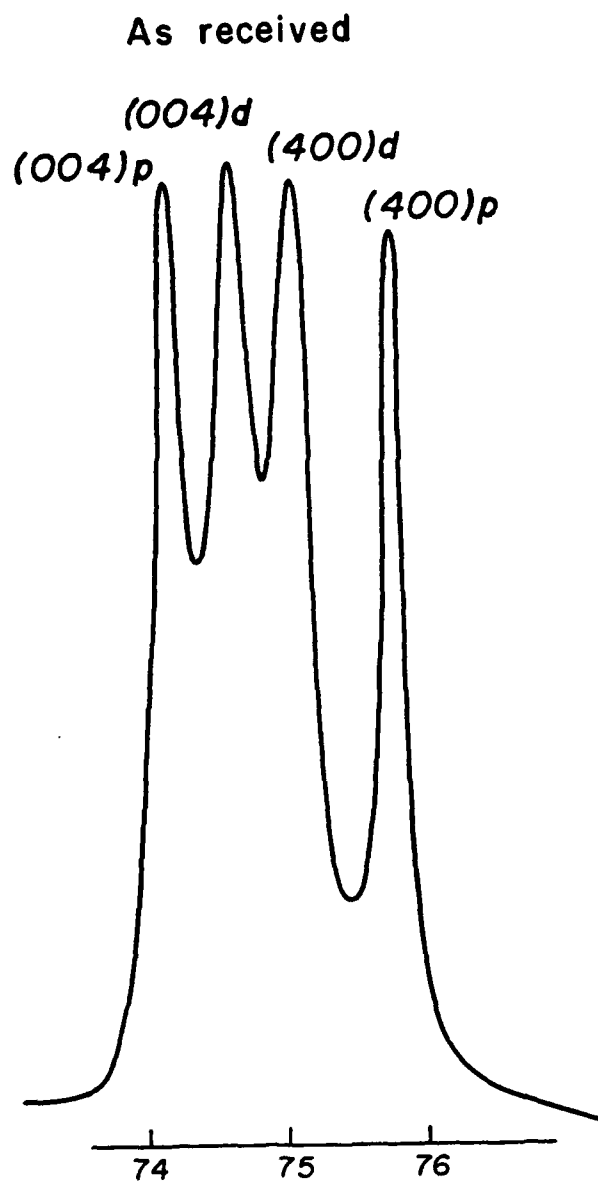
REFERENCES

1)   R. P. Ingel, D. Lewis, B. A. Bender and R. W. Rice, "Temperature Dependence of Strength and Fracture Toughness of ZrO_2 Single Crystals", *J. Am. Ceram. Soc.*, 65 [9] C-150 - C-151, (1982).

2)   R. P. Ingel, D. Lewis, B. A. Bender and R. W. Rice, "Physical, Microstructural and Thermomechanical Properties of ZrO_2 Single Crystals", pp. 408-414 in Advances in Ceramics, vol. 12, Science and Technology of Zirconia II, edited by N. Clausen, M. Rühle and A. H. Heuer, American Ceramic Society, Columbus, Ohio, 1984.

3)   D. Michel, L. Mazerolles and M. Perez y Jorba, "Fracture of Metastable Tetragonal Zirconia Crystals", *J. Mater. Sci.*, 18, 2618-2628, (1983).

4)   T. C. Yuan, G. V. Srinivasan, J. F. Jue and A. V. Virkar, "Dual Phase Magnesia-Zirconia Ceramics with Strength Retention at Elevated Temperatures", accepted for publication in the *J. Mater. Sci*, (1989).

5)   A. V. Virkar and R. L. K. Matsumoto, "Ferroelastic Domain Switching as a Toughening Mechanism in Tetragonal Zirconia", *J. Am. Ceram. Soc.*, 69 [10] C-224 - C-226, (1986).

6)   K. Aizu, "Possible Species of "Ferroelastic" Crystals and of Simultaneously Ferroelectric and Ferroelastic Crystals", *J. Phys. Soc. Japan*, 27, 387, (1969).

7)   K. Aizu, "Possible Species of Ferromagnetic, Ferroelectric and Ferroelastic Crystals", *Phys. Rev. B*, 2 [3], 754-772, (1970).

8) A. V. Virkar and R. L. K. Matsumoto, "Toughening Mechanism in Tetragonal Zirconia Polycrystalline (TZP) Ceramics", p. 653-662, in Advances in Ceramics, Vol. 24, Science and Technology of Zirconia III, edited by S. Somiya, N. Yamamoto and H. Yanagida, a publication of the American Ceramic Society, Westerville, Ohio (1988).

9) K. Mehta and A. V. Virkar, "Fracture Mechanisms in Ferroelectric-Ferroelastic Lead Zirconate Titanate Ceramics", submitted to the *J. Am. Ceram. Soc.*, (1988).

10) V. Lanteri, R. Chaim and A. H. Heuer, "On Microstructure Resulting from the Diffusionless Cubic $\rightarrow$ Tetragonal Transformation in ZrO_2-Y_2O_3 Alloys", *J. Am. Ceram. Soc.*, **69** [10] C258-C261 (1986).

11) T. Sakuma, Y. A. Yoshizawa and H. Suto, "The Microstructure and Mechanical Properties of Yttria-Stabilized Zirconia prepared by Arc-Melting", *J. Mater. Sci.*, **20** [10] 2399-2407 (1985).

12) J. C. Tolenado, "Symmetry-Determined Phenomena at Crystalline Phase Transitions", *J. of Solid State Chemistry*, **27** 41-49 (1979).

13) K. Nagita, "Lattice Vibrations and Cubic to Tetragonal Phase Transition in ZrO_2", *Acta Met.* **37** [1] 313-317 (1989).

14) G. V. Tendeloo and S. Amelinckx, "Group-Theoretical Considerations Concerning Domain Formation in Ordered Alloys", *Acta Cryst.* A30 431-440 (1974).

15) A. H. Heuer, R. Chaim and V. Lanteri, "The Displacive Cubic $\rightarrow$ Tetragonal Transformation in ZrO_2 Alloys", *Acta Metall.*, **35** [3] 661-666, (1987).

16) T. Sakuma, "Development of Domain Structure Associated with the Diffusionless Cubic-to-Tetragonal Transition in ZrO_2-Y_2O_2 Alloys", *J. Mater. Sci.*, **22** 4470-4475, (1987).

17) J. Lankford, L. Rabenberg and R. A. Page, "Deformation Mechanisms in Yttria-Stabilized Zirconia", *J. Mater. Sci.*, **23** 4144-4156 (1988).

18) P. E. Reyes-Morel, Jyh-Shiarn Cherng and I-Wei Chen, "Transformation Plasticity of CeO_2-Stabilized Tetragonal Zirconia Polycrystals: II, Pseudoelasticity and Shape Memory Effect", *J. Am. Ceram. Soc.*, **71** [8] 648-657, (1988).

19) H. G. Scott, "Phase Relations in the Zirconia-Yttria System", *J. Mater. Sci.*, **10** [9] 1527-1535, (1975).

20) E. D. Whitney, "Effect of Pressure on Monoclinic-Tetragonal Transition of Zirconia; Thermodynamics", *J. Am. Ceram. Soc.*, **45** [12] 612-613 (1962).

21) A. H. Heuer, V. Lanteri and A. Dominguez-Rodriguez, "High Temperature Precipitation Hardening on Y_2O_3 Partially-Stabilized ZrO_2 (Y-PSZ) Single Crystals", *Acta Met.* **37** [2] 559-567 (1989).

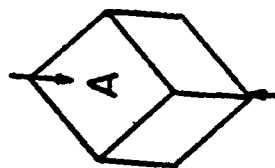22) V. K. Wadhavan, "Ferroelasticity and Related Properties of Crystals", *Phase Transitions* **3** 3-103 (1982).

FIGURE CAPTIONS

Figure #1(a):   X-ray diffraction trace in the 2θ range between 72° and 76° from an as-received crystal (cube faces orthogonal to <100> on the basis of the pseudocubic symmetry) showing peaks from the displacively formed and precipitated tetragonal phases.

Figure #1(b):   X-ray diffraction trace in the 2θ range between 72° and 76° from an annealed ($\geq$ 2100°C) crystal (cube faces orthogonal to <100> on the basis of the pseudocubic symmetry) showing peaks from the displacively formed tetragonal phase.

Figure #2:   X-ray diffraction traces from an annealed, cube-shaped sample subjected to compressive loading at room temperature showing ferroelastic domain switching.

Figure #3:   X-ray diffraction traces from an annealed, cube-shaped sample subjected to compressive loading at 1400°C showing ferroelastic domain switching.

Figure #4(a):   Electron diffraction pattern from an as-received crystal along zone axis <001> on the basis of the pseudocubic symmetry. The labeled spots correspond to the tetragonal symmetry. Additional spots are due to the monoclinic phase.

Figure #4(b):   Electron diffraction pattern from an annealed crystal along zone axis <001> on the basis of a pseudocubic symmetry. The presence of the three variants of the displacively formed tetragonal phase is evidenced by the existence of additional spots indicated by the arrow.

Figure #5:   Bright-field image of a single phase, annealed crystal showing the presence of 90° domains.

Figure #6:   An optical micrograph of a polycrystalline sample (5.4 wt.% or 3 mol% Y_2O_3) heat treated at $\geq$ 2100°C. The sample was etched using HF. X-ray diffraction shows only the presence of the tetragonal phase.

Figure #7(a):   X-ray diffraction traces from pristine and fracture surfaces of an SENB sample broken at room temperature showing the occurrence of ferroelastic domain switching during fracture.

Figure #7(b):   X-ray diffraction traces from pristine and fracture surfaces of an SENB sample broken at 1000°C showing the occurrence of ferroelastic domain switching.
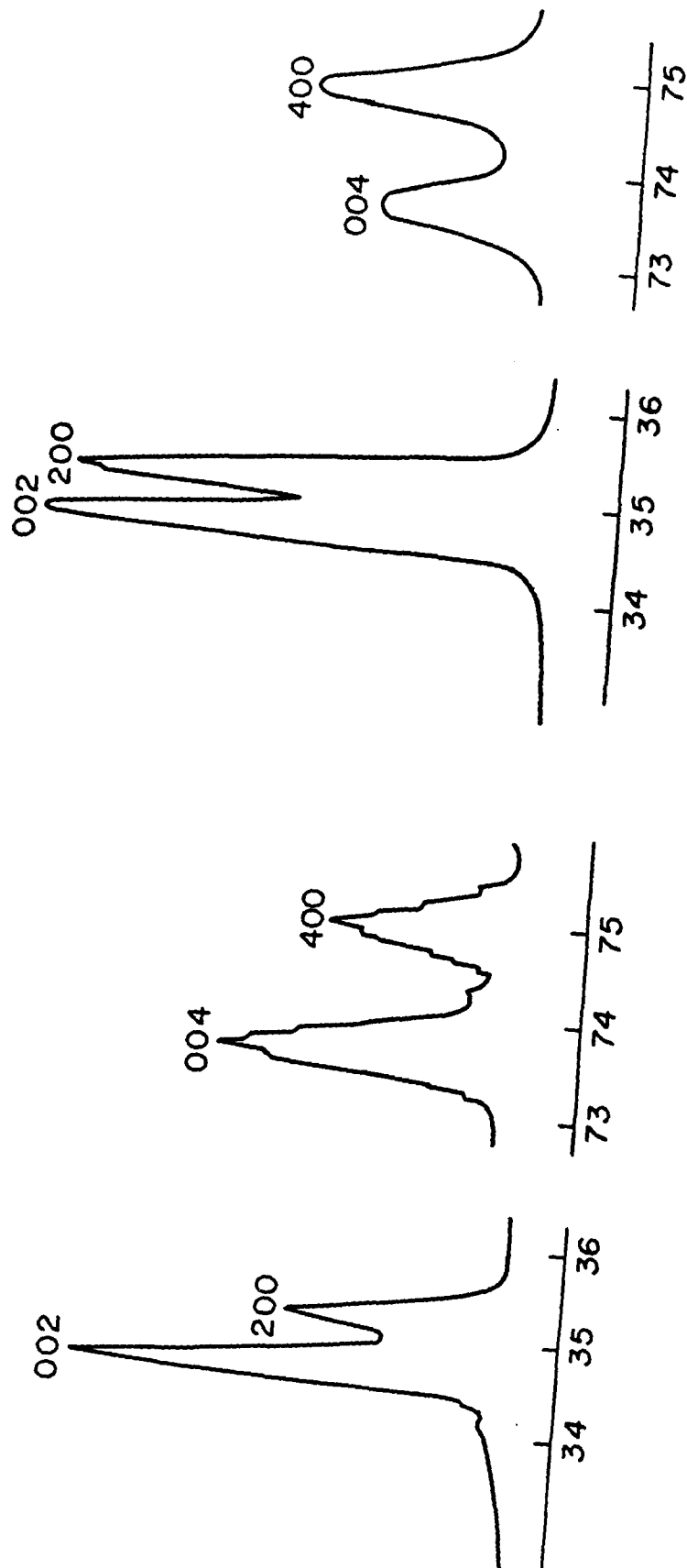
$ZrO_2 + 4.2$ wt % Y_2O_3
Single Crystal

As received

(004)d
(004)p
(400)d
(400)p

74   75   76

After heat treatment
$T \gtrsim 2100°C$

(004)d
(400)d

73   74   75

Room Temperature
$\dot{\epsilon} = 4.6 \times 10^{-4}$/sec

$\sigma \sim 2.25$ GPa

After Testing

Before Testing

Temperature = 1400°C
$\dot{\epsilon} = 4.6 \times 10^{-4}$ /sec

XRD from Side A

XRD from Side B

Before Testing

After Testing

Before Testing

After Testing

$\sigma \sim 300$ MPa

002

200

220

200

020

000

0.5 μ

100 μm
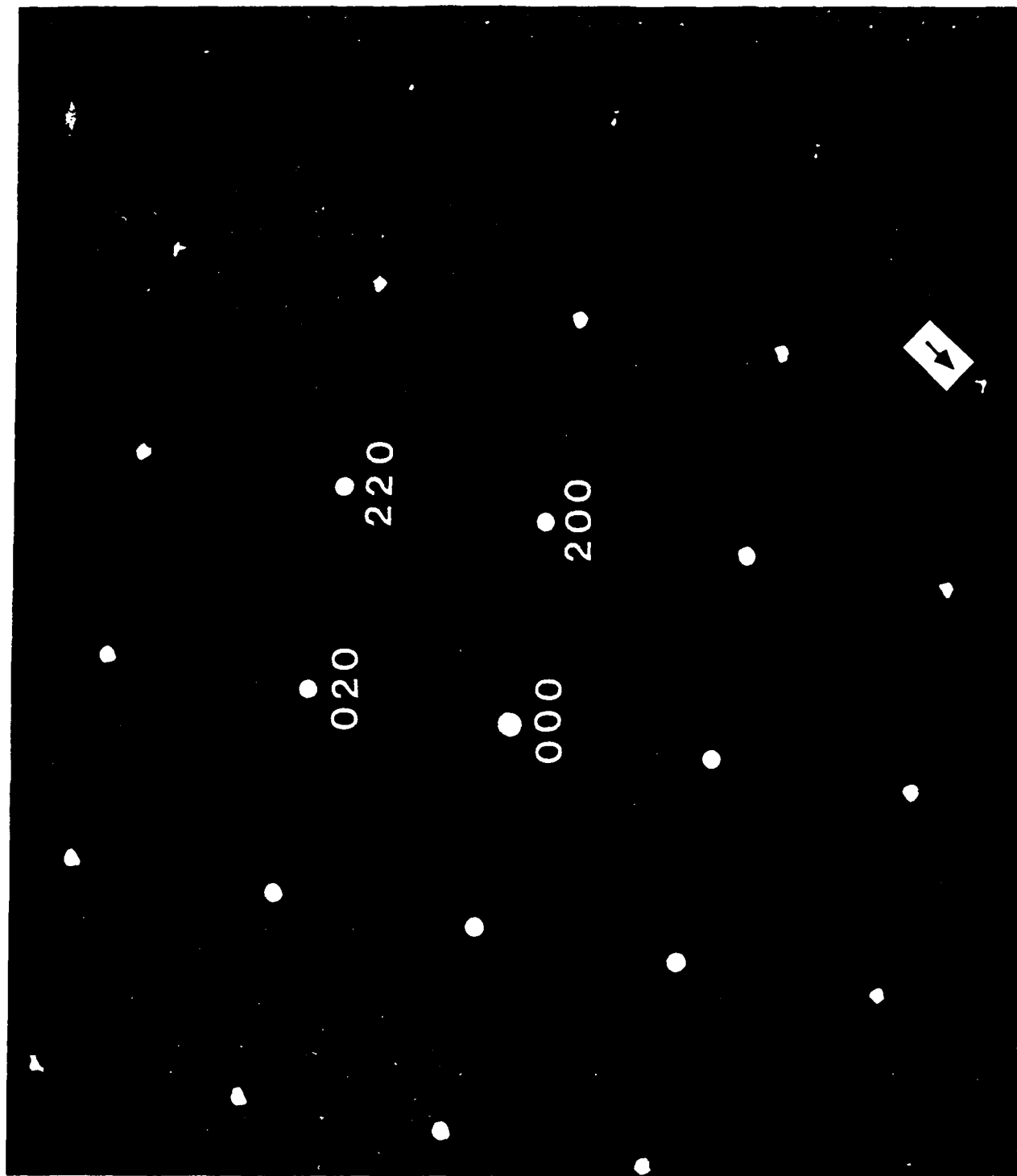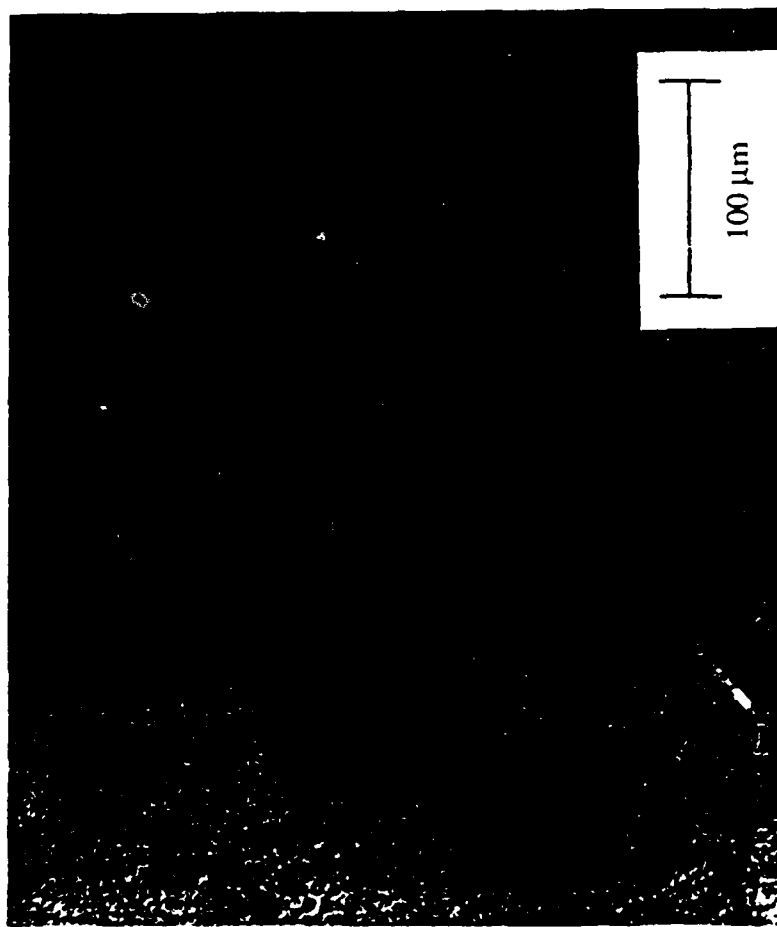
Fig 4 6

$ZrO_2 + 4.2$ w/o Y_2O_3

Single Crystal

<100> Orientation

Heat Treated at 2100°C
R.T. SENB Toughness: 12 Mpa $\sqrt{m}$

After Testing

002

200

34   35   36

Before Testing

200

002

34   35   36

ZrO$_2$ + 4.2 w/o Y$_2$O$_3$
Single Crystal

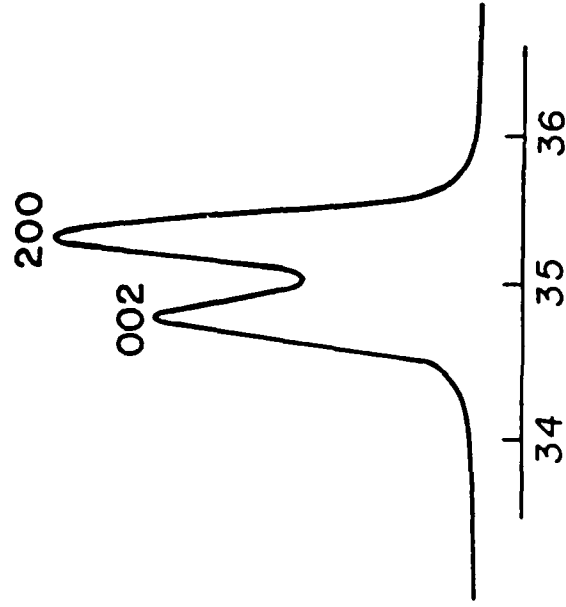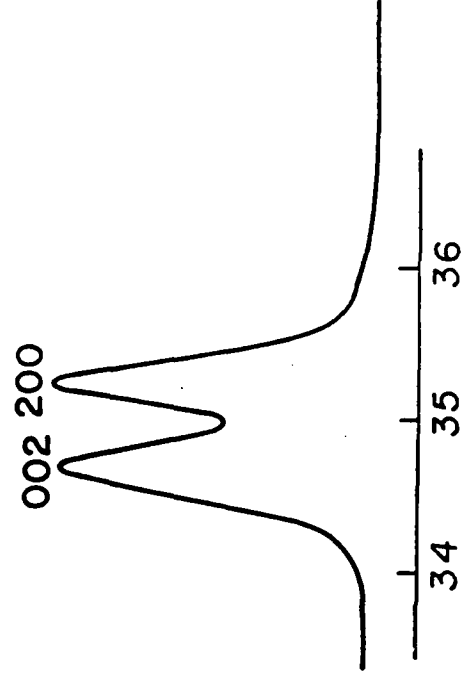<100> Orientation

Heat Treated at 2100°C
1000°C SENB Toughness: 8 Mpa √m

Before Testing

After Testing

FRACTURE MECHANISMS IN FERROELECTRIC-FERROELASTIC LEAD ZIRCONATE TITANATE CERAMICS

by

Karun Mehta and Anil V. Virkar

Department of Materials Science & Engineering
University of Utah
Salt Lake City, Utah 84112

ABSTRACT

Commercial polycrystalline lead zirconate titanate (PZT) ceramics were subjected to various mechanical and electromechanical tests including the measurement of fracture toughness, K_{Ic}, as a function of temperature both above and below the Curie temperature, domain switching (poling) under electrical and mechanical loading, kinetics of domain switching under the application of an electrical field and indentation studies on mechanically and electrically poled materials. Samples were characterized by scanning electron and optical microscopy. The degree of domain switching in electrically and mechanically poled ceramics, on ground surfaces and on fracture surfaces was determined by X-ray diffraction. It was observed that either the application of an electrical field or a compressive stress led to domain switching. For example, the intensity of (002) peak increased and that of (200) peak decreased on th : face perpendicular to the direction of the application of the electric field. Similarly, the process of surface grinding also led to the development of texture consistent with the occurrence of domain switching. Domain switching was also observed on fracture surfaces of many samples (although not all) fractured at room temperature. X-ray diffraction of fracture surfaces also showed that no stress-induced phase transformation had occurred. The toughness of samples which exhibited domain switching was greater than samples which did not. For example, at room temperature, the highest K_{Ic} measured was 1.85 MPa$\sqrt{m}$ while above the Curie temperature it was about 1.0 MPa$\sqrt{m}$. Indentations were introduced on samples that were both mechanically and electrically poled. It was observed that the sizes of cracks emanating from the indents were not the same in all directions. The difference in the crack sizes can be explained on the basis of the occurrence of domain switching during crack growth in certain directions. These results indicate that ferroelastic domain switching does contribute to the overall toughness in the PZT materials tested. The experiments on the time dependence of domain switching indicated that the kinetics can be adequately described by a first order kinetic equation with a single relaxation time. The relaxation time was observed to decrease with increasing

temperature. The significance of the relaxative process with regard to the occurrence of domain switching during fracture is discussed.

I. INTRODUCTION

Lead zirconate titanate ($PbZr_xTi_{(1-x)}O_3$) or PZT ceramics are ferroelectric-ferroelastic ceramics that are used in numerous piezoelectric devices. Fracture behavior of ferroelectric materials as a function of composition and grain size has been examined by Pohanka and coworkers [1-4]. These authors identified microcracking and twinning as toughening mechanisms. In $BaTiO_3$, it was observed that the fracture energy exhibited a maximum at some grain size. Scanning electron micrographs of samples fractured at room temperature (in ferroelectric state) exhibited twins while no twins were observed in samples fractured at 150°C, which is in the paraelectric state. The ferroelectric phase exhibited significantly higher fracture energy. In PZT also the fracture energy was significantly higher at room temperature (in ferroelectric state) than at 200°C (paraelectric state).These authors also observed that pressure-depoled PZT exhibited higher fracture energy. McHenry and Koepke [5] examined the effect of applied a.c. electric fields of various frequencies on the slow crack growth behavior of unpoled PZT ceramics. It was observed in their study that the application of an electric field in general enhanced the propensity to crack growth. Cook et. al. [6] examined the strength of fine grained $BaTiO_3$ as a function of temperature by introducing controlled flaws by indentation. These authors observed that the strength decreased with increasing temperature from room temperature to 150°C (Curie temperature) above which the strength remained constant.

PZT is a simultaneously ferroelectric-ferroelastic material [7] according to the classification scheme advanced by Aizu [8]. The phenomenology of ferroelastic materials suggests that absorption of mechanical energy in domain alignment or switching (by twinning, for example) in the near stress field of a crack tip is a possible mechanism of toughening. The objective of the present work was: 1) to determine if domain switching can occur during fracture, 2) to assess the contribution of domain switching to the overall toughness, and 3) to identify parameters which affect the contribution of domain switching to toughness. In view of the potential abundance of ferroelastic materials, it is conceivable that if such a mechanism of toughening is indeed operative, structural ceramics toughened by this mechanism may emerge as a new class of materials. PZT was chosen as a model material for the present study since this material has been extensively characterized with regards to its electrical and electro-mechanical properties. Also, as PZT is simultaneously ferroelectric- ferroelastic, domain switching may be effected by the application of an electric field as well by the application of mechanical stress. This is particularly useful for the study undertaken here as discussed later.

The experimental work included the measurement of fracture toughness of commercial PZT ceramics and subsequent determination of the degree of texture caused by the fracture process using X-ray diffraction. The degree of texture which occurs due to the reorientation of the 90° degree domains under the action of an electric field or a mechanical stress was also determined using X-ray diffraction. The kinetics of the domain reorientation process was measured under the action of an applied electric field and its significance in fracture processes is described. Finally, the effect of anisotropy induced by mechanical and electrical poling on fracture toughness is determined.

II. EXPERIMENTAL PROCEDURE

II.(a): Grinding and Annealing Studies: Some of the as-received samples were diamond ground. After grinding, X-ray diffraction traces were obtained using CuKα radiation. Subsequently, the samples were annealed at 500°C for periods of time between 1 hour and 4 hours. X-ray diffraction traces were again obtained. The principal objective was to determine if the process of grinding creates surface texture and whether the texture can be removed by annealing.

II.(b): Measurement of Fracture Toughness: The as-received, unpoled PZT ceramic samples which were in the form of rectangular bars and discs, were machined in the geometry of single edge notched beam (SENB) specimens for the measurement of fracture toughness. The typical dimensions were 35 mm x 6.5 mm x 3 mm. Notch of 0.25 mm width and 3 mm depth was machined into every sample. After machining, the samples were annealed at 500°C for 4 hours to ensure that domain orientation is completely random. The samples were then fractured in four point bending under a cross head speed of 0.125 mm/min over a range of temperatures between room temperature and 500°C. Fracture toughness, K_{Ic}, was determined using the pertinent equation. Some of the samples were electrically poled after the annealing treatment at 500°C. One set of samples were poled with an electric field of strength 15.7 kV/cm applied perpendicular to the notch surface (along the long direction of the sample) and another set was poled with an electric field of strength 15.7 kV/cm parallel to the notch surface and perpendicular to the notch edge. Samples were poled for 30 minutes at 100°C in a dielectric oil. X-ray diffraction traces were obtained from fracture surfaces to determine the degree of texture, if any.

II.(c): Switching under the Application of an Electric Field and Relaxation Experiments: The objective of these experiments was to examine the kinetics of switching of 90° domains. As the switching of 90° degree domains is expected to cause dimensional changes in the poling and orthogonal directions, mechanical transducer is an ideal device to follow the kinetics. The following experiments were designed using a universal testing machine. Thin rectangular-shaped samples of

dimensions 10 mm x 6 mm x ~400 μm were machined from the as-received, unpoled PZT samples. The samples were then annealed at 500°C for 4 hours to ensure complete randomness of domains. The two large faces (10 mm x 6 mm) of each sample were silver painted which served as the electrodes in the subsequent poling experiments. Care was taken to ensure that the two electrodes were not shorted. A loading (actually load sensing) fixture was designed and built with fused quartz rods of 2.5 cm diameter. The quartz rod assembly was mounted on a universal testing machine and an electroded sample was secured between the two rods under a very light load (typically ≤ 4 N). The corresponding mechanical stress was on the order of 1.6 MPa or less (on the order of 240 p.s.i. or less). This stress is too small to cause any domain switching. Electrical contacts were attached to the two electrodes which were connected to a regulated d.c. power supply. Figure #1 shows a schematic of the assembly. The sample/quartz rod assembly was heated to the desired temperature which was typically between room temperature and 180°C. The quartz rods were used to minimize load fluctuations due to thermal expansion. After the temperature had equilibrated, which was judged on the basis of the thermocouple readout as well as the constancy of load with time, a d.c. voltage was applied across the two electrodes. The corresponding field across the sample was ~10 kV/cm. As soon as the field was applied, the load on the sample began to drop. The drop was initially rapid but decreased with increasing time. The typical load-time trace is analogous to load relaxation experiments carried out under fixed imposed deflection, such as those used in creep or in slow crack growth studies. The rate of drop was greater at higher temperatures. The load relaxation data were subsequently analyzed using a first order kinetic equation. After the relaxation experiments, the electroded samples were placed in a bath containing HNO_3 which dissolved the silver electrodes. Subsequently, X-ray diffraction traces were obtained from the large faces in order to determine the degree of texture developed by domain switching.

II.(d): Switching under the Application of a Mechanical Stress: Bar-shaped specimens of dimensions 3 mm x 3 mm x 5 mm were machined out of the as-received, unpoled samples. The specimens were subsequently annealed at 500°C for 4 hours. The specimens were then placed, one at a time, in the quartz rod assembly. In these experiments, the specimens were subjected to a compressive stress as high as about 300 MPa. The actual procedure consisted of loading the samples at a cross head speed of 0.125 mm/min followed by arresting the crosshead once the stress reached about 300 MPa. As soon as the deflection was arrested, the load began to drop. The drop in the load was, however, much more gradual than in the experiments involving switching under the action of an electrical field. Specimens were then examined using X-ray diffraction in order to determine the degree of texture caused by mechanical poling. Experiments were conducted over a range of temperatures between room temperature and 200°C.

II.(e): Indentation Experiments on Mechanically and Electrically Poled Specimens: Bar-shaped specimens of dimensions 3 mm x 3 mm x 6 mm were machined out of the as-received, unpoled samples. One surface of each of the specimens was polished down to 1 μm finish. The specimens were then annealed at 500°C for 4 hours. The polished surface was examined by X-ray diffraction to ensure that the domains are randomly oriented. Some of the samples were then subjected to a compressive stress of 250 MPa at 100°C with the polished surface being parallel to the loading direction. After the compression test, the polished surface of every sample was again examined by X-ray diffraction. Vicker's hardness indentations were then introduced on the polished surface with one of the pyramid diagonals being parallel to the loading axis during the prior compression testing. Indentations were introduced using an indentation load between 200 gm. and 500 gm. applied for 10 seconds.

On some of the polished and annealed samples, electrodes were deposited on two opposite surfaces. The samples were then electrically poled with the polished surface being parallel to the poling direction. After poling, indentations were introduced on the polished surface with one of the pyramid diagonals being parallel to the poling direction.

III. RESULTS

III.(a): Grinding and Annealing Studies: Figure #2(a) shows an X-ray diffraction trace of an as-received sample between $2\theta = 43°$ and $2\theta = 46°$ which shows the (002) and the (200) peaks of the tetragonal structure. As seen in the figure, the intensity of the (002) peak is lower than that of the (200) peak. The ratio of the two intensities, i.e., $I_{(002)}/I_{(200)}$ is approximately 0.52. Figure #2(b) shows a trace of a sample after surface grinding in which the intensity of the (002) peak is seen to be significantly greater than that of the (200) peak. The corresponding ratio $I_{(002)}/I_{(200)}$ is ~ 1.82 which is considerably greater than that from surfaces of the as-received samples. X-ray diffraction trace of the same sample (surface ground) after annealing at 500°C is shown in Figure #2(c). The intensity of the (002) peak after annealing is lower than that of the (200) peak and that the intensity ratio was determined to be ~0.57, which is about the same as the value exhibited by the pristine surfaces. In samples that had been annealed for times less than about 2 hours, the intensity ratio although less than the as-ground surfaces, had not fully recovered.

III.(b): Fracture Toughness: Fracture toughness, K_{Ic}, of unpoled samples as a function of temperature is shown in Figure #3. As seen in the figure, K_{Ic} decreases with increasing temperature. At room temperature, the highest value of K_{Ic} was measured to be ~ 1.85 MPa√m. With increasing temperature, the K_{Ic} decreases to ~ 1.0 MPa√m and remains constant up to the maximum test temperature of 500°C. X-ray diffraction traces of fracture surfaces showed that the

5

ratio of the intensities of (002) and (200) peaks was typically greater for samples fractured at room temperature in comparison to the samples fractured near or above the Curie temperature.

Fracture toughness of samples that had been poled after machining and an annealing treatment at 500°C showed that the toughness of samples poled along the length of the test bars was ~ 0.98 MPa√m compared to ~1.2 MPa√m for samples that had been poled along the notch surface. The toughness of unpoled samples from the same set was ~ 1.45 MPa√m.

III.(c): Switching under an Electric Field: A typical load-time trace for a sample under the application of an electric field of intensity 10 kV/cm is shown in Figure #4. As seen in the figure, prior to the application of the electric field, the load is essentially constant indicating that the temperature was essentially constant everywhere within the loading set up. As soon as the field is applied, the load rapidly drops indicating a decrease in the vertical dimension of the sample. The rate of decrease continuously decreases with increasing time. About 90 % of the total load drop occurs in approximately the first 2 to 4 seconds. Over this range, the data could be adequately described by a first order kinetic equation with a single relaxation time constant, τ. In terms of the initial load, P(0), and load after infinite time, P(∞), the relaxation time, τ, and the time, t, the instantaneous load, P(t), may be given by

$$P(t) = P(\infty) + \{P(0) - P(\infty)\} \exp\left[-\frac{t}{\tau}\right] \quad \text{-------------------(1)}$$

Equation (1) shows that a plot of $\ln\left(-\frac{dP(t)}{dt}\right)$ vs. t should yield a straight line with $-\frac{1}{\tau}$ as the slope and $\ln\left(\frac{P(0) - P(\infty)}{\tau}\right)$ as the intercept.

After the electric field is removed, a slight increase in the load is noted. For the most part, the load remains unchanged after the field is removed. This suggests that the domain switching is essentially irreversible. Also, it is assumed that contribution of piezoelectric and electrostrictive effects is negligible. A typical plot of the logarithm of the rate of load relaxation vs. time is shown in Figure #5. A linear fit supports the choice of a first order kinetic equation. The relaxation behavior was studied over a range of temperatures between room temperature and 135°C under an applied field of 10 kV/cm. The relaxation time, which ranged between ~ 0.3 and ~ 1.8 seconds, was found to decrease with increasing temperature. A plot of the relaxation time vs. temperature is shown in Figure #6. A plot of ln τ vs. 1/T is shown in Figure #7. From the slope, the activation energy was determined to be ~4.65 kcal/mol.

X-ray diffraction traces of the samples after dissolving away the silver electrodes in HNO_3 indicated that the intensity of the (002) peak increased while that of the (200) peak decreased as

shown in Figure #8. The increase in the intensity of the (002) peak indicates that the 90° domains aligned themselves along the the poling direction. Under the action of the applied electric field, it is expected that both the 90° and the 180° domains will align. There, however, is no dimensional change due to the alignment of the 180° domains and thus will not be reflected in the relaxation behavior which is recorded on the basis of dimensional change or in the X-ray peak intensities. That is, the relaxation studies represent the alignment kinetics of the 90° domains.

III.(d): Switching under a Mechanical Stress: During the mechanical poling tests it was observed that the load relaxed at a considerably lower rate after the cross head deflection was arrested as compared to the electrical poling experiments. In the mechanical poling experiments, it took typically several seconds to load the samples to the final desired load. The electrical poling tests showed that much of the 90° domain switching occurred in the first 2 to 4 seconds. Therefore, the early stages of 90° domain switching could not be studied in mechanical poling experiments. Thus, switching under an electric field in the manner studied here provides a better representation of the process which occurs under a mechanical stress during the early stages. After the relaxation experiments under a mechanical stress, X-ray diffraction traces were obtained from surfaces parallel to the loading axis. These clearly showed an enhancement of the (002) peak intensity indicating that domain reorientation had occurred under mechanical loading. The intensity ratio, $I_{(002)}/I_{(200)}$ was however lower than that in the case of electrically poled samples. These experiments, however, indicated that the 90° domains in polycrystalline PZT can be reoriented at a stress on the order of 70 MPa. In order to determine the magnitude of the strain generated, a strain gage was mounted on a sample which was subsequently subjected to a compressive stress on the order of 250 MPa. Three important features were observed: (i) The stress-strain trace exhibits permanent retained strain (on the order of 4.6×10^{-4}), (ii) there is no unique yield stress (i.e., there is no unique switching stress), and (iii) nonlinearity sets in at stresses as low as about 25 to 30 MPa.

III.(e): Indentation Experiments on Mechanically and Electrically Poled PZT: Vickers microindentation crack lengths were measured on samples that had been subjected to a compressive stress of 250 MPa prior to the introduction of indentations. Microindentations were also introduced in samples that were electrically poled under a poling field of 15.7 kV/cm. It was observed that the crack lengths were longer in the direction of the loading (during the compression test) compared to the orthogonal direction. Similarly, in the electrically poled samples, the crack lengths were longer in a direction orthogonal to the poling direction. Figure #9 shows a typical photomicrograph of an indented sample that was mechanically poled. The length of the crack in the loading direction (compression) is ~ 105 μm while that in the orthogonal direction is ~ 67 μm. The corresponding anisotropic toughnesses were determined to be ~ 0.35 and ~ 0.73 MPa√m, respectively. Similar

results were obtained by Yamamoto et. al.[9] on lanthanated $PbTiO_3$ and by Okazaki [10] on PLZT. These authors explained the observations on the basis of an internal stress.

IV. DISCUSSION

<u>IV.(a): Domain Switching as a Toughening Mechanism:</u> It was observed that the fracture toughness, K_{Ic}, decreased with increasing temperature and above ~350°C the K_{Ic} was independent of temperature up to the maximum test temperature of 500°C. The Curie temperature for the material used in the present work is ~350°C. The c/a ratio of the PZT used in this work is 1.019. Unidirectional compression tests indicated that the domain switching can be effected at stresses as low as 50 MPa. X-ray diffraction patterns taken from fracture surfaces of samples fractured at room temperature often showed that the ratio of the intensities of the (002) and (200) peaks was greater (in some of the samples) than that from the as-fired surfaces indicating that domain reorientation occurred during fracture in such a way that the c axes of many of the domains became orthogonal to the fracture surfaces. In some cases, however, the ratio $I_{(002)}/I_{(200)}$ was about the same as from pristine surfaces. If the coordinate system is chosen such that the crack surface is identified with the xz plane and the crack front is parallel to the z axis, for $\theta = 0$, $\sigma_{rr} = \sigma_{\theta\theta} = \sigma_{yy} = \sigma_{xx}$, as $r \rightarrow 0$. However, for $\theta = \pi/2$, $\sigma_{rr} = \sigma_{yy} = 3\sigma_{\theta\theta} = 3\sigma_{xx}$. Thus, just off the crack plane, normal stress perpendicular to the crack plane (i.e. along y direction) is greater than the normal stress in the x direction. Assuming plane strain conditions to prevail, the normal stress in the z direction is given by $\sigma_{zz} = \nu (\sigma_{yy} + \sigma_{xx})$. If the Poisson's ratio, ν, can be assumed to be 0.25, the normal out-of-plane stress in the z direction near the crack tip, σ_{zz}, would be the same as σ_{xx}. The net tensile stress experienced by an element of material just ahead and off the crack tip is given by $2\sigma_{xx}$ or $2/3\sigma_{yy}$. If this stress exceeds the coercive stress, σ_c, necessary for the 90° domains to switch, domain switching can occur during fracture. That is, domain switching will occur in the near crack tip region if $\sigma_{yy} \geq 1.5 \sigma_c$. An increase in the ratio of the intensities of the (002) and (200) peaks from fracture surfaces is in accord with this expectation.

If the depth to which domain switching occurs is given by 'h', the elastic energy release rate, G_{Ic}, is given by

$$G_{Ic} \approx G_{Ic}^o + 2h\sigma_c\epsilon_s \quad \text{-----------------------------------} (2)$$

where ϵ_s is the switching strain and G_{Ic}^o is the elastic energy release rate in the paraelastic state. The depth to which switching occurs, h, is related to the fracture toughness, K_{Ic}, by

$$h \approx \alpha \left(\frac{K_{Ic}}{\sigma_{yy}^c} \right)^2 \qquad ----------------------------- (3)$$

where α is a constant and σ_{yy}^c is the magnitude of σ_{yy} corresponding to σ_c.

The near tip stress field is given by

$$\sigma_{yy} = \frac{K_I}{\sqrt{2\pi r}} \cos\left(\frac{\theta}{2}\right)\left[1 + \sin\left(\frac{\theta}{2}\right)\sin\left(\frac{3\theta}{2}\right)\right] \qquad ------------(4)$$

For $\theta = \pi/2$, with $K_I = K_{Ic}$, the zone depth, h, is given by

$$h \approx 0.179 \left(\frac{K_{Ic}}{\sigma_{yy}^c} \right)^2 \approx 0.08 \left(\frac{K_{Ic}}{\sigma_c} \right)^2 \qquad -------------------- (5)$$

Substituting in (2) gives

$$K_{Ic} \approx \frac{K_{Ic}^o}{\sqrt{1 - \dfrac{0.16\varepsilon_s E}{\sigma_c}}} \qquad --------------------- (6)$$

In the preceding, the relation $K_{Ic}^2 = G_c E$ has been used. The c/a for the PZT used in this work was ≈ 1.019. In a polycrystalline material with domains randomly distributed, the maximum possible value of ε_s is given by $\varepsilon_s \approx 2/3$ (c/a - 1) or 0.0127, provided all of the domains switch. In a compression test, the remnant strain was measured to be 4.6×10^{-4}. Thus, in a corresponding tensile test it should be on the order of 9.2×10^{-4}. Young's modulus of this material is given by E $\approx 6.6 \times 10^{10}$ N/m^2. The nonlinearity in the stress-strain curves sets in at ~ 25 MPa. Thus, the lower estimate of σ_c in compression can be taken as 25 MPa. Assuming it to be the same in tension and noting that K_{Ic}^o (above the Curie temperature) ≈ 1.0 MPa$\sqrt{m}$, K_{Ic} is calculated to be $\approx$ 1.28 MPa$\sqrt{m}$. This number is in accord with experimental observation in that the measured toughness at room temperature is between 1.3 and 1.85 MPa$\sqrt{m}$. The preceding only gives an approximate estimate because the domain switching does not occur at a fixed stress but occurs over a range of stresses. The average switching stress is obviously greater than 25 MPa which would make the contribution of domain switching to toughness less than given here. Alternatively, however, as the magnitude of stress in the near tip region is much greater than 250 MPa (the maximum unaxial compressive stress in the compression tests), the actual switching strain would be expected to be greater than 9.2×10^{-4} which would enhance the magnitude of the contribution to the overall toughness. A more realistic estimate must await the determination of the depth to which

9

switching occurs as well as the degree of switching. The preceding, however, does show that ferroelastic domain switching is a viable toughening mechanism, which in this material enhances the toughness by about 30 %.

Indentation experiments on mechanically poled samples are also in accord with the hypothesis of domain switching. X-ray diffraction from the face subjected to compression showed that the ratio of the intensities of (002) and (200) peaks decreased while that from the faces parallel to the loading axis showed an increase in the ratio. This suggests that the application of a compressive stress led to the domain realignment with the c axes of several of the domains orienting perpendicular to the loading axis. When the faces parallel to the loading axis were subsequently indented with one of the diagonals parallel to the loading axis, it was observed that the crack lengths were different in the two directions. Specifically, the indentation cracks were longer in the direction of loading than in the orthogonal direction. This observation can be rationalized as follows.

Many of the domains were poled during the compression testing such that their c axes are orthogonal to the loading direction. During fracture, domains with c-axes parallel to the crack surface are expected to switch in such a way that the domains in the crack tip region orient orthogonal to the crack surface. This process is expected to absorb some energy which should reflect as enhanced toughness. By contrast, domains that are already orthogonal to the crack surface should remain unaltered in orientation. Thus, no energy is absorbed by these domains. With reference to the mechanically poled samples then, a large number of domains are switched during the compression loading such that a large number of domains have their c-axes orthogonal to the loading axis. *When indented with one of the diagonals parallel to the loading direction, no switching is expected for a crack along the loading direction as the domains are already oriented perpendicular to the prospective crack as shown in Figure #10. By contrast, for a crack orthogonal to the loading direction, a large number of domains have their c-axes parallel to the prospective crack.* Thus, as a crack is formed by indentation, domain reorientation can occur such that their c-axes become perpendicular to the crack surface. This is shown schematically in Figure #10 in which the arrows A & B indicate the orientations of the domains before & after the introduction of the crack. Since energy is absorbed in the switching process, it is expected that the crack will be shorter in the direction perpendicular to the loading direction. This is precisely what was observed. Similar effects were also observed in electrically poled samples. Specifically, indentation cracks were shorter in the direction of poling as the field aligns the domains along the field. The indentation K_{Ic} for a crack orthogonal to the compressive loading direction was ~ 0.73 MPa$\sqrt{m}$ compared to ~ 0.35 MPa$\sqrt{m}$ in the direction of loading indicating a substantial contribution of domain switching to the overall toughness, on a percentage basis. The indentation toughnesses are considerably lower than those obtained by SENB technique. However, their relative magnitudes

are in accord with the analysis presented here.

Okazaki and coworkers [9,10] who examined the anisotropy of indentation crack lengths in electrically poled $PbTiO_3$ and PLZT polycrystalline ceramics also observed similar effects. However, they interpreted their results on the basis of an internal stress. In analogy with the indentation work on tempered glass [11] in which the apparent toughness K_{Ic} depends upon the true toughness K_{Ic}^o, the crack length (radius) c and _uniform_ residual stress σ_i, via

$$K_{Ic} = K_{Ic}^o - \frac{2}{\sqrt{\pi}}\sigma_i\sqrt{c} \quad \text{------------------------------(7)}$$

Okazaki et. al. [9,10] deduced that there must be a uniform stress in their poled and unpoled samples. In equation (7), for a compressive stress, $\sigma_i < 0$. Thus, if a surface compressive stress exists, the apparent toughness will be higher. Similar effects have been observed in zirconia-containing ceramics that are surface ground [12]. Okazaki et. al. [9,10] observed that the crack sizes were of the same lengths in unpoled samples (similar to the present work) but were different in the two directions in the poled samples. They suggested that there must be an internal stress in all of the ferroic samples used in their study and that the stresses must be aniostropic, macroscopically, in the poled samples.

Residual stresses determined by Okazaki [10] in PLZT ceramics were as high as 14.5 GPa while the hardness was only 0.47 GPa. Clearly, such high stresses can not be sustained by the material. It can be shown that their interpretation is incorrect. It is to be noted that no _uniform_ stress is expected in either unpoled or poled samples. In the unpoled samples, as the sample is cooled through the Curie temperature, cubic → tetragonal transition occurs such that c/a >1.0. This leads to the establishment of a complex state of internal stress. To a first approximation, some of the grains are under compression while the others are under tension, with the spatial average of the stress however being zero. Thus, there would be a periodic distribution of residual stresses with the wavelength on the order of twice the grain size. If the magnitude of the internal stress is σ_i, then the additional toughening that can be realized is ~ 1.2 σ_i √d where d is the grain size [13,14]. The stress intensity factor due to the periodic internal stress is also periodic and oscillates between two values [14]. According to the work of Freiman and coworkers [15], the magnitude of the internal stress is on the order of 25 MPa. The linear dependence of K_{Ic} on √c with positive slope observed in the work of Okazaki et. al. [9,10] is probably due to an R-curve behavior similar to the one often observed in transformation toughened materials and cannot be identified with residual stress. In tempered glass plates [11] and surface ground zirconia ceramics [12], the slope is identified with the surface stress since the surface is under a uniform stress unlike the $PbTiO_3$ and PLZT materials used by Okazaki et. al. [9,10].

Anisotropy in fracture toughness of piezoelectric ceramics has recently been analyzed by Pisarenko et. al. [16]. These authors have attributed the observed behavior on the concept of domain reorientation and have further pointed out the errors in the interpretation based on an internal stress. Freiman et. al. [15] have suggested microcracking and crack/twin interactions as the mechanisms of toughening. Further, the enhanced toughness of pressure-depoled PZT ceramics was interpreted on the basis of antiferroelectric domains transforming into ferroelectric domains. In their work, however, the anisotropy of toughness was not examined. Also, the nature of twin/crack tip interaction was not explicitly identified.

Fracture toughness of electrically poled samples using the SENB technique showed that the toughness of samples poled in a direction along the notch surface was ~1.2 MPa$\sqrt{m}$ while of the samples poled in a direction perpendicular to the notch surface was ~0.98 MPa$\sqrt{m}$. This observation is in accord with the preceding analysis. The unpoled samples, however, exhibited the highest toughness ~1.45 MPa$\sqrt{m}$. This result suggests that domain switching in unpoled samples is apparently easier. Further work is needed to explore this effect.

IV.(b): Kinetics of Domain Switching: Domain switching was not observed on fracture surfaces of all of the samples fractured at room temperature. An obvious conclusion one is inclined to draw is that in those samples domain switching probably did not occur. It is important to emphasize that this may not be the case. In transformation toughened materials, the common practice is to obtain X-ray diffraction patterns from fracture surfaces in order to determine the amount of the monoclinic phase formed during fracture. The fact that the monoclinic phase is often observed on fracture surfaces in a large number of zirconia ceramics is indeed a unique characteristic of transformation toughened materials as compared to other toughening mechanisms. Martensitic transformation is athermal and known to occur almost instantaneously. The parent phase/martensitic phase boundary can propagate at velocities near the sound velocity in martensitic transformations. By contrast, most other phenomena, such as plastic deformation, viscous deformation, are time dependent. For example, plastic deformation is almost always strain rate dependent. Thus, if a material such as a hard metal containing a crack is subjected to external loads, a plastic zone develops at the crack tip. Once the stress intensity factor exceeds the fracture toughness, the crack begins to propagate in almost a brittle manner. In such a case, while at the tip of the crack a plastic zone develops during quasistatic loading, essentially no plastic deformation occurs along the crack surfaces when the crack propagation is rapid. Clearly the fact that no deformation can be observed along the crack surfaces does not imply that it did not occur before the crack became critical and that it did not contribute to the quasistatic fracture toughness. To illustrate this point, a photomicrograph showing an arrested crack (which was produced by thermal shock) in an MgO crystal is shown in Figure

#11. It is seen that no dislocations can be seen along the crack surfaces. However, at the tip a high density of dislocations is seen. As the crack propagated rapidly and then arrested, a high level of stress existed at the tip for a long enough of time for the formation and motion of dislocations. During the crack propagation stage, on the other hand, time was too short for dislocations to form and propagate. The implication is that the stress intensity factor necessary to initiate crack propagation is expected to be greater than that necessary to continue crack propagation. This indeed is a common observation in many metallic materials including many steels.

The phenomenon of domain switching is also known to be time dependent. Most of the commercial ferroelectric materials such as $BaTiO_3$ and PZT are typically poled for several minutes to ensure that poling is complete. The process of domain switching can often be described as a relaxative phenomenon. Recently, Rudyak [17] for example, examined domain switching and viscosity phenomenon in ferroelectric and ferroelastic materials.

In the present work the electrical switching experiments were designed to determine the time dependence of the domain switching process. The 90° domain switching in PZT is identical with ferroelastic domain switching. This, however, is not the case with 180° domain switching as no changes in physical dimensions of the material occur due to the 180° switching. However, from the standpoint of toughening, only the 90° domains are relevant. If one were to determine the magnitude of the permanent polarization as function of time, it would reflect the time dependence of both types of switching. In the present work, the dimensional change was measured as a function of time under the action of an externally applied electric field. The reason for applying an electric field instead of a mechanical stress for the relaxation studies is that the electrical field can be applied almost instantaneously and thus the early stages of domain switching can be studied. From the standpoint of toughening by ferroelastic domain switching, it is essential to determine the kinetics of domain switching during the early stages.

It was observed that the relaxation time was typically ranged between 0.3 to 3 seconds. The relaxation time decreased with increasing temperaure. As shown in Figure #5, first order kinetics adequately describes the kinetics and the activation energy was ~4.65 kcal/mol. A few experiments were also done under an applied mechanical load, similar to the work of Esaklul [18]. Typical time required to load the sample to ~ 250 MPa stress was on the order of several seconds. Electrical switching experiments, on the other hand, showed that much of the 90° domain switching was complete within the first couple of seconds. As a result, relaxation experiments under a mechanical load are not meaningful from the point of examining the early stages of the switching process, which are relevant to fracture processes. It was further observed that the relaxation in mecahnical loading was considerably slower than that observed during the early stages in the electrical

switching experiments. This relaxation, however, was similar to the later stages of relaxation in the electrical experiments. This suggests that there are two mechanisms of load relaxation in PZT ceramics. The first stage can be satisfactorily described by simple first order kinetics. In the work of Esaklul et. al. [18], only the later stages were studied since relaxation under only a mechanical load was examined. The fact that these authors measured a much higher activation energy also indicates that the mechanisms of relaxation are different in the early and the later stages. Syrkin and Elgard [19] have determined the dependence of anelastic strain under constant stress in BaTiO₃. They measured a relaxation time of ~10 minutes with an activation energy of ~7.5 kcal/mol. Since their experiments were also under a mechanical load, only the later stages could be studied.

In order to ensure that switching of 90° domains does occur relatively rapidly (relaxation time on the order of second or seconds rather than on the order of minutes), some of the samples were rapidly (within 3 to 5 seconds) loaded to 250 MPa in compression and rapidly unloaded. That is, in these samples the load was not allowed to relax. X-ray diffraction traces (Figure #12) before and after loading clearly show that domain switching did occur . In these experiments, the sample was at ~ 250 MPa for a fraction of a second. Based on electrical switching experiments, this time is sufficient to switch a significant number of domains. These experiments also confirm the validity of electrical switching experiments for the analysis of fracture processes.

V. CONCLUSIONS

Based on the present work the following conclusions may be drawn.

1) The fracture toughness of polycrystalline PZT ceramics decreases with increasing temperature and above the Curie temperature it is independent of temperature up to 500°C, the maximum test temperature in the present work. X-ray diffraction traces of fracture surfaces in some cases showed that the ratio of the intensities of the (002) and the (200) peaks was greater than that from pristine surfaces.

2) Indentation experiments on mechanically and electrically poled samples exhibited an anisotropy in crack lengths. It was observed that the crack length was shorter in the direction in which the domains tended to line up during the poling (mechanical and electrical) proces . The alignment of the domains that occurs during the poling process was confirmed by X-ray diffraction.

3) On the basis of these observations, it is proposed that ferroelastic domain switching in the stress field of a crack tip is a viable toughening mechanism in PZT ceramics.

14

4) Kinetics of 90° domain switching could be satisfactorily explained by a first order kinetic equation. The relaxation time was less than 3 seconds, and typically on the order of 1 second at room temperature. The kinetics of domain switching is thermally activated with an activation energy on the order of 4.65 kcal/mol.

5) The fact that an increase in the ratio of the intensities of (002) and (200) peaks, i.e., $I_{(002)}/I_{(200)}$, is some times not observed on fracture surfaces of samples fractured in the ferroic state is rationalized on the premise that crack propagation is often too rapid to allow domain switching on the overall fracture surface. However, during the quasistatic loading of a crack, domain switching would occur near the crack tip and thus would contribute to the overall toughness, much in the same way as a plastically deformed zone forms near a crack tip prior to catastrophic growth in a brittle manner.

REFERENCES

1) R. C. Pohanka, S. W. Freiman, K. Okazaki and S. Tashiro, "Fracture of Piezoelectric Materials", Fracture Mechanics of Ceramics, Vol. 5, edited by R. C. Bradt, A. G. Evans, D. P. H. Hasselman and F. F. Lange, Plenum Press, p. 353-364, New York, (1983).

2) R. C. Pohanka, S. W. Freiman and B. A. Bender, "Effect of Phase Transformation on the Fracture Behavior of BaTiO$_3$", *J. Am. Ceram. Soc.*, **61**, 72, (1978).

3) R. C. Pohanka, S. W. Freiman and R. W. Rice, "Fracture Processes in Ferroic Materials", *Ferroelectrics*, **28**, 337, (1980).

4) R. C. Pohanka, R. W. Rice and B. E. Walker, Jr., "Effect of Internal Stress on the Strength of BaTiO$_3$", *J. Am. Ceram. Soc.*, **59**, 71, (1976).

5) K. D. McHenry and B.G. Koepke, "Electric Field Effects on Subcritical Crack Growth in PZT", Fracture Mechanics of Ceramics, Vol. 5, edited by R. C. Bradt, A. G. Evans, D. P. H. Hasselman and F. F. Lange, Plenum Press, p. 337-352, New York, (1983).

6) R. F. Cook, S. W. Freiman, B. R. Lawn and R. C. Pohanka, "Fracture of Ferroelctric Ceramics", *Ferroelectrics*, **50**, 267-272, (1983).

7) S. C. Abrahams and E. T. Keve, "Structural Basis of Ferroelectricity and Ferroelasticity", *Ferroelectrics*, **2**, 129-154, (1971).

8) K. Aizu, "Possible Species of Ferromagnetic, Ferroelectric and Ferroelastic Crystals", *Physical Review B*, **2** [3], 754-772, (1970).

9)   T. Yamamoto, H. Igarashi and K. Okazaki, "Internal Stress Anisotropies induced by Electric Field in Lanthanum Modified $PbTiO_3$ Ceramics", *Ferroelectrics*, **50**, 273-278, (1983).

10)   K. Okazaki, "Mechanical Behavior of Ferroelectric Ceramics", *Ceramic Bulletin*, **63**, [9], 1150, (1984).

11)   D. B. Marshall and B. R. Lawn, "An Indentation Technique for Measuring Stress in Tempered Glass Surfaces", *J. Am. Ceram. Soc.*, **60** [1-2] 86-87, (1977).

12)   Y. Ikuma and A. V. Virkar, "Crack Size Dependence of Fracture Toughness in Transformation Toughened Ceramics", *J. Mater. Sci.*, **19**, 2233. (1984).

13)   A. V. Virkar and D. L. Johnson, "Fracture Behavior of ZrO_2-$Zr(O)$ Composites", *J. Am. Ceram. Soc.*, **60**, 514, (1977).

14)   R. A. Cutler and A. V. Virkar, "The Effect of Binder Thickness and Residual Stresses on the Fracture Toughness of Cemented Carbides", *J. Mater. Sci.*, **20**, 3557-3573, (1985).

15)   S. W. Freiman, L. Chuck, J. J. Mecholsky, D. L. Shelleman and L. J. Storz, "Fracture Mechanisms in Lead Zirconate Titanate Ceramics", in 'Fracture Mechanics of Ceramics', Vol.8, Edited by Bradt, Evans, Hasselman and Lange, Plenum Press, p.175-185, (1986).

16)   G. G. Pisarenko, V. M. Chushko and S. P. Kovalev, "Anisotropy of Fracture Toughness of Piezoelectric Ceramics", *J. Am. Ceram. Soc.*, **68** [5] 259-265 (1985).

17)   V. M. Rudyak, Viscosity Phenomenon and Switching Processes in Ferroelastics", *Ferroelectrics*, **48**, 131-141, (1983).

18)   K. A. Esaklul, W. W. Gerberich and B. G. Koepke, "Stress Relaxation in PZT", *J. Am Ceram. Soc.*, **63** [1-2] 25-30 (1980).

19)   L. N. Syrkin and A. M. Elgard, "Influence of the Domain Structure of Ceramic Ferroelectrics on Their Mechanical Properties", *Sov. Phys.-Solid State*, **7** [4] 967-971 (1965).

FIGURE CAPTIONS

Figure #1: A schematic of the load recording assembly used for the relaxation studies under the application of an electric field. The enlarged view in the inset shows the sample with silver electrodes.

Figure #2(a): An X-ray diffraction trace of an as-received sample showing the (002) and the (200) peaks. Note that the peak intensity of the (002) peak is less than that of the (200) peak. The ratio of the intensities, namely $I_{(002)}/I_{(200)}$ is about 0.52.

Figure #2(b): An X-ray diffraction of the same sample after surface grinding. The intensity of the (002) peak is greater than that of the (200) peak $(I_{(002)}/I_{(200)} = 1.82)$ showing the occurrence of domain switching.

Figure #2(c): An X-ray diffraction of the same sample which was annealed at 500°C for 4 hours. Note that the texture induced during grinding is removed after annealing. $(I_{(002)}/I(200) = 0.57)$.

Figure #3: Fracture toughness of unpoled samples as a function of temperature.

Figure #4: Load vs. time trace for a sample under the application of an electric field of magnitude 10 kV/cm.

Figure #5: A plot of ln {-dP/dt} vs. time for the trace shown in Figure #4. Note that the data can be described by first order kinetics.

Figure #6: Relaxation time, τ, as a function of temperature.

Figure #7: A plot of ln{τ} vs. 1000/T for the determination of the activation energy. The activation energy was determined to be ~4.56 Kcal/mol.

Figure #8: X-ray diffraction traces of the as-annealed and electrically poled samples. The trace of the poled sample, which was taken on one of the surfaces perpendicular to the poling direction, clearly shows the occurrence of domain switching.

Figure #9: A photomicrograph showing a microindent (500 g for 10 seconds) introduced in a mechanically poled sample. Note the anisotropy in crack 'ngths. The arrows indicate the direction of compression.

Figure #10: A schematic showing the anisotrpoy of crack lengths in a mechanically poled sample. The horizontal cracks are shorter because domain reorientation is expected to occur once the indentation is introduced. The arrows A & B indicate the orientations of the domains before & after introduction of the indent. By contrast, for the vertical cracks, no reorientation is expected since the domains are already oriented in the prospective direction.

Figure #11: (a): A photomicrograph showing a crack introduced in an MgO single crystal by thermal shock. Note that dislocations are present near the crack tip but not along the crack surfaces. (b): An enlarged view of the dislocation pits near the crack tip.

Figure #12: X-ray diffraction traces of as-annealed and rapidly loaded (in compression) & unloaded sample showing the occurrence of domain switching. The entire loading and unloading was done in about 5 seconds. The figure shows that domain switching occurs relatively fast and that slow relaxation, such as that observed by Esaklul et. al. [18], does not represent the early stages of domain switching.
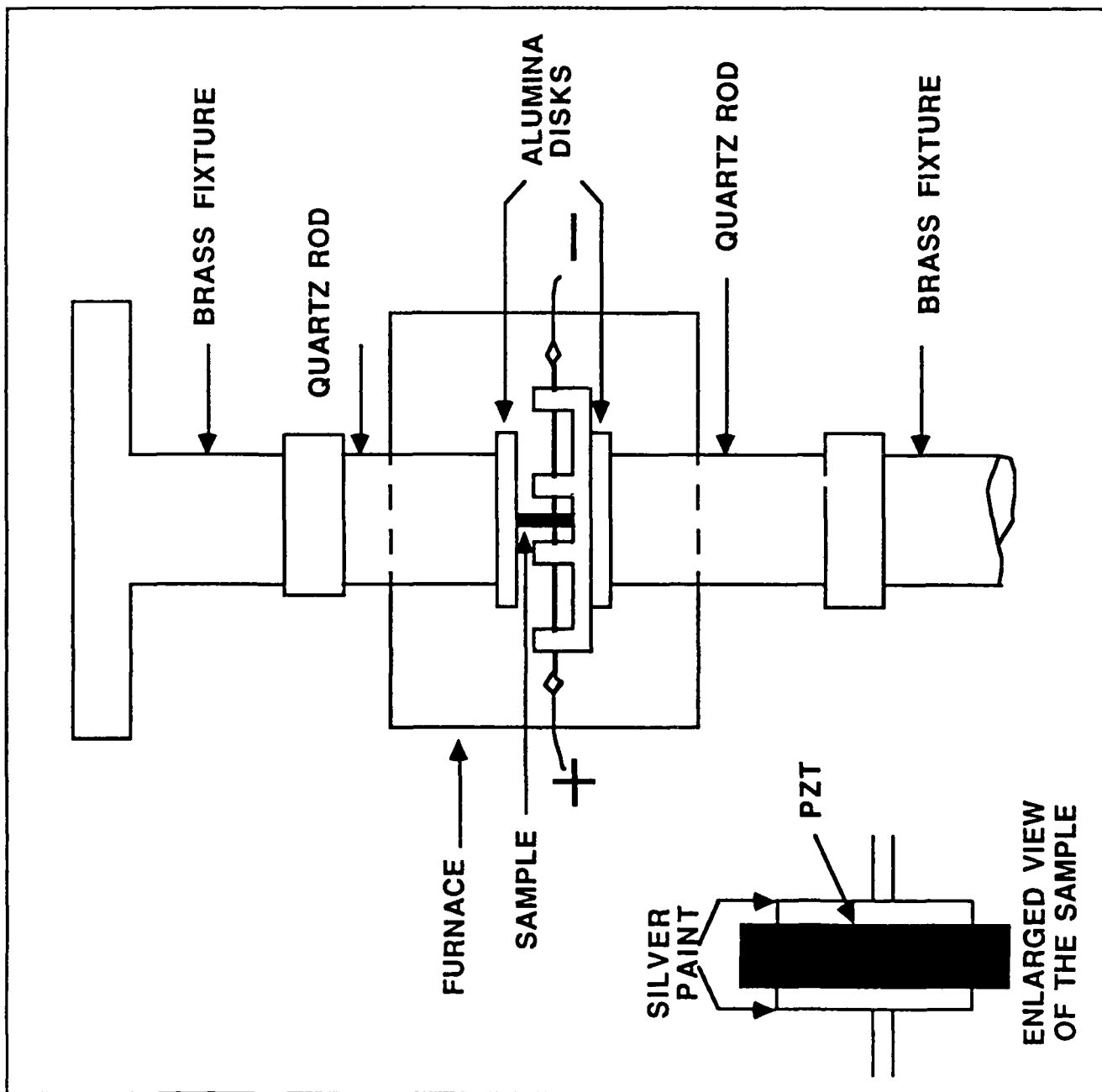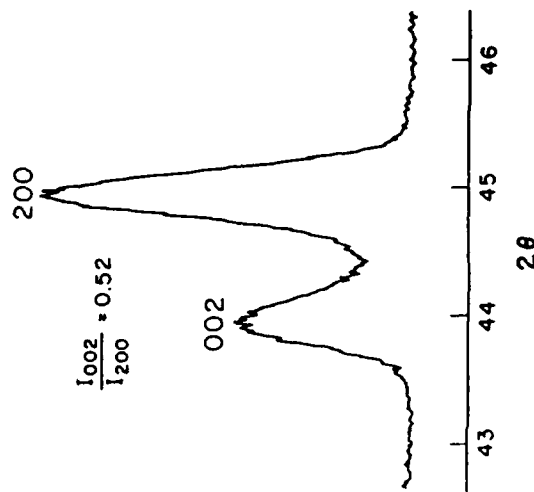
17

BRASS FIXTURE

QUARTZ ROD

ALUMINA
DISKS

QUARTZ ROD

BRASS FIXTURE

FURNACE

SAMPLE

SILVER
PAINT

PZT

ENLARGED VIEW
OF THE SAMPLE

Fig 1

AS RECEIVED

$\frac{I_{002}}{I_{200}} = 0.52$
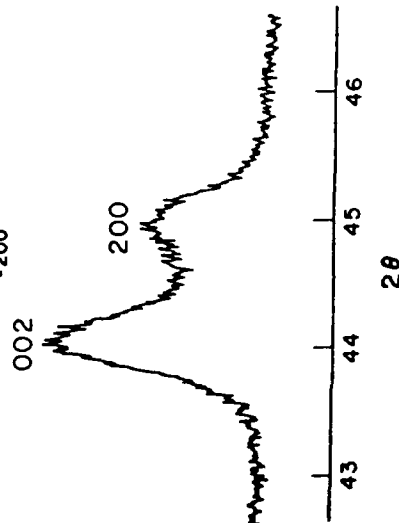
200

002

2θ

2(a)

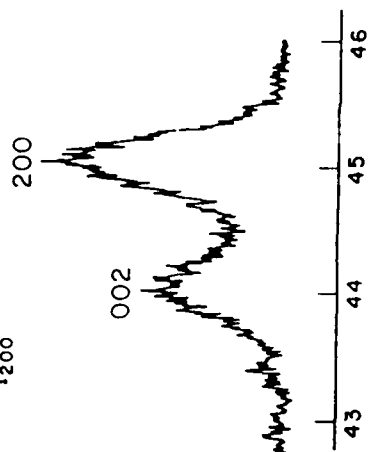AFTER SURFACE GRINDING

$\frac{I_{002}}{I_{200}} = 1.82$
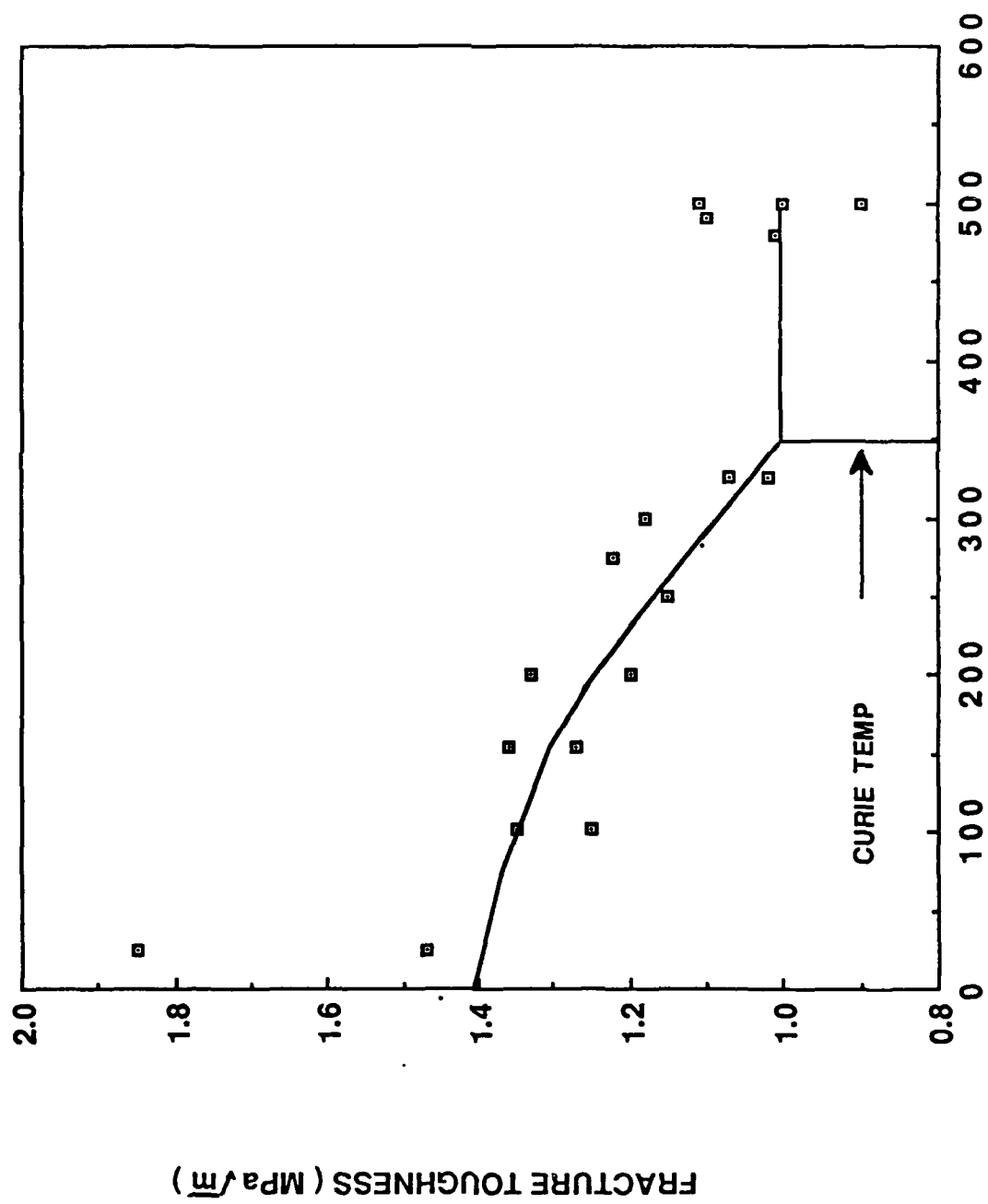
002

200

2θ

2(b)

AFTER SURFACE GRINDING
AND ANNEALING

$\frac{I_{002}}{I_{200}} = 0.57$

200

002

2θ

2(c)

Fig. 2
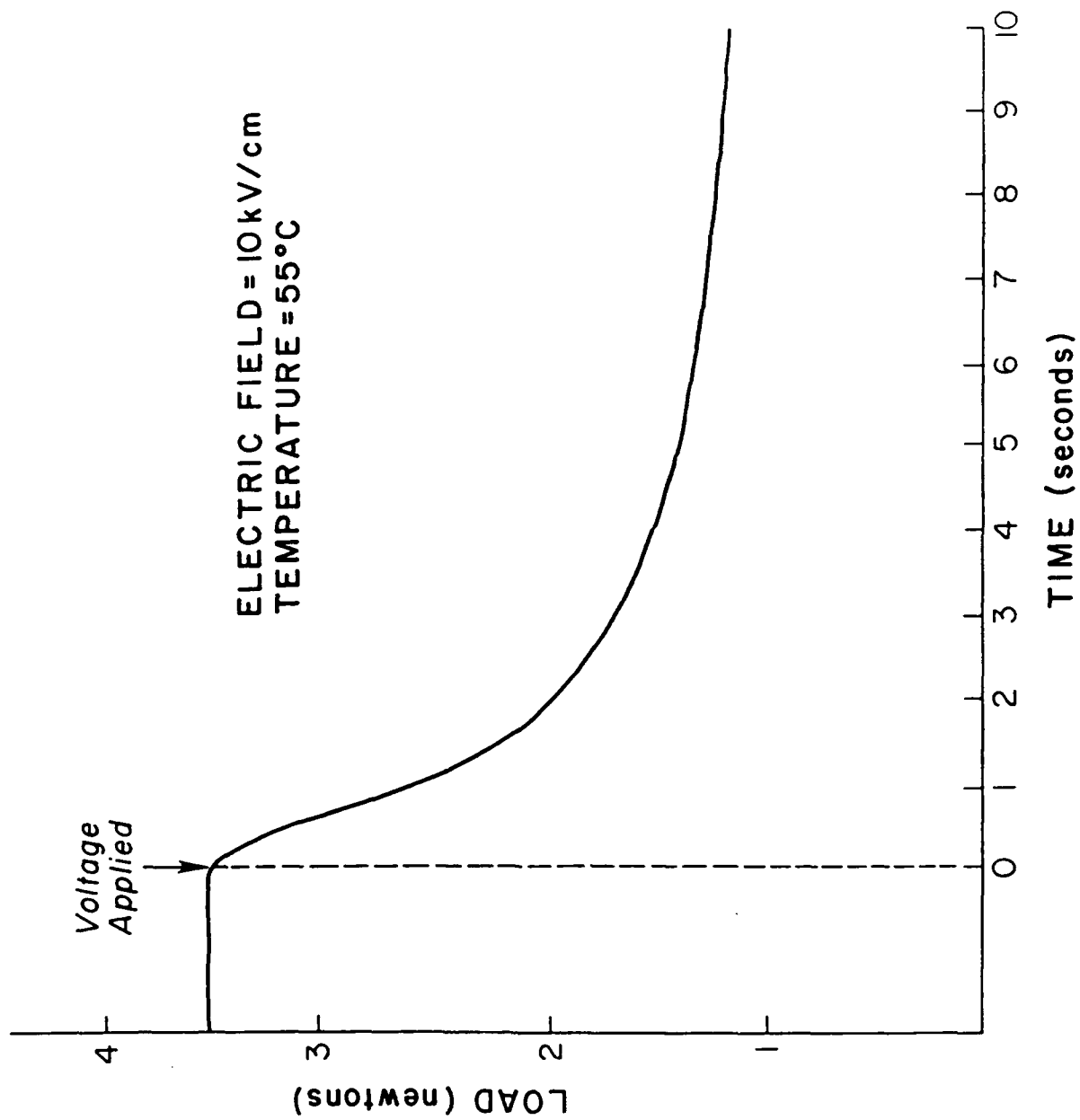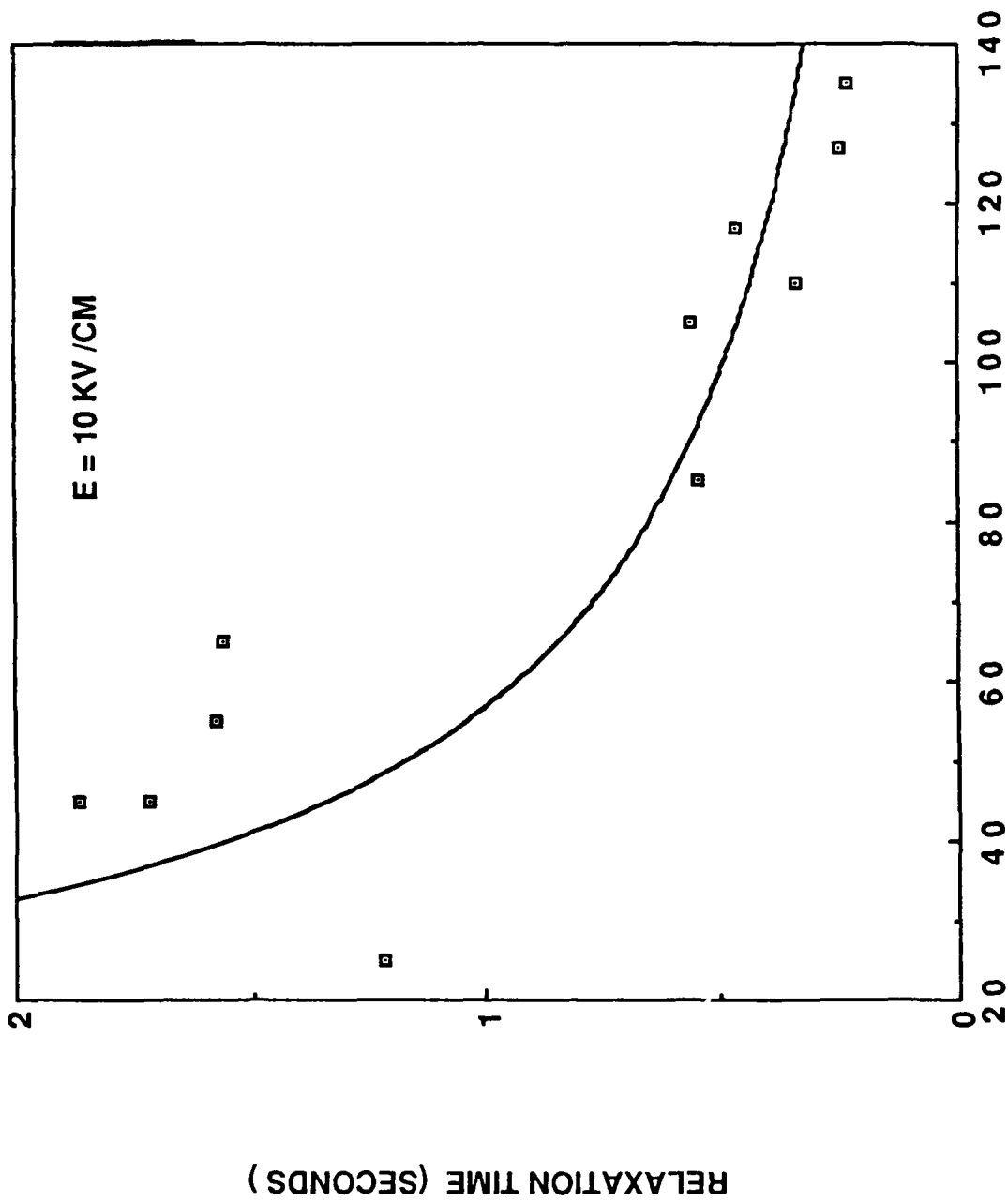
Fig 3.

ELECTRIC FIELD = 10 kV/cm
TEMPERATURE = 55°C

Voltage Applied

LOAD (newtons)

TIME (seconds)

fig. 4

E = 10 KV / CM   T = 55 C

RELAXATION TIME =1.6 SEC

TIME (SEC)

LN (- STRESS RATE)

fig. 5

E = 10 KV/CM

TEMPERATURE (C)

RELAXATION TIME (SECONDS)

Fig 6

ACTIVATION ENERGY = 4560 Cal / mole

LN RELAXATION TIME

1000 / TEMPERATURE   (1/ K)
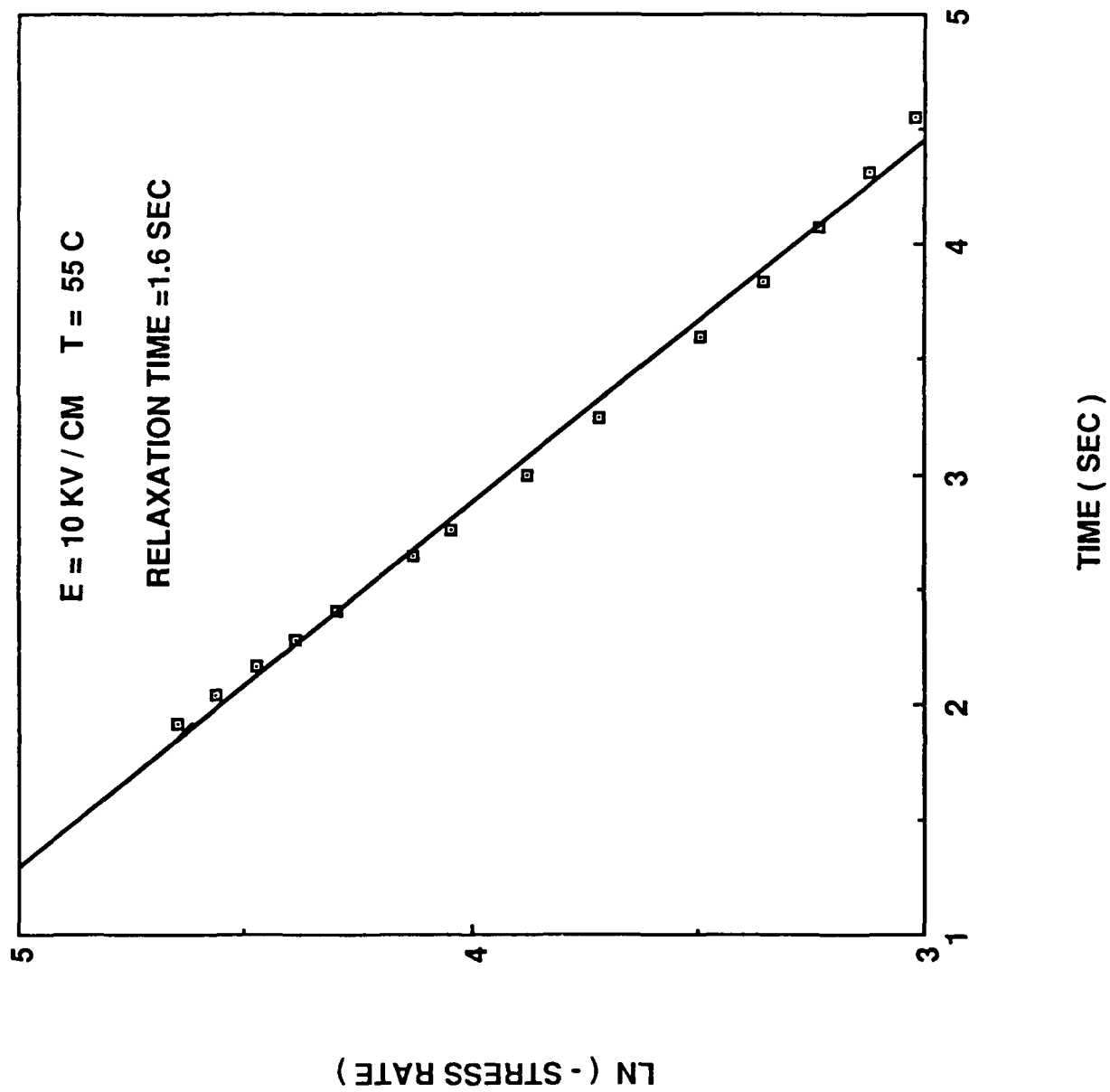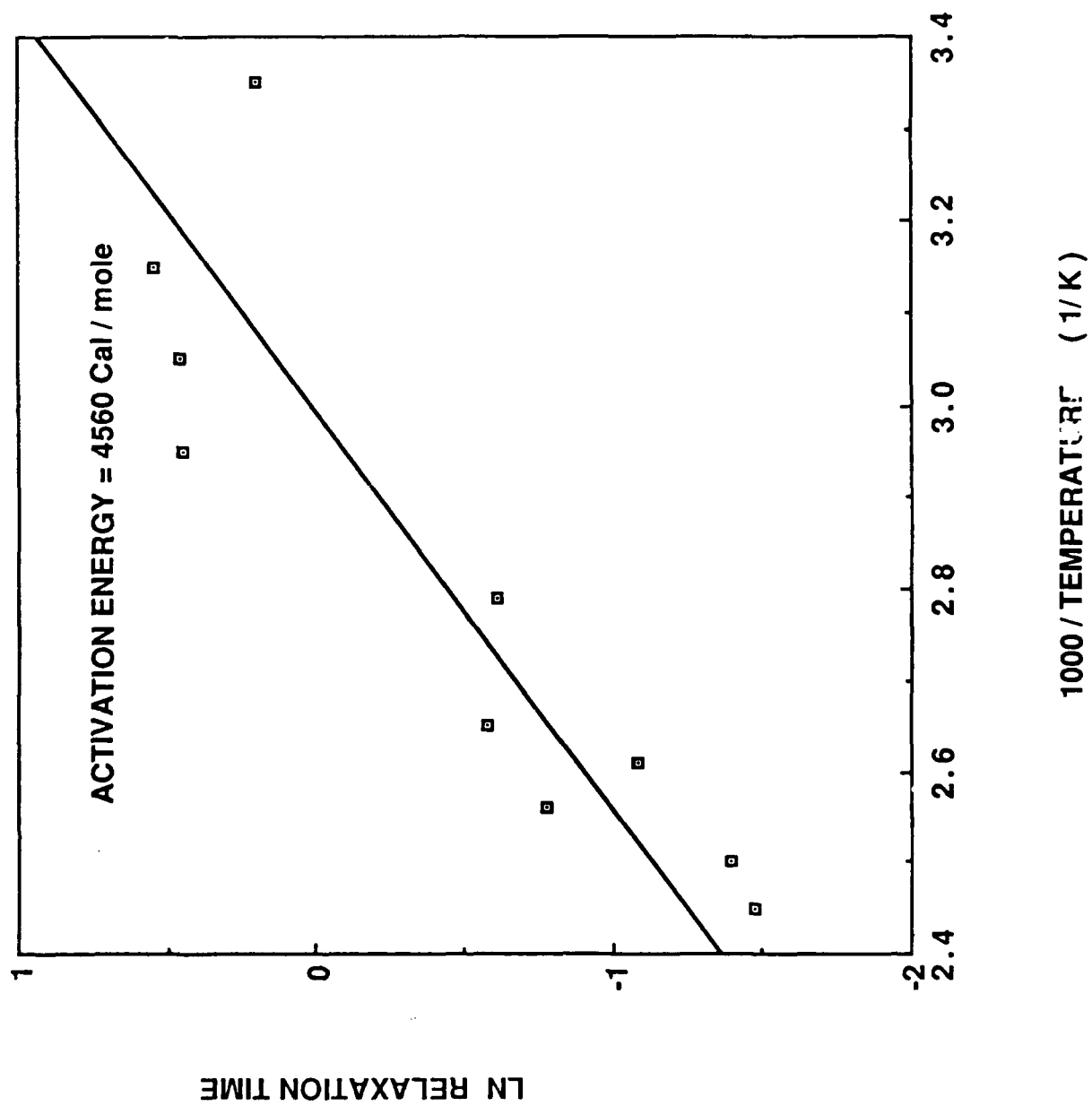
fig 1.
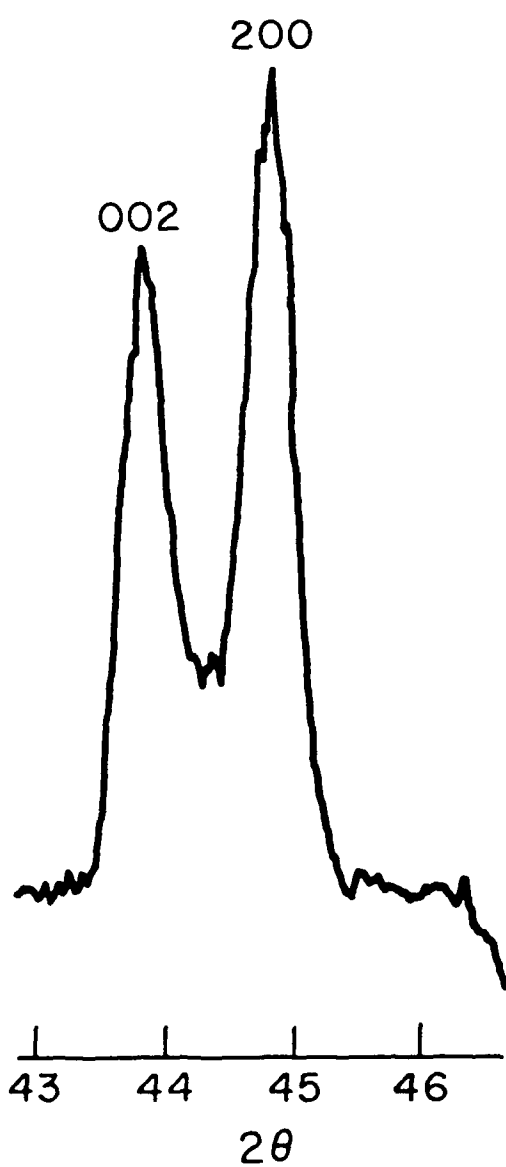
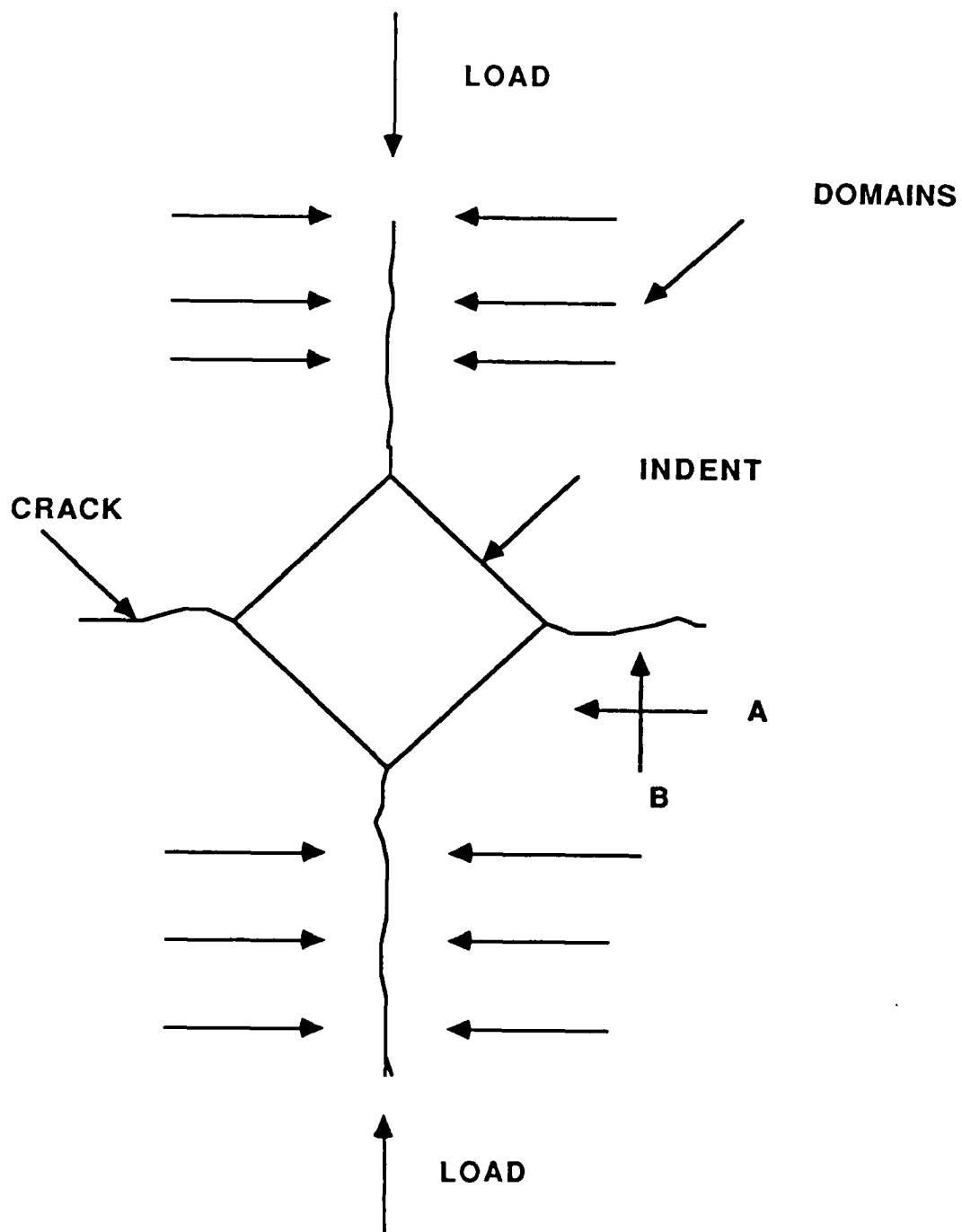AFTER
ANNEALING

AFTER APPLYING
ELECTRIC FIELD
(10kV/cm)

002

200
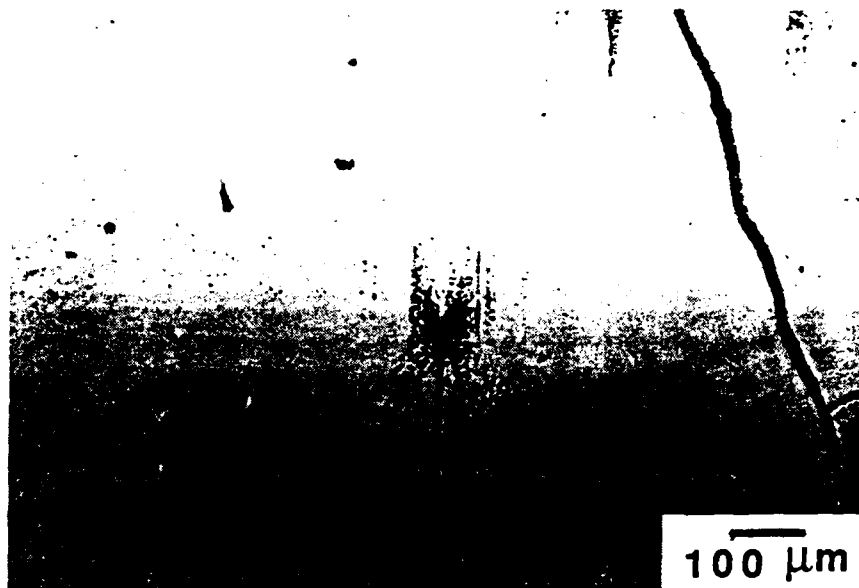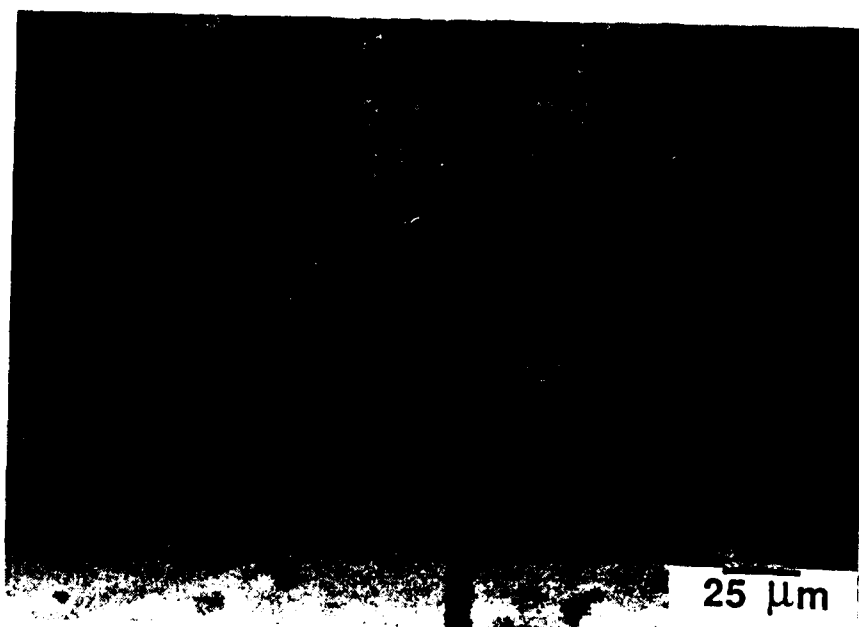
002

200

43   44   45   46

2θ

43   44   45   46

2θ

25 μm

LOAD

DOMAINS

INDENT

CRACK
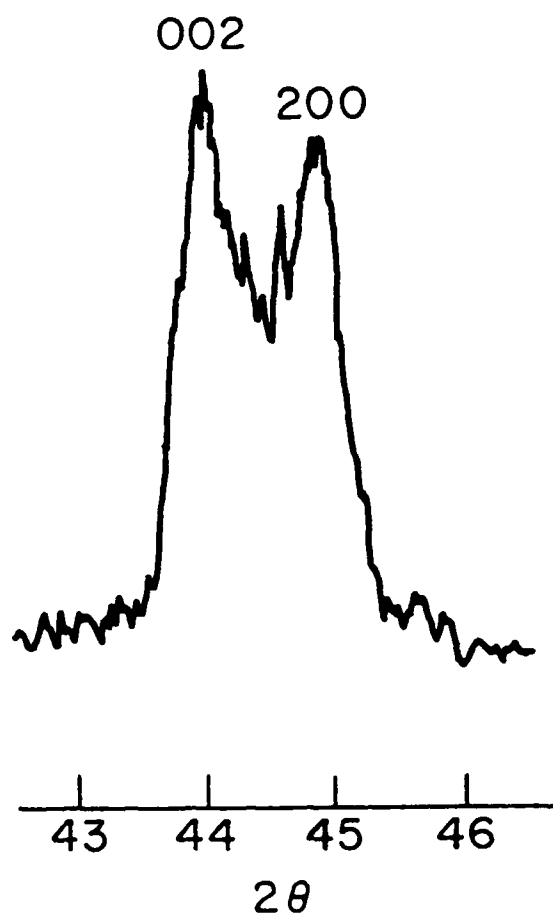
A

B

LOAD

Fig 10.

(a)

100 μm
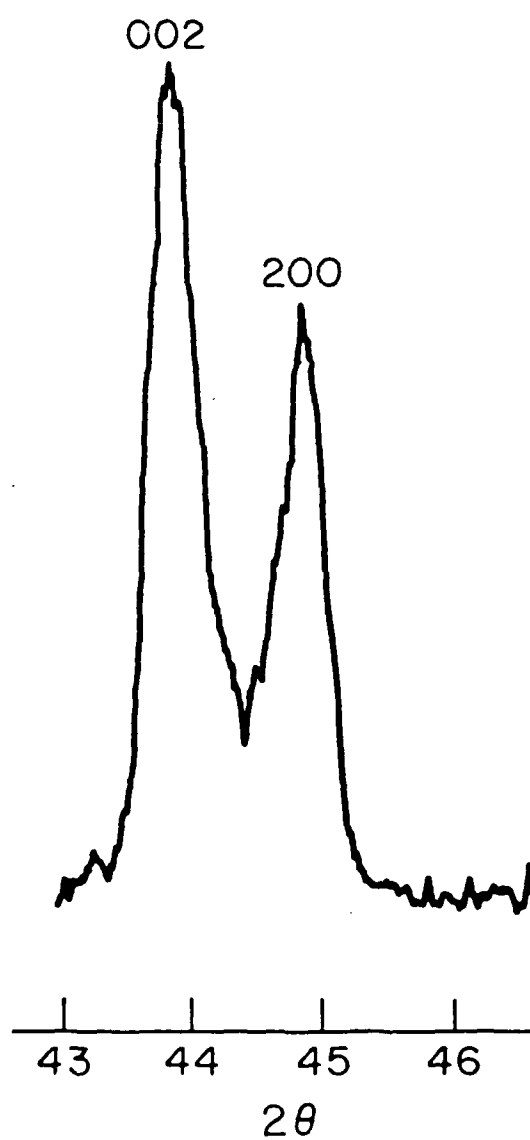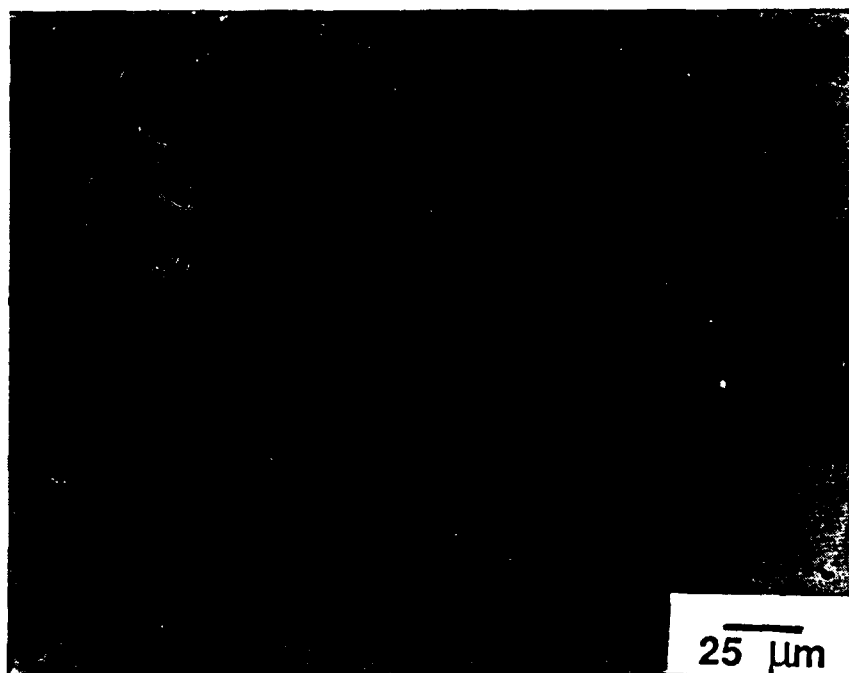
25 μm

b

Fig. 11

AFTER ANNEALING

AFTER RAPID LOADING TO 250 MPa (COMPRESSION) AND UNLOADING